

การศึกษาเปรียบเทียบผลของตัวทำละลายและตัวกระตุ้นการเกิดปฏิกิริยาคู่ด้วยตัวเร่งปฏิกิริยาไททานเนียม
ด้วยการพอลิเมอไรซ์ของเอทิลีน/แอลฟาโอเลฟิน



นาย นวพร อินทรกำจร

สถาบันวิทยบริการ
จุฬาลงกรณ์มหาวิทยาลัย

วิทยานิพนธ์นี้เป็นส่วนหนึ่งของการศึกษาตามหลักสูตรปริญญาวิศวกรรมศาสตรดุษฎีบัณฑิต

สาขาวิชาวิศวกรรมเคมี ภาควิชาวิศวกรรมเคมี

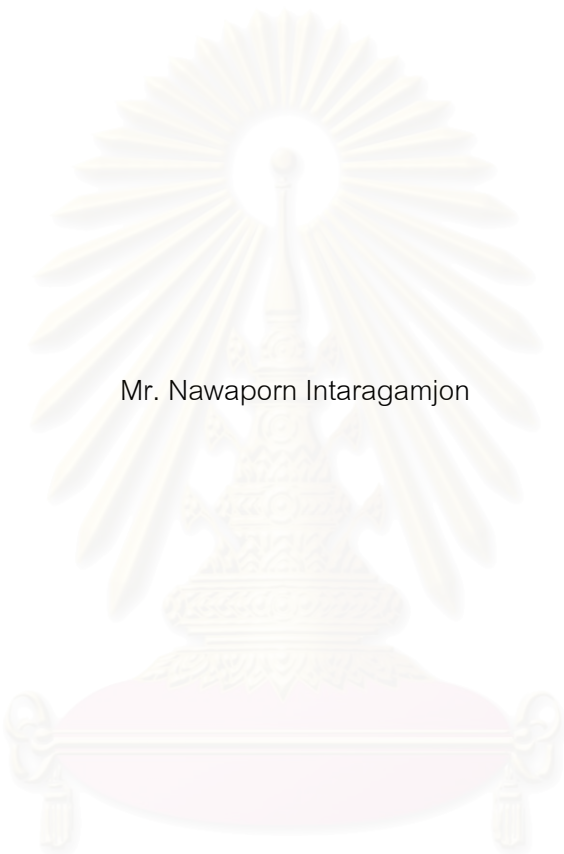
คณะวิศวกรรมศาสตร์ จุฬาลงกรณ์มหาวิทยาลัย

ปีการศึกษา 2548

ISBN 974-17-2104-4

ลิขสิทธิ์ของจุฬาลงกรณ์มหาวิทยาลัย

COMPARATIVE STUDY OF SOLVENT EFFECT AND ACTIVATORS WITH TITANOCENE CATALYSTS
ON ETHYLENE/ALPHA-OLEFINS POLYMERIZATION



Mr. Nawaporn Intaragamjon

สถาบันวิทยบริการ
จุฬาลงกรณ์มหาวิทยาลัย

A Dissertation Submitted in Partial Fulfillment of the Requirements
for the Degree of Doctor of Engineering Program in Chemical Engineering

Department of Chemical Engineering

Faculty of Engineering

Chulalongkorn University

Academic year 2005

ISBN 974-17-2104-4

นพพร อินทรกำจร : การศึกษาเปรียบเทียบผลของตัวทำละลายและตัวกระตุ้นการเกิดปฏิกิริยาด้วยตัวเร่งปฏิกิริยาไททานินขึ้นด้วยการพอลิเมอไรซ์ของเอทิลีน/แอลฟาโอเลฟิน.

(COMPARATIVE STUDY OF SOLVENT EFFECT AND ACTIVATORS WITH TITANOCENE CATALYSTS ON ETHYLENE/ALPHA-OLEFINS POLYMERIZATION) อ. ที่ปรึกษา :

ศ.ดร.ปิยะสาร ประเสริฐธรรม, อ.ที่ปรึกษาร่วม : Prof.Takeshi SHIONO จำนวนหน้า 129 หน้า. ISBN 974-14-2104 -4.

การศึกษาโคพอลิเมอไรเซชัน ของ เอทิลีน/แอลฟา-โอเลฟิน ในระบบตัวเร่งปฏิกิริยาไททานินขึ้น ได้ถูกศึกษาในระบบการพอลิเมอไรซ์แบบสเลอรีเฟส โดยใช้ตัวเร่งปฏิกิริยาร่วมหลายชนิดเช่น โบเรน ($B(C_6F_5)_3$) โบเรท ($Ph_3CB(C_6F_5)_4$) เมทิลอะลูมิเนียมออกเซน (MAO) เมทิลอะลูมิเนียมออกเซนแห้ง (d-MAO) โมนิฟายเมทิลอะลูมิเนียมออกเซน (MMAO) โมนิฟายเมทิลอะลูมิเนียมออกเซนแห้ง (d-MMAO) ในส่วนแรกการพอลิเมอไรซ์ด้วย ตัวเร่งปฏิกิริยาเทอทาร์บิวทิลอะมิโดไซลิลไดเมทิลฟลูออรีนไททานเนียมไดเมทิล ($[t-BuNSiMe_2Flu]TiMe_2$) การพอลิเมอไรเซชันได้ทำที่ความดันบรรยากาศของเอทิลีนในถังปฏิกรณ์แบบแก้ว จากผลการศึกษาพบว่าชนิดของตัวเร่งปฏิกิริยาร่วมส่งผลกระทบต่อพฤติกรรมของระบบและสมบัติของพอลิเมอร์ที่ได้เช่น โบเรทให้การเข้าร่วมของ 1-เฮกซีน สูงที่สุด นอกจากนี้ ได้ทำการศึกษาผลของตัวทำละลาย 4 ชนิด คือ เฮกเซน โทลูอิน คลอโรเบนซีน และ ไดคลอโรมีเทน โดยใช้ MMAO เป็นตัวเร่งปฏิกิริยาร่วม โดยใช้ระบบการพอลิเมอไรซ์แบบความดันสูง ได้แสดงให้เห็นว่ายิ่งตัวทำละลายมีขั้วมาก ระบบจะมีความว่องไวสูงและพบว่ามีความว่องไวสูงสุดเมื่อใช้โทลูอินเป็นตัวทำละลาย การใช้มอนิเมอร์ที่ในการผลิตพอลิเอทิลีนแบบเชิงเส้นที่มีความหนาแน่นต่ำ (LLDPE) ได้ทำการศึกษาและพบว่า 1-ฮ็อกทีนเป็นโคมอนอเมอร์ที่ดีที่สุดในการบวนการผลิต . นอกจากนั้นได้ทำการเปลี่ยนโครงสร้างของตัวเร่งปฏิกิริยาจาก $[t-BuNSiMe_2Flu]TiMe_2$ เป็นตัวเร่งปฏิกิริยาเทอทาร์บิวทิลอะมิโดไซลิลไดเมทิลเตตระเมทิลไซโคเพนตะไดอินิลไททานเนียมไดเมทิล ($[t-BuNSiMe_2Cp^*]TiMe_2$) เพื่อศึกษาผลของโครงสร้างของตัวเร่งปฏิกิริยาและพบว่าพอลิเมอร์ที่ได้จากการสังเคราะห์ด้วยตัวเร่งปฏิกิริยาระบบแรกมีความสามารถในการเข้าร่วมของแอลฟาโอเลฟินได้ดีกว่าระบบที่สอง พอลิเมอร์ที่ได้ทั้งหมดจะวิเคราะห์ด้วย เครื่องเจลเพอมีเอชันโครมาโตกราฟี (GPC) เครื่องนิวเคลียร์แมกเนติกเรโซแนนซ์ (NMR) และเครื่องดิฟเฟอเรนเชียลสแกนนิ่งแคลอริมิเตอร์ (DSC) เพื่อวัดคุณสมบัติของพอลิเมอร์และ โครงสร้างย่อยของพอลิเมอร์

ภาควิชา.....วิศวกรรมเคมี.....ลายมือชื่อนิสิต..... นพพร อินทรกำจร.....
 สาขาวิชา.....วิศวกรรมเคมี..... ลายมือชื่ออาจารย์ที่ปรึกษา..... *Takeshi Shiono*.....
 ปีการศึกษา 2548 ลายมือชื่ออาจารย์ที่ปรึกษาร่วม..... *Takeshi Shiono*.....

4571809721 : MAJOR CHEMICAL ENGINEERING

KEY WORD: METALLOCENE / COCATALYST / SOLVENT EFFECT / OLEFIN POLYMERIZATION /
STERIC EFFECT

NAWAPORN INTARAGAMJON : COMPARATIVE STUDY OF SOLVENT EFFECT AND
ACTIVATORS WITH TITANOCENE CATALYSTS ON ETHYLENE/ALPHA-OLEFINS
POLYMERIZATION. THESIS ADVISOR : PROF. PIYASAN PRASERTHDAM, Dr.Ing.,
THESIS COADVISOR : PROF.TAKESHI SHIONO D.Eng., 129 pp.
ISBN 974-17-2104-4.

Copolymerizations of ethylene/ α -olefin were investigated with homogeneous Ti-based catalysts. In the first part slurry phase of polymerizations by using various cocatalyst such as, borane ($B(C_6F_5)_3$), borate ($Ph_3CB(C_6F_5)_4$), methylaluminoxane (MAO), dried-methylaluminoxane (d-MAO), modified-methylaluminoxane (MMAO) and dried-modified-methylaluminoxane (d-MMAO) were conducted with [*t*-BuNSiMe₂Flu]TiMe₂ catalyst. Polymerization was conducted in the atmospheric pressure of ethylene by using a glass reactor. It revealed that the types of activators had influence on the polymerization behavior and polymer microstructure, for example borate system gave the highest insertion of 1-hexene. Moreover, the effect of solvent medium was chosen to study. Four solvents were selected: heptane, toluene, chlorobenzene, dichloromethane. To investigate the effect of solvent, polymerization proceeded in a high pressure autoclave system, and it was revealed that the solvent with high polarity showed high activity and the optimum value of dielectric constant was found to be used of toluene. The different kind of co-monomers for linear low density polyethylene (LLDPE) were also investigated in this polymerization system and found that 1-octene exhibited the best co-monomer to produce LLDPE. Moreover, we have modified the catalyst structure form [*t*-BuNSiMe₂Flu]TiMe₂ to [*t*-BuNSiMe₂Cp*]TiMe₂ to investigate the effect of catalyst structure, and found that LLDPE produced from the former system had a better ability for the insertion of α -olefins. All the polymers obtained were characterized by gel permeation chromatography (GPC), nuclear magnetic resonance (NMR) and differential scanning calorimetry (DSC) to observe the polymer properties and polymer microstructure.

Department...Chemical EngineeringStudent's signature.....*N. Intaragamon*

Field of study...Chemical Engineering.....Advisor's signature.....*P. Praserttham*

Academic year 2005..... Co-advisor's signature.....*T. Shiono*

ACKNOWLEDGEMENTS

I would like to give special recognition to Professor Dr. Piyasan Praserttham, my advisor, and Professor Takeshi SHIONO, co-adviser, for their generosity in providing guidance and sharing their idea on the interesting work. Their advice is always worthwhile and without him this work could not be possible.

I wish to thank Asst. Prof. Dr. Montri Wongsri chairman of the committee and all of the members of the examining committee including Asst. Prof. Dr. Meundeun Phisalaphong, Asst. Prof. Dr. Bunjerd Jongsomjit and Dr. Chariya Chao for their valuable guidance and revision throughout my thesis. Especially Asst. Prof. Dr. Bunjerd Jongsomjit who always corrected for my English and gave a great recommendation for writing strategy.

Sincere thanks are given to the Thailand Research Fund (TRF), the AIEJ scholarship and financial support in Japan and the graduate school and department of chemical engineering at Chulalongkorn University for the financial support of this work.

I wish to thank the staff of SUITOMO chemical (Japan); Yuki Iseki, Satoru Hosoda, who assisted me to measure the ^{13}C -NMR of my sample.

I wish to extend my thanks to the chemical resource Ikeda-Shiono laboratory, Tokyo Institute of Technology: Prof. Tomaki Ikeda who concerned me and thanks for so warm farewell party. Miss. Ikeda, Miss. Murase, Mr. Cai, Mr. Sukimoto, Mr. Okada, Mr. Hasan, Mr. Nishii to take care and look after me while I was spending my time in Japan including all of my friends in Japan: Mr. Cha, Mr. Bang, Miss. Num, Miss. Wang and everybody in Ikeda-Shiono Laboratory and all Thai students at the Tokyo Institute of Technology for giving me strength and encouragement.

And for my friend, Mr. Sutti to discuss the problem with me, Mr. Pichet, Miss. Aumpaipan, Mr. Sonti and Mr. Kitti to participate in measuring DSC. Miss. Nattinee, Miss. Lerdlusana, Mr. Satit, Miss. Tidarat for support. And all freshmen students in ZM group especially Miss. Chanintorn encouraged me and corrected my document. And the unforgettable person in our lab.

Finally, I would like to express my parents and family and sisters for their tremendous support and overwhelming encouragement.

CONTENTS

	Page
ABSTRACT(IN THAI)	iv
ABSTRACT(IN ENGLISH)	v
ACKNOWLEDGMENTS	vi
CONTENTS	vii
LIST OF TABLES	xi
LIST OF FIGURES	xii
CHAPTER I INTRODUCTION	1
CHAPTER II LITERATURE REVIEWS	5
2.1 Classification of polyethylene.....	5
2.2 General aspect of metallocene.....	6
2.2.1 Metallocene.....	7
2.2.2 Cocatalysts.....	10
2.2.3 Mechanism.....	13
2.2.3.1 Mechanism of polymerization.....	13
2.2.3.2 Chain transfer mechanism.....	15
2.2.3.3 Mechanism of catalyst deactivations.....	17
2.3 Classification of metallocene catalyst systems.....	19
2.3.1 Homogeneous metallocene catalyst with Aluminoxane systems.....	20
2.3.2 Homogeneous metallocene catalyst with Lewis base Activators systems.....	20
2.3.3 Supported metallocene system.....	21
2.4 Effect of polymerization parameters to characteristic of polymer.....	22
2.4.1 Effect of substitute ligand and center metal atom.....	22
2.4.2 Effect of cocatalysts and/or activators.....	25
2.4.3 Effect of solvent medium.....	26
CHAPTER III EXPERIMENTAL	27
3.1 Objective.....	27
3.2 Scope of investigation.....	27
3.3 Experimental.....	28

	Page
3.3.1 Material.....	28
3.3.2 Equipments.....	30
3.3.2.1 Cooling system.....	30
3.3.2.2 Inert gas supply.....	30
3.3.2.3 Magnetic stirrer and heater.....	31
3.3.2.4 Reactors.....	31
3.3.2.5 Schlenk line.....	31
3.3.2.6 Schlenk tube.....	32
3.3.2.7 Vacuum pump.....	33
3.3.2.8 Polymerization line.....	33
3.3.3 Catalyst synthesis.....	33
3.3.3.1 Synthesis of t-BuNHSiMe ₂ FluH.....	33
3.3.3.2 Synthesis of [t-BuNSiMe ₂ Flu]TiMe ₂	34
3.3.3.3 Synthesis of t-BuNHSiMe ₂ C ₅ HMe ₄	35
3.3.3.4 Synthesis of [t-BuNSiMe ₂ C ₅ Me ₄]TiMe ₂	35
3.3.4 Preparation of d-MAO and d-MMAO.....	36
3.3.5 Polymerization procedure.....	37
3.3.5.1 Atmospheric pressure semibatch system.....	37
3.3.5.2 High pressure autoclave system.....	37
3.3.6 Characterization methods.....	37
3.3.6.1 Gel Permeation Chromatography (GPC).....	38
3.3.6.2 Nuclear magnetic resonance spectroscopy (NMR).....	38
3.3.6.3 Differential Scanning Calorimeter (DSC).....	38
CHAPTER IV EFFECT OF COCATALYST.....	39
4.1 Ethylene/1-hexene polymerization results.....	40
4.2 Discussion of polymer microstructure.....	44
4.3 Summary.....	45
CHAPTER V EFFECT OF SOVENT MEDIUM.....	46
5.1 Effect of solvent on the catalytic activity.....	46
5.2 Polymer microstructure.....	53
5.3 Thermal properties.....	54

	Page
5.4 Summary.....	55
CHAPTER VI EFFECT OF SECOND MONOMER.....	56
6.1 Effect of α -olefin comonomer on productivity.....	57
6.2 Polymer microstructure.....	61
6.3 Thermal analysis of the polymer.....	63
6.4 Summary.....	64
CHAPTER VII EFFECT OF CATALYST STRUCTURE.....	65
7.1 Effect of solvent on the catalytic activity.....	65
7.2 Polymer microstructure.....	71
7.3 Thermal properties.....	74
7.4 Summary.....	74
CHAPTER VIII CONCLUSIONS AND RECOMMENDATIONS.....	75
8.1 Conclusions.....	75
8.1.1 Effect of cocatalysts.....	75
8.1.2 Effect of solvents.....	75
8.1.3 Effect of second monomers.....	76
8.1.4 Effect of catalyst structure.....	76
8.2 Recommendations.....	77
REFERENCES.....	78
APPENDICES	
APPENDIX A. GEL PERMEATION CHROMATROGRAPHY.....	87
APPENDIX B. NUCLEAR MAGNETIC RESONANCE.....	98
APPENDIX C. DIFFERENTIAL SCANNING CALORIMETER.....	118
APPENDIX D. CALUCATION OF POLYMER PROPERTIES.....	125
VITA.....	129

LIST OF TABLES

Table	Pages
2.1 Density range, molecular structure, synthesis, and applications of various type polyethylenes.....	6
4.1 Results of polymerization of ethylene/1-hexene polymerization with catalyst 1	41
4.2 Triad distribution of ethylene/1-hexene copolymer.....	43
4.3 Relative reactivity value of ethylene and 1-hexene.....	44
5.1 Polymerization results.....	47
5.2 Solubility of ethylene in different solvents obtained from this study.....	51
5.3 Triad distribution of copolymer obtained from ¹³ C NMR.....	54
5.4 Monomer incorporation and the reactivity ratio.....	55
5.5 Melting temperature and % crystallinity of polymer produced.....	56
6.1 Polymerization results.....	58
6.2 Triad distribution of copolymer.....	62
6.3 Monomer incorporation and its structure.....	62
7.1 Polymerization results with CGC/MMAO system.....	66
7.2 Triad distribution of copolymer obtained from ¹³ C NMR.....	72
7.3 Monomer incorporation and the reactivity ratios.....	73
7.4 Melting temperature and % crystallinity of polymer produced.....	73

LIST OF FIGURES

Figure	Page
2.1 Typical chemical structure of a metallocene catalyst	8
2.2 Schematic representations of metallocene symmetry.....	9
2.3 Several kinds of MAO.....	10
2.4 Proposed structure of MAO.....	11
2.5 Cossee mechanisms for Ziegler-Natta olefin polymerization.....	13
2.6 Types of olefin polymer tacticity.....	14
2.7 Chain transfer via β -H elimination.....	15
2.8 Chain transfer via β -Me elimination.....	16
2.9 Chain transfer to aluminum.....	16
2.10 Chain transfer to monomer.....	17
2.11 Chain transfer to hydrogen.....	17
2.12 Mechanism showing the deactivation of active center.....	18
2.13 Mechanism of reversible second-order deactivation.....	19
2.14 Bridging moiety on bite angle in zirconium dichloride complexes.....	23
2.15 2-substitute catalyst, bis(2-Rindenyl)zirconium dichloride.....	24
3.1 Inert gas supply system.....	31
3.2 Schlenk line.....	32
3.3 Schlenk tube.....	32
3.4 Diagram of system in slurry phase polymerization.....	33
4.1 Ethylene rate consumption profile of ethylene/1-hexene copolymerization with catalyst 1 / activators.....	42
4.2 Ethylene rate consumption profile of ethylene polymerization with catalyst 1 / activators.....	42
5.1 Ethylene consumption rate for ethylene/1-hexene copolymerization with various solvent mediums at 70°C.....	48
5.2 Ethylene consumption rate for ethylene polymerization with various solvent medium at 70 °C.....	48
5.3 Ethylene consumption rate for ethylene/1-hexene . copolymerization with various solvent mediums at 0°C.....	49

	Page
5.4 Ethylene consumption rate for ethylene polymerization with various solvent mediums at 0°C.....	49
6.1 Ethylene rate consumption profile of ethylene/ α -olefin copolymerization and ethylene polymerization at 70 °C.....	59
6.2 Ethylene rate consumption profile of ethylene/ α -olefin copolymerization and ethylene polymerization at 0 °C.....	59
7.1 Ethylene rate consumption profile of ethylene/1-hexene copolymerization with various solvent of CGC/MMAO at 70 °C.....	68
7.2 Ethylene rate consumption profile of ethylene polymerization with various solvent of CGC/MMAO at 70 °C.....	68
7.3 Ethylene rate consumption profile of ethylene/1-hexene copolymerization with various solvent of CGC/MMAO at 0 °C.....	69
7.4 Ethylene rate consumption profile of ethylene polymerization with various solvent of CGC/MMAO at 0 °C.....	69
A1 GPC curve of ethylene/1-hexene copolymerization with catalyst1/d- MAO at 40 °C.....	88
A2 GPC curve of ethylene/1-hexene copolymerization with catalyst1/MAO at 40 °C.....	88
A3 GPC curve of ethylene/1-hexene copolymerization with catalyst1/MMAO at 40 °C.....	89
A4 GPC curve of ethylene/1-hexene copolymerization with catalyst1/d- MMAO at 40 °C.....	89
A5 GPC curve of ethylene/1-hexene copolymerization with catalyst1/Borate at 40 °C.....	90
A6 GPC curve of ethylene with catalyst1 1. MAO 2. d-MAO 3. Borate cocatalyst at 40 °C.....	90
A7 GPC curve of ethylene/1-hexene copolymerization with catalyst1/MMAO in heptane at 70 °C.....	91
A8 GPC curve of ethylene/1-hexene copolymerization with catalyst1/MMAO in toluene at 70 °C.....	91

	Page
A9 GPC curve of ethylene/1-hexene copolymerization with catalyst1/MMAO in chlorobenzene at 70 °C.....	92
A10 GPC curve of ethylene polymerization with catalyst1/MMAO in heptane at 70 °C.....	92
A11 GPC curve of ethylene polymerization with catalyst1/MMAO in toluene at 70 °C.....	93
A12 GPC curve of ethylene polymerization with catalyst1/MMAO in chlorobenzene at 70 °C.....	93
A13 GPC curve of ethylene/1-octene copolymerization with catalyst1/MMAO in heptane at 70 °C.....	94
A14 GPC curve of ethylene/1-decene copolymerization with catalyst1/MMAO in heptane at 70 °C.....	94
A15 GPC curve of ethylene/1-hexene copolymerization with catalyst2/MMAO in heptane at 70 °C.....	95
A16 GPC curve of ethylene/1-hexene copolymerization with catalyst2/MMAO in toluene at 70 °C.....	95
A17 GPC curve of ethylene/1-hexene copolymerization with catalyst2/MMAO in chlorobenzene at 70 °C.....	96
A18 GPC curve of ethylene polymerization with catalyst2/MMAO in heptane at 70 °C.....	96
A19 GPC curve of ethylene polymerization with catalyst2/MMAO in toluene at 70 °C.....	97
A20 GPC curve of ethylene polymerization with catalyst1/MMAO in chlorobenzene at 70 °C.....	97
B1 ¹³ C-NMR spectrum of ethylene/1-hexene copolymer with catalyst 1/d-PMAO system at 40 °C.....	99
B2 ¹³ C-NMR spectrum of ethylene/1-hexene copolymer with catalyst 1/d-MMAO system at 40 °C.....	100
B3 ¹³ C-NMR spectrum of ethylene/1-hexene copolymer with catalyst 1/MMAO system at 40 °C.....	101
B4 ¹³ C-NMR spectrum of ethylene/1-hexene copolymer with catalyst 1/Borate system at 40 °C.....	102

	Page
B5	¹³ C-NMR spectrum of ethylene/1-hexene copolymer with catalyst 1/MMAO in heptane at 70 °C.....103
B6	¹³ C-NMR spectrum of ethylene/1-hexene copolymer with catalyst 1/MMAO in toluene at 70 °C.....104
B7	¹³ C-NMR spectrum of ethylene/1-hexene copolymer with catalyst 1/MMAO in chlorobenzene at 70 °C.....105
B8	¹³ C-NMR spectrum of ethylene/1-hexene copolymer with catalyst 1/MMAO in heptane at 0 °C.....106
B9	¹³ C-NMR spectrum of ethylene/1-hexene copolymer with catalyst 1/MMAO in toluene at 0 °C.....107
B10	¹³ C-NMR spectrum of ethylene/1-hexene copolymer with catalyst 1/MMAO in chlorobenzene at 0 °C.....108
B11	¹³ C-NMR spectrum of ethylene/1-octene copolymer with catalyst 1/MMAO in heptane at 70 °C.....109
B12	¹³ C-NMR spectrum of ethylene/1-octene copolymer with catalyst 1/MMAO in heptane at 0 °C.....110
B13	¹³ C-NMR spectrum of ethylene/1-decene copolymer with catalyst 1/MMAO in heptane at 70 °C.....111
B14	¹³ C-NMR spectrum of ethylene/1-decene copolymer with catalyst 1/MMAO in heptane at 0 °C.....112
B15	¹³ C-NMR spectrum of ethylene/1-hexene copolymer with catalyst 2/MMAO in heptane at 70 °C.....113
B16	¹³ C-NMR spectrum of ethylene/1-hexene copolymer with catalyst 2/MMAO in toluene at 70 °C.....114
B17	¹³ C-NMR spectrum of ethylene/1-hexene copolymer with catalyst 2/MMAO in chlorobenzene at 70 °C.....115
B18	¹³ C-NMR spectrum of ethylene/1-hexene copolymer with catalyst 2/MMAO in heptane at 0 °C.....116
B19	¹³ C-NMR spectrum of ethylene/1-hexene copolymer with catalyst 2/MMAO in toluene at 0 °C.....117
C1	DSC scanning of Ethylene/1-hexene copolymer with catalyst 1/MMAO In heptane at 70° C.....119

	Page
C2 DSC scanning of Ethylene/1-hexene copolymer with catalyst 1/MMAO in toluene at 70° C.....	119
C3 DSC scanning of Ethylene/1-hexene copolymer with catalyst 1/MMAO in chlorobenzene at 70° C.....	120
C4 DSC scanning of Ethylene/1-octene copolymer with catalyst 1/MMAO In heptane at 70° C.....	120
C5 DSC scanning of Ethylene/1-decene copolymer with catalyst 1/MMAO In heptane at 70° C.....	121
C6 DSC scanning of polyethylene with catalyst 1/MMAO in heptane at 70° C.....	121
C7 DSC scanning of polyethylene with catalyst 1/MMAO in toluene at 70° C.....	122
C8 DSC scanning of polyethylene with catalyst 1/MMAO in chlorobenzene at 70° C.....	122
C9 DSC scanning of polyethylene with catalyst 2/MMAO in heptane at 70° C.....	123
C10 DSC scanning of polyethylene with catalyst 2/MMAO in toluene at 70° C.....	123
C11 DSC scanning of polyethylene with catalyst 1/MMAO in chlorobenzene at 70° C.....	124

CHAPTER I

INTRODUCTION

Nowadays, polymer and plastics are playing the important role on the material industry. Since their physical properties such as, toughness, strength, low density and resistance to corrosion have enabled them to replace the metal in construction of household tools and create comforts. Otherwise the demands for the plastics increase in huge quantities every year [1]. Among synthetic polymers, polyethylene is the major polymer and the largest of production in plastic industry. [2, 3]. Thus, it has chemical stability and great range of physical properties, polyethylene is the large usage polymer in many kind of industry such as from the strong flexible films and coating to rigid containers. It is the variations in molecular structure that results in this range of physical properties. The first step of development occurred in the ability to control the molecular weight in the commercial scale of ethylene production in 1930s [4]. In 1970s, the industrial scale of linear low density polyethylene (LLDPE) was commercialized [5]. The development of industrial LLDPE has the largest going rate in all type of polyethylene production until present. [6,7]

In the pioneer generation of ethylene polymerization, polyethylene was produced from the free radical initiation of high pressure process. The low pressure process was developed and invented by using metal alkyls as catalyst [8]. Karl Ziegler et al. (1953) [8] discovered a catalyst for ethylene polymerization in mild conditions, and Giulio Natta et al. (1955) [9] adapted this catalyst for propylene polymerization. With this catalyst we call Ziegler-Natta catalyst, ethylene polymerization can be conducted at the low pressure and low temperature system ($P < 2 \text{ MPa}$, $T = 60\text{-}100 \text{ }^\circ\text{C}$) compared with the free radical process at high pressure and high temperature ($P = 300 \text{ MPa}$, $T = 300 \text{ }^\circ\text{C}$). In the early decade, Ziegler-Natta catalyst consisted of a transition metal compound as an active component and alkyl or hydride of main group element as a cocatalyst. TiCl_3 was chosen to be active component and triethylaluminum (AlEt_3) was used to be a cocatalyst. The next evolution of Ziegler-Natta catalyst is based on electron donor-containing MgCl_2 -supported Ziegler-Natta catalyst system, which shows about 100 times higher activity

than the conventional Ziegler-Natta catalyst. At the beginning, the improvement of catalyst was tending to increase the activity of HDPE by charging a third component, such as, electron donor or Lewis base. The next development of Ziegler-Natta catalyst has been concentrated on the copolymerization ability to produce LLDPE. Unfortunately, the third generation of Ziegler-Natta catalyst was limited by the heterogeneous nature of active species to give nonuniform copolymer with broad molecular weight distribution. The fourth generation of Ziegler-Natta catalyst was paid attention to improve the properties, such as heteroplastics, olefin copolymers, reactor blends, multiphase alloys, and non-olefin grafted polyolefin alloys in the production process.

The next step of development on the polyolefin industry was the introduction of metallocene catalysts. The general aspect of metallocene catalysts consist of the transition metal group IV (Ti, Zr and Hf) which was sandwiched between parallel planner two organic molecules, such as cyclopentadienyl group (Cp, C₅H₅), including those substitute of Cp group such as, indenyl (Ind), fluorenyl (Flu). The first metallocene catalyst was invented by Giulio Natta and Ronald Breslow [11] in 1957. The catalyst was bis(cyclopentadienyl)titanium dichloride (Cp₂TiCl₂) activated with alkylaluminum chloride (AlR₂Cl). At first, these catalysts were generating the low activity of polymerization for ethylene. In 1980, Kaminsky et al. explored that a small amount of water greatly increased the activity of metallocene catalyst with trimethylaluminum (TMA) as the cocatalyst. This result is due to the formation of methylaluminoxane (MAO); the hydrolysis product of TMA.

The Ziegler-Natta and metallocene catalysts have one clear difference in the characteristic of active sites. Since the Ziegler-Natta catalysts were the heterogeneous catalyst and contain a variety of active site swchich are different in propagation rate, stereospecificity, monomer reactivity ration, etc., we call them multi-site catalysts [8]. In the contrary, metallocene catalysts are homogeneous catalyst. Every active site in the catalyst plays the same characteristic in polymerization. Therefore, metallocene catalysts are referred to a single site catalyst and offer the potential advantages over the traditional multi site Ziegler-Natta catalysts. The major ability of metallocene catalyst is controlling the polymer structure and properties by variation of catalyst structure. Furthermore, these catalyst can fix the disadvantage of Ziegler-Natta

catalyst such as, low comonomer insertion, low molecular weight and broad molecular weight distribution, caused by multi site catalyst [12].

Due to the numerous advantage of metallocene catalyst, the research and development of metallocene catalyst was growing very fast in this decade. One branch of exploring on the catalyst has been concentrated on the polymerization ability of LLDPE, because the difference in polymer microstructure affects polymer properties such as, melting and glass transition temperatures, melt viscosity, and mechanical and optical properties, all of which define the type and useful range of application of LLDPE in material industry.

At present, many studies have paid attention to the polymerization ability to study the effect of polymer microstructure to the polymer properties. Polymerization ability depends on several reasons such as, the ligand of catalyst structure, the geometry of catalyst and the cocatalyst which might take part in the formation of bimetallic active species. Many points still remain broadly open research and development to use for the polyolefin industry in the future.

In this thesis was divided to eight chapters. Chapter I involved an overview of the use of metallocene catalyst for the polyolefin industry. In Chapter II, knowledge and open literature dealing with metallocene catalysis for olefin polymerization were presented. The literature review was accentuated metallocene catalyst system used for copolymerization of ethylene with α -olefins and also the major parameter that can alter the properties of polymer and further on the microstructure such as, effect of cocatalyst, effect of solvents, effect of second monomer and effect of catalyst structures. The experimental procedure as well as the instrument and techniques used for characterizing the resulting polymers were also described in Chapter III. Moreover, in this chapter, the most important data: the procedure of catalyst synthesized was reported. The obtained polymer in all experiment was characterized by using differential scanning calorimetry (DSC), gel permeation chromatography (GPC) and ^{13}C -nuclear magnetic resonance (^{13}C -NMR)

In Chapter IV, the results on ethylene and α -olefins copolymerization with the different of co-catalyst were presented. Effects of various activators in ethylene/1-hexene, comonomer impact on nature of active site on the catalyst content in the copolymer. Effect of system between homopolymer and copolymer can be changed other polymer properties.

In Chapter V, the effect of solvent medium were reported with the different structure and polarity of solvent, it could altered the formation of the active species. Thus polymerization activities and polymer microstructure of the produced polymer from various kind of solvent were investigated.

In Chapter VI, the result of ethylene/1-olefins were report. Chaging the second monomer from 1-hexene to 1-octene and 1-decene, polymerization was study on heptane solvents. From the result it revealed that with the different of second monomer applied to the LLDPE production system will obtain the different in ethylene incorporation on the polymer backbone.

In Chapter VII, one of the most important parameter in these study. The catalyst strucure was altered by changing the ligand of the catalyst from the above chapter(Flurine system) to the Cp* as constrain geometry catalyst (CGC). The result of polymerization, polymer microstructure and thermal properties of polymer were reported in this chapter.

Finally, conclusions of this work and some recommendations for future research work were provided in Chapter VIII.



สถาบันวิทยบริการ
จุฬาลงกรณ์มหาวิทยาลัย

CHAPTER II

LITERATURE REVIEW


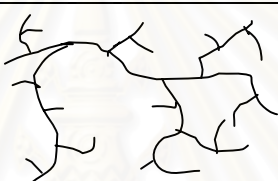
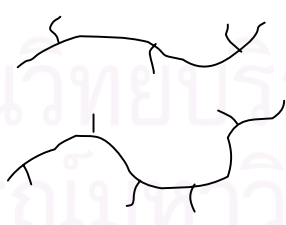
2. Studying in metallocene catalyst polymerization

2.1 Classification of polyethylene

Polyethylene (PE) is the most important material in plastic and polymer type. Normally, polyethylene is classified to three type according to its density and structure, high density polyethylene (HDPE), low density polyethylene (LDPE) and linear low density polyethylene (LLDPE). The numerous studies show that the global market of LLDPE was increased in very interesting rate about 10 % per annum [13]

Table 2.1 summarized the characteristic of three type of polyethylene. The different in structure of polymer affects to the physical properties of polymer i.e. density of polymer and hence the application of polymer. HDPE is the polymer that has very less or does not have any branch in the polyethylene backbone. From this microstructure HDPE has very high crystalline phase in polymer morphology and highest density about 0.96 g/cm^3 . Polyethylene which has many long and short chain branching formed by radical process is LDPE. The amount of long chain branching (LCB) and short chain branching (SCB) also affect the crystalline and others physical properties too. Normally, long chain branching has the main effect on the polymer viscosity and melt rheology due to the molecular size and shape. On the other hands, short chain branching has the influence to polymer morphology and solid state properties of polyethylene. LLDPE was produced by the copolymerization of ethylene and α -olefins such as propylene, 1-butene, 1-hexene and 1-octene. Mostly, side chain in LLDPE distributed in short chain branching type by non-uniformly with linear microstructure of backbone polyethylene chain. The properties of LLDPE such as, thermal, physical and mechanical properties depend on the distribution of short chain in the copolymer and polymer microstructure (triad and dyad distribution). Thus, the several LLDPE grades are classified by the primarily result via microstructure of polymer and molecular weight of polymer.

Table 2.1 Density range, molecular structure, synthesis, and applications of various type polyethylenes. [13]

Type of PE	Density (g/cm ³)	Molecular structure	Synthesis	Common uses
HDPE	0.945-0.965		Polymerization of ethylene on Philips, Ziegler-Natta and metallocene catalyst	Gas pipe, car gas tanks, bottles, rope and fertilizer bag
LDPE	0.890-0.940		Free radical polymerization of ethylene at high temperature and high pressure	Packing film, bags, wire, sheathing, pipes, waterproof membrane
LLDPE (VLDPE,ULDPE)*	0.910-0.925		Copolymerization of ethylene with α -olefins on Ziegler-Natta and metallocene catalysts	Shopping bag, stretch wrap, greenhouse film

* A family of LLDPE with density of 0.87-0.915 g/cm³

2.2 General aspects of metallocene

One of the greatest challenges in organometallic complex is to synthesize the metallocene complex and apply for new polymerization technology with transition group IV metals. Metallocene complexes are become an important class of polymerization catalyst in the research and industrial area since it have many advantage in polymerization such as [14],

1. The homogeneous nature of catalysts provides the active sites that have the great number of activity in olefin polymerization. Comparison to conventional Ziegler-Natta catalyst or Philips catalyst, it was found that metallocene complex gave the higher activity about 100 times.
2. Metallocene catalysts have ability to control the stereoregularity (isotactic, atactic, syndiotactic and hemitactic polypropylene) of the polymers produced from prochiral olefins, such as propylene
3. According from the narrow molecular weight distribution of polymer about 1-2, we can call metallocene catalyst as single site catalysts.
4. Their potential for producing polyolefin with regularly distributed short and long chain branches in the polymer chain. These parameters determine the properties of new materials for applications i.e. LLDPE and thus generate new markets.
5. Heterogeneous catalyst provide the different active sites than those in solution and can have an enormous effect on catalyst activity and the properties of the produced polyolefins in term of molecular weights, branching and stereospecificity.

2.2.1 Metallocene

Metallocene catalysts are the organometallic coordination compounds in which one or two π -carbocyclic ligands such as cyclopentadienyl ring, substituted cyclopentadienyl ring, or derivative of cyclopentadienyl ring (such as fluorenyl and indenyl etc.) are bonded to central transition metal atom. The cyclopentadienyl ring of metallocene singly bonded to the ring-metal bond is not centered on any one of the five

carbon atoms in the ring but equally on all of them [15]. The typical structure of a metallocene catalyst is represented by Figure 2.1 where M is the group 4B, 5B, or 6B transition metal, normally group 4B (Ti, Zr and Hf); A is an optional bridging atom usually Si or C atom; R is a σ -homoleptic hydrocarbyl such as H, alkyl, or other hydrocarbon groups; and X is chlorine or other halogens from group 7A or an alkyl group. The cyclopentadienyl ligands, halides and σ -homoleptic hydrocarbyl represent the three classes of ligands of the metallocene catalysts and variation of, and/or substitutions within some of these ligands could result in variation of the catalytic activity, polymer stereoregularity, and average molecular mass. In case of metallocene catalyst, which have only one π -carbocyclic ligand with a hetero atom that is attached to the bridging atom.



Figure 2.1 Typical chemical structure of a metallocene catalyst

Compositions and types of metallocene have several varieties. When the two cyclopentadienyl (Cp) rings on either side of the transition metal are unbridged, the metallocene is non-stereorigid and it is characterized by C_{2v} - symmetry. The Cp_2M (M = metal) fragment is bent back with the centroid-metal-centroid angle θ about 140° due to the interaction with the other two σ bonding ligands [16]. When the Cp rings are bridged (two Cp rings arranged in the chiral array and connected together with chemical bonds by a bridging group), the stereorigid metallocene, called ansa-metallocene, could be characterized by either a C_1 , C_2 or C_s symmetry depending upon the substitutions on two Cp rings and the structure of the bridging unit as schematically illustrated [17] in the figure 2.2

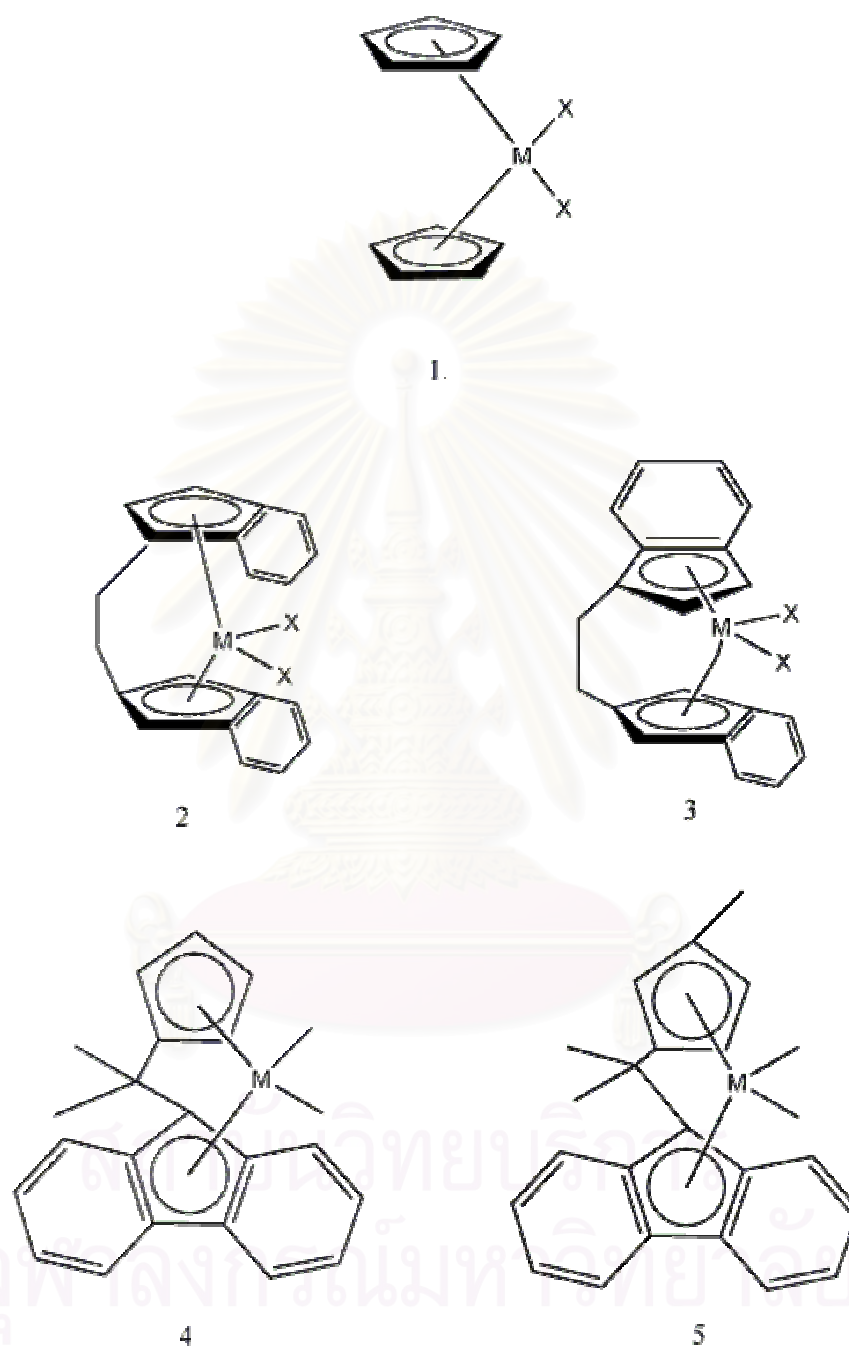


Figure 2.2 Schematic representations of metallocene symmetry (Type 1: C_{2v} -symmetric, Type 2: C_2 -Symmetric, Type 3 and Type 4: C_s -symmetric, Type 5: C_1 -symmetric)(C, italic. It is better to draw all the structures in a similar way)

2.2.2 Cocatalyst

Aluminoxane, especially methylaluminoxane (MAO) plays the very important role to activate metallocene catalyst. Before the MAO was discovered, in Ziegler-Natta catalyst alkylaluminumchloride was used to activate Cp_2TiCl_2 but it exhibited the very poor activity. Using of MAO as cocatalyst can promote the productivity of polymerization by several order of magnitude. Otherwise using of MAO, the other aluminoxanes such as, ethylaluminoxane (EAO) or iso-buthylaluminoxane (iBAO) or modified methylaluminoxane was employed to use as cocatalyst too. (Structure of MAO, EAO, iBAO and MMAO was shown in **Figure 2.3**)

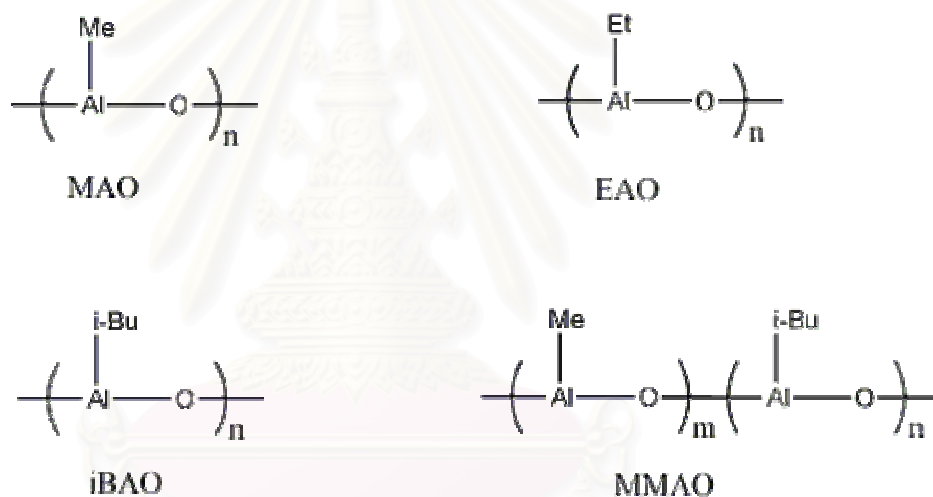


Figure 2.3 several kinds of MAO

MAO $\left[\text{-Al}(\text{Me})\text{O-} \right]_n$, $n = 5-20$, one of oligomeric alkylaluminoxane, is generated by controlled hydrolysis of AlMe_3 by crystal water of $\text{CuSO}_4 \cdot 5 \text{H}_2\text{O}$, $\text{MgCl}_2 \cdot 6\text{H}_2\text{O}$ or $\text{Al}_2(\text{SO}_4)_3 \cdot 14-18\text{H}_2\text{O}$ [18, 19]. Although several researchers have made a lot of effort to clarify the structure and functions of MAO, the details are still open to discussion. Attempts were, of course, made to elucidate the MAO structure, e.g. with the help of size exclusion chromatography, NMR, mass balance and phase separation experiments. The structure of MAO can, however, only be postulated as follow.

The proposed structures of MAOs now have several models, not only 1-dimensional model but also 2-dimension model and 3-dimensional model too. For the simple 1-dimensional models, linear chain, cyclic chain structures are shown in figure 2.4. [20] Moreover Sinn et. al proposed the 3-dimensional model structure, in which MAO was based on structural similarities with tert-buthylaluminoxanes with cage structure and a major component of MAO contain hexamethyltetraaluminoxane $[Al_4O_3(CH_3)_6]_4$

However, now, several kinds of MAO structure have been proposed but the exact model of MAO is still unknown. Because of the multiple equilibriums are present in MAO solution, and residual $AlMe_3$ in MAO solutions would participate in the interconversion of various MAO oligomers.

Naturally, the size and structure of MAO depend on the dynamic equilibrium of them. It has molecular weight around 900-1000 g/mol for commercial in toluene solution.

Except the organoaluminum compounds described above, some of organoborane compound or lewis acid e.g. $B(C_6F_5)_3$ (Borane), $Ph_3CB(C_6F_5)_4$ (Borate) and $PhMe_2NHB(C_6F_5)_4$ have been discovered that it could be employed as cocatalyst too.

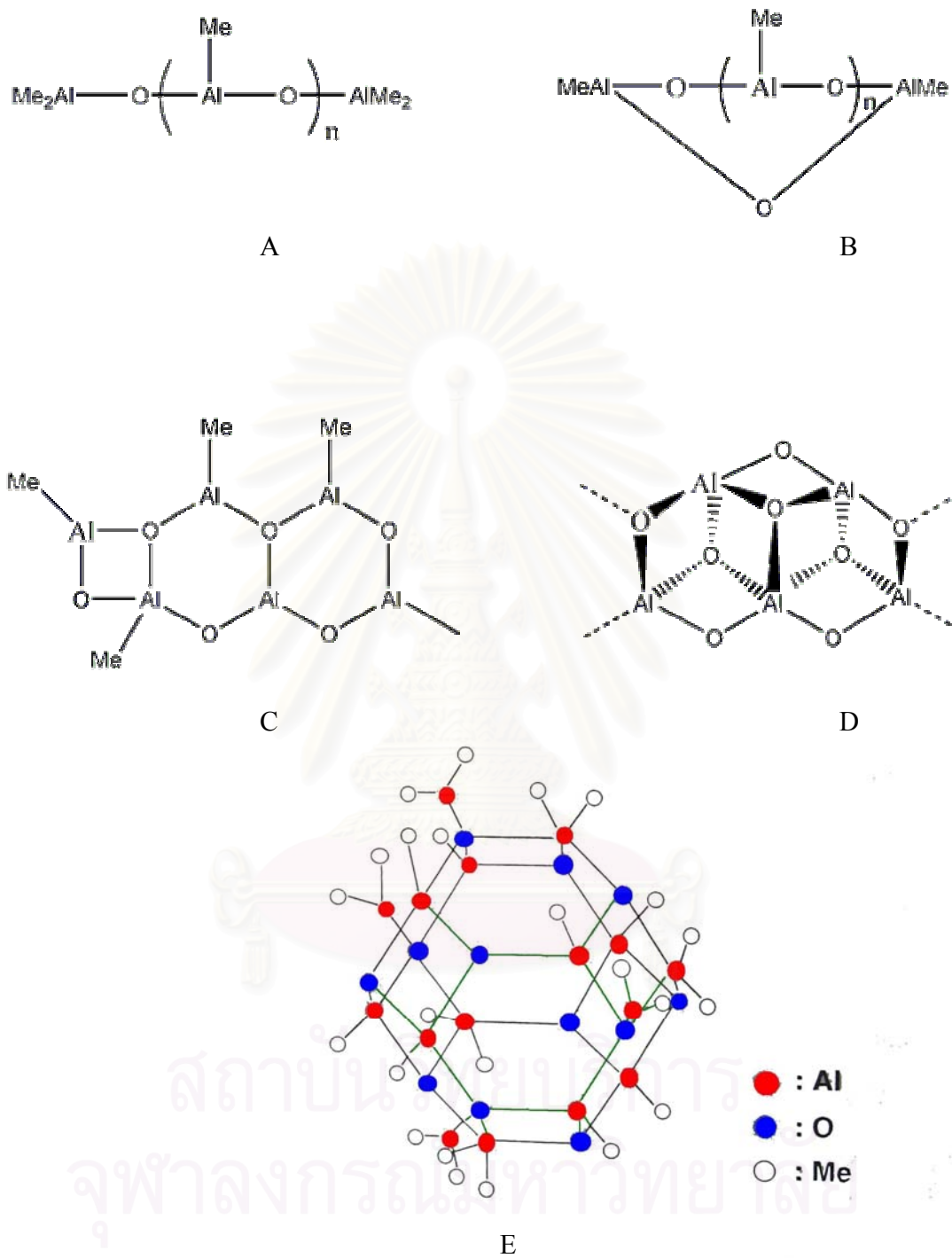


Figure 2.4 Proposed structures of MAO [20]

2.2.3 Mechanism

2.2.3.1 Mechanism of polymerization

The mechanisms for olefin polymerization by metallocene-aluminoxane system have been picked up to investigate in several experiment and theoretical study. [21-25] These study have shown that the Cossee mechanism of polymerization is indeed viable for metallocene catalysts (Figure 2.5). In the cationic metallocene species, the metal atom is coordinated with the π -ligands and alkyl group (growing polymer chain). During polymerization, the monomer coordinates with a highly electrophilic and coordinatively unsaturated cationic complex. It is followed by insertion of a monomer in the metal-carbon bond to produce a polymer chain. The migration of the polymer chain, P, and the formation of the metal-carbon bond occur in concert through a four center transition state. These results in a new vacant coordination site which was originally occupied by the polymer chain. These processes involving shifting of the growing chain to the position previously occupied by a coordinated monomer continue until termination of polymer chain.

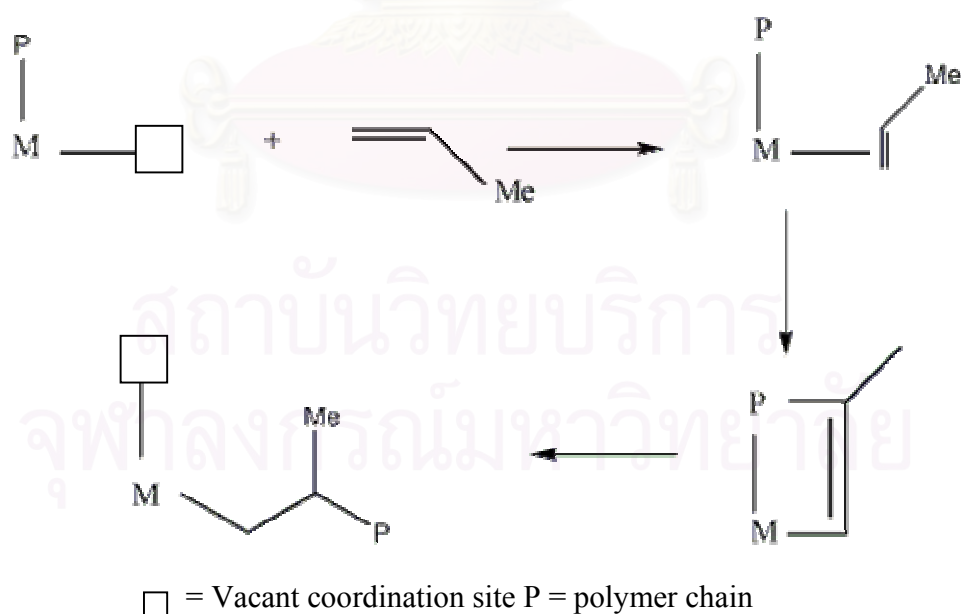


Figure 2.5 Cossee mechanisms for Ziegler-Natta olefin polymerization [21]

The other one more advantage of metallocene catalyst in α -olefin polymerization is the ability to control the stereoregularity of polymer. Propylene polymerization by metallocene catalyst can produce in four types of polypropylene (atactic, isotactic, syndiotactic and hemitactic) [26] (Figure 2.6). In order to control the stereospecificity 2 types of mechanism are present, i.e., stereo control via the chirality of catalyst (catalyst side control) and stereo control due to the last insert monomer unit (chain end control). Ewen et al. [27] reported that a bridged metallocene catalyst $\text{Me}_2\text{C}(\text{3-MeC}_5\text{H}_3)(9\text{-Fluorenyl})\text{ZrCl}_2/\text{MAO}$ produced the hemiisotactic PP, whereas the substitute of cyclopentadienyl ring at third position with H and t-Bu gave the stereospecificity in syndiotactic and isotactic instead. From this evidence we could say that metallocene catalyst can be used to control the stereospecificity in propylene polymerization.

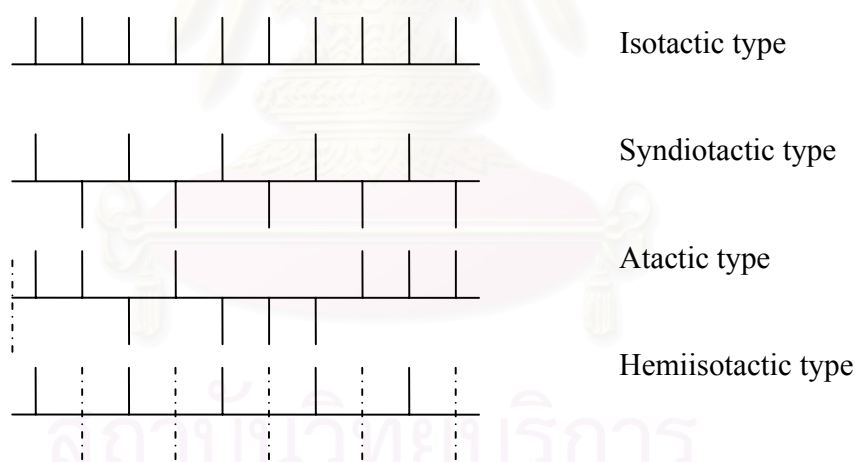


Figure 2.6 Types of olefin polymer tacticity

2.2.3.2 Chain transfer mechanism

One important reaction in polymerization of metallocene catalyst is chain transfer and chain termination reaction. Chain termination reaction can occur due to many reasons, such as chain transfer to β -H elimination (Figure 2.7) [28], chain transfer to β -Me elimination reaction (Figure 2.8) [29], chain transfer reaction to aluminum (Figure 2.9) [30], chain transfer to monomer (Figure 2.10) [31] and chain transfer to hydrogen (Figure 2.11) [32]. Metallocene catalyst and activator used in each system has the different characteristic of behavior in polymerization. Resconi et.al [33] reported that chain transfer reaction depended on the metallocene catalyst, aluminoxane and polymerization condition employed to the system in propylene polymerization.

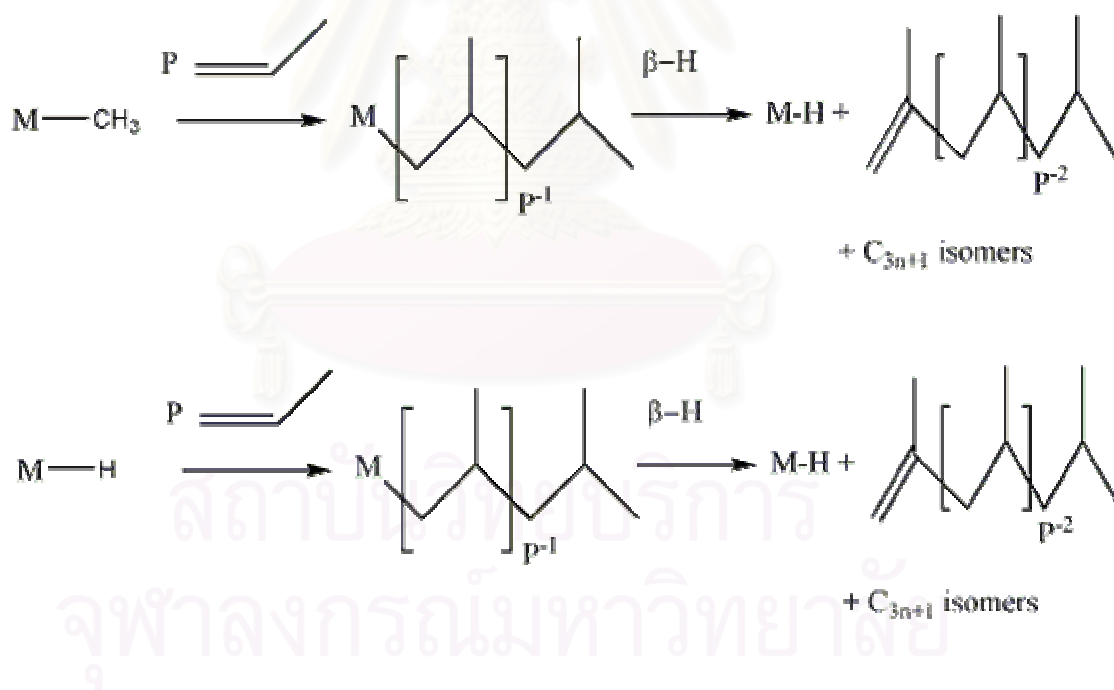


Figure 2.7 Chain transfer via β -H elimination [28]

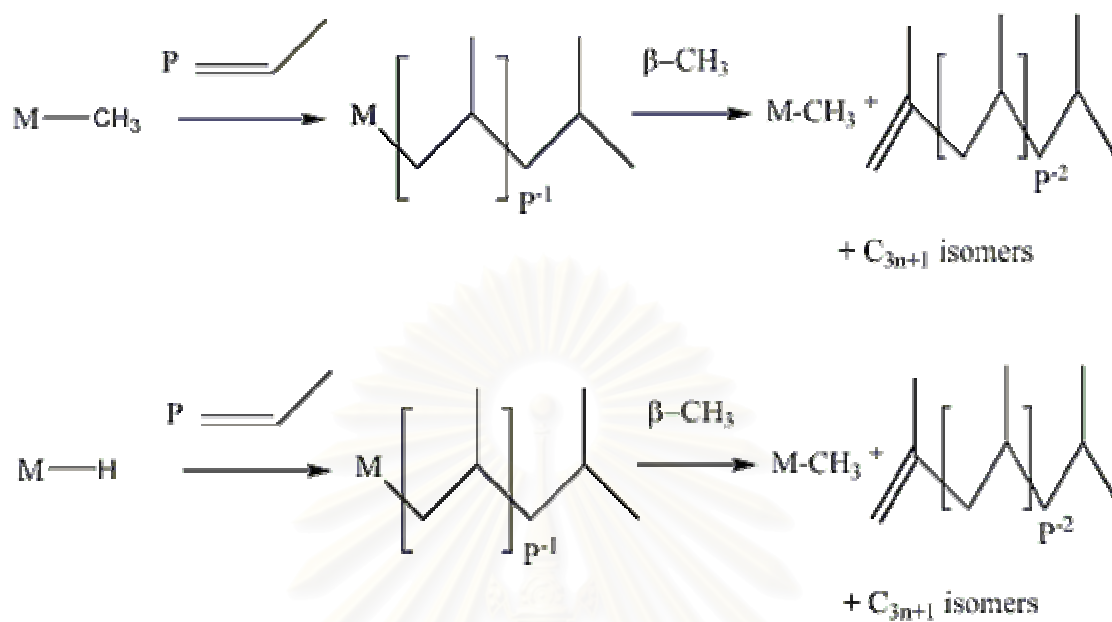


Figure 2.8 Chain transfer via β -Me elimination [29]

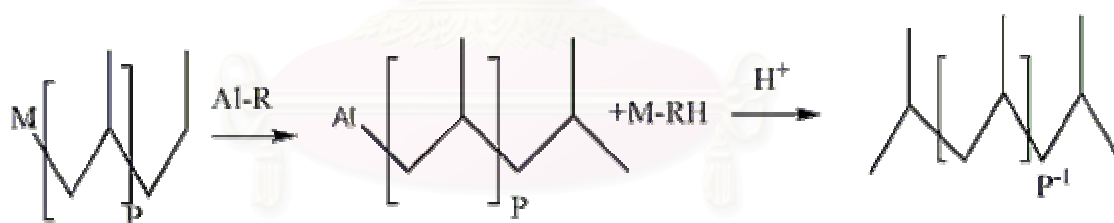


Figure 2.9 Chain transfer to aluminum [30]

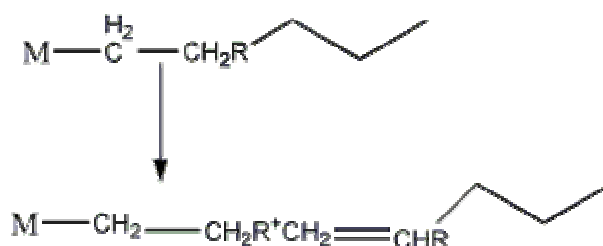


Figure 2.10 Chain transfer to monomer [31]



Figure 2.11 Chain transfer to hydrogen [32]

2.2.3.3 Mechanism of catalyst deactivation

Some metallocene catalyst systems exhibit the gradually decreased rate of polymerization due to the catalyst deactivation of active species with metallocene/MAO system or metallocene/Borate catalyst. Kaminsky et al. [34] proposed one mechanism of deactivation of active species with a M-CH₂-Al (Figure 2.12). However these inactive species can be reactivated by transmetallation reaction with MAO and lost Al-CH₂-Al structure at high concentration of anion MAO as MAO is consumed during the polymerization by side reactions, by impurity, by chain transfer and by recreating active sites. The regeneration of active sites will decrease at lower concentration of MAO but it cannot compensate to the loss of active site in polymerization process, thus a polymerization rate will gradually decrease.

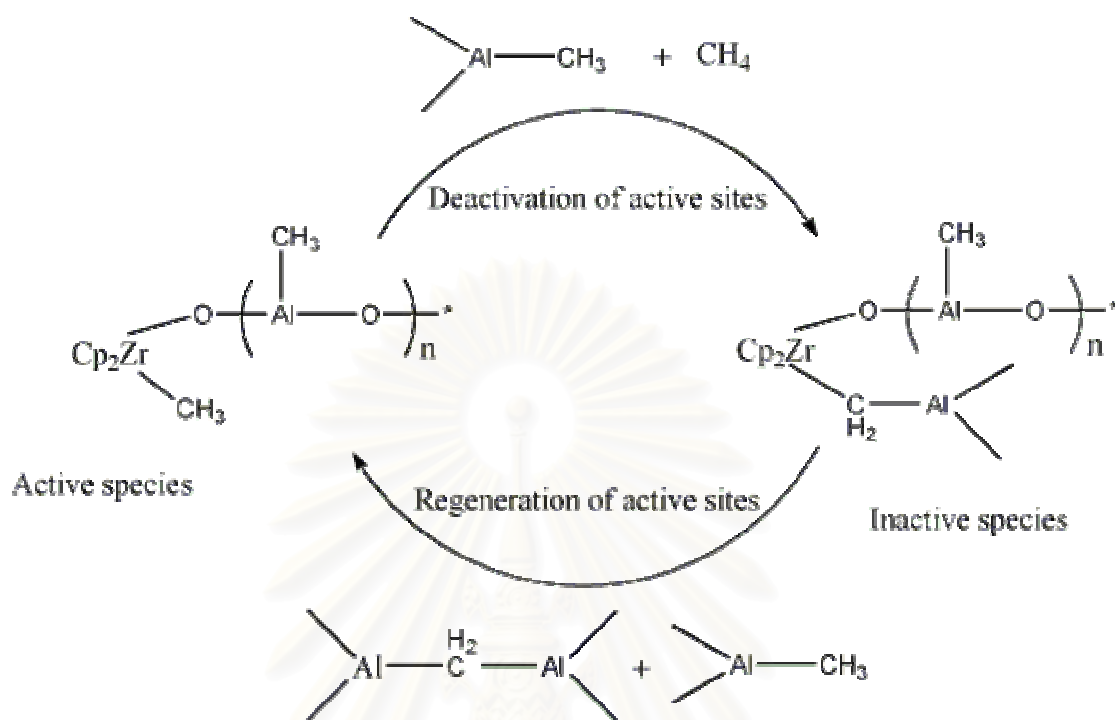


Figure 2.12 Mechanism showing the deactivation of active center for Cp_2ZrCl_2 -MAO catalyst system [34]

Moreover, Mulhaupt et al. [35] proposed another kind of reaction of deactivation of metallocene catalyst. In this model the deactivation rate was faster than the activation rate of active species in second order relatively in the Cp_2ZrCl_2 /MAO system. Deactivations of active species occur after the active species was fully activated. The Mulhaupt deactivation model was shown in figure 2.13

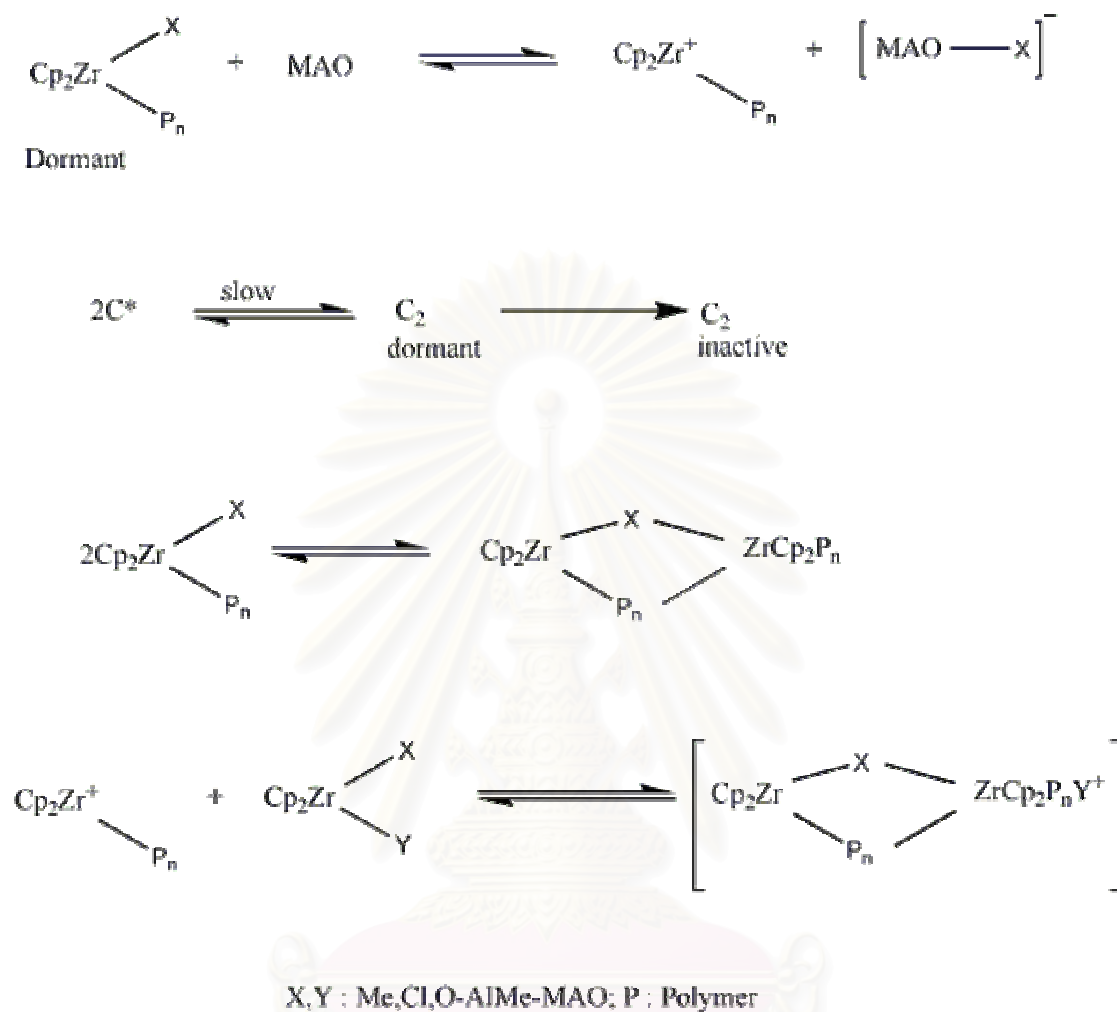


Figure 2.13 Mechanism of reversible second-order deactivation [35]

2.3 Classification of metallocene catalyst systems

Polymerization with metallocene catalyst can be arranged to 2 major types, the supported system and non-supported system. For the non-supported system, the cocatalyst was a mobile phase in the polymerization medium. On the other hands, the supported metallocene catalyst system, the co-catalyst mostly was immobilized on the organic support. In the early category, the activity was very high and easy to control the molecular weight. These systems still can divide to 2 sub-categories, aluminoxane system and cationic metallocene system. To study the metallocene catalyst behavior by changing

the substitute bridge or effect of activator are very famous to pick the homogenous metallocene catalyst system to study, because it did not have effect of interaction between inorganic support (silica or alumina) and metallocene catalyst systems.

2.3.1 Homogeneous metallocene catalyst with aluminoxane systems

At the first generation of this system, metallocene catalyst was a simple model which assembled from the cyclopentadienyl or substituted cyclopentadienyl ligands were π -bonded to the central metal atom. The development of metallocene catalyst was going on the synthesis of metallocene compounds. Breslow and Newbreg were the first researchers who apply the metallocene catalyst for polymerization [36]. They used the soluble bis(cyclopentadienyl)titanium derivative and alkylaluminum for ethylene polymerization. However, it was found that the productivity of these catalyst system was very low and the low molecular weight of polymer too. Moreover, these catalysts systems did not show activity when propylene was chosen to be a monomer for olefin polymerization. The breakthrough step of this typical metallocene occurred when Kaminsky and co-workers observed that the addition of water to trialkylaluminum in molar ratio 1:1 during the polymerization of ethylene could improve the productivity rate in significance [37]. It was known that the improved activity in the event above came from the reaction between water and trialkylaluminum to produce alkylaluminoxane in the system. Thus, Kaminsky and his group decided to use the alkylaluminoxane as the cocatalyst coupling with the metallocene compound. From this combination, the next generation of metallocene catalyst was born. It brought to the development in olefins polymerization because the metallocene/aluminoxane system sowed the activity higher than conventional Ziegler-Natta catalyst. In addition, the produced polymer from metallocene system gave the narrower polymer distribution than the traditional system.

2.3.2 Homogeneous metallocene catalyst with Lewis base activators systems

In this decade, not only the aluminoxane can activate the metallocene catalysts. Lewis bases can be used to produce the activator for metallocene catalyst system too. Naturally, metallocene catalyst will be active when the positive ion charged to the metal

central atom. And to stabilize the cation of metal complex, the anion must be introduced to the system. Now we have enough experimental evidence to prove the hypothesis that all active center types operative with metallocenes are cation that stabilized with the counter anion derived from the cocatalyst.

Cationic metallocene are prepared by combination of at least 2 compounds. The first one is the metallocene and the other is an activator that exchanges to charge the metallocene complex from neutral state to cationic state and forms a counter anion. The later component is the new step of development in polymerization from the aluminum activators. This compound must be capable of stabilizing the cationic metallocene complex and must be labile enough to displace with monomer the insertion step of polymerization too.

Non-aluminum activators such as $B(C_6F_5)_3$ (Borane), $Ph_3CB(C_6F_5)_4$ (Borate) and $PhMe_2NHB(C_6F_5)_4$, maybe replace the disadvantage of MAO as an activator for metallocene complexes. Several cations (metallocene) have been developed for the $[B(C_6F_5)_4]^-$ anion. Recently the silysium salts prepared by methathesis of $Li[B(C_6F_5)_4]$ with R_3SiCl [38] can be used as an activator for polymerization. In addition, tris(pentafluorophenyl)boron is a widely used activator for converting metallocene dihydrides and dialkyls to cationic catalyst. It has been prepared by the reaction of C_6F_5MgBr (from C_6F_5Br and alkylmagnesium halides) with BF_3 etherate [39]

These systems are very interesting in development to replace the disadvantage of MAO since it produced the near productivity. Unfortunately the active species of metallocene catalyst with these counter anions is very sensitive to air and any impurities during the polymerization.

2.3.3 Supported metallocene catalyst

A large proportion of polyolefin production is currently achieved by slurry- and gas-phase polymerization process. The major advantage of supported catalytic system is the desired polymer morphology and avoiding reactor fouling with finely dispersed swelling polymers. In the contrary, this system still has several disadvantages too. For example, low activity of polymerization due to the formation of inactive species between

catalyst and support, low molecular weight of polymer due to the rate of chain transfer reaction increased, low stereoregularity of polymer that can be controlled in homogenous system although the metallocene complex is the same.

There are roughly two basic methods of supporting the MAO-activate metallocene catalysts: (1) Supporting the metal complex on the carrier first, then react with MAO and (2) Supporting on MAO first, then react with the metal complex.

The most commonly employ inorganic support for catalysts are silica (SiO_2), alumina (Al_2O_3) and magnesium chloride (MgCl_2). And many supporting materials have been on the research such as, zeolite, nanocomposite material and etc.

2.4 Effect of polymerization parameters to characteristic of polymer

Naturally, the characteristic of polymer such as, stereoregularity, dyad distribution, triad distribution and monomer insertion depend on the polymerization parameters. The major parameters in the experiment can be classified in three categories: (1) Catalyst structure, substitute ligand and metal center atom, (2) Cocatalyst and/or activator including the structure of the cocatalyst employed in the polymerization, and (3) The solvent medium in experiment.

2.4.1 Effect of substitute ligand and center metal atom

In metallocene catalytic systems, the widest investigation is studying the effect of several kind of substitute ligand or the center metal atom. Metallocene complexes were synthesized in order to modified not only the bridge type [40-42] (such as, Si bridge and C bridge metallocene), but also the substitute of the position of the cyclopentadienyl ring [43-45] and the center metal atom [46]

A.Koppel et al. [41] investigated the effect of bridge type by using various *ansa*-bis(fluorenylidene) and *ansa*-fluorenylidene cyclopentadienyliidene zirconium dichloride complexes with PHT (PHT partially hydrolyzed trimethylaluminum) by using various bridge types. This study showed that the relationship between “bite angle” and what? is

effect on the productivity rate and comonomer insertion. A larger bite angle of bridge type (Figure 2.14) should allow the better access of comonomer insertion. However the different in dihedral angles also influence the electron density on metal atom and therefore the stability of *ansa*-metallocene dichloride complex. On one hand, ligand systems with a larger opening angle and a lower electron density on the center metal atom should exhibit higher activity, on the other hand, their thermal stability decreases in the same order. Decreased stability should lead to a loss in catalytic activity.

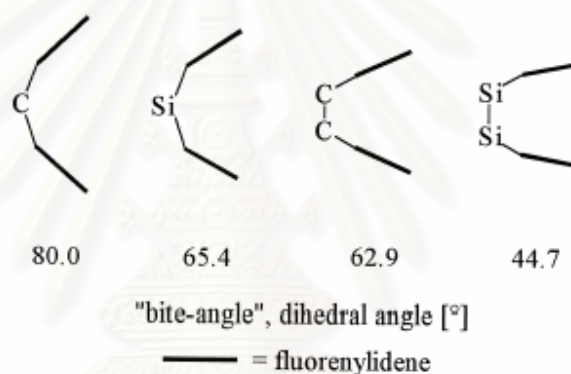


Figure 2.14 Bridging moiety on bite angle in *ansa*-bis(fluorenylidene) zirconium dichloride complexes

Waymouth et al.[45] reported that the effect of substitute of methyl group at the second position on the indenyl ring catalyst, bis(2-methylindenyl)zirconium dichloride or bis(2-phenylindenyl)zirconium dichloride, exhibits the higher insertion of 1-hexene than bis(indenyl)zirconium dichloride system. In addition, these studies reported that bridge metallocene catalytic system has the incorporation of 1-hexene more than unbridged metallocene system. One explanation proposed for this phenomenon is that the larger coordination gap aperture of the bridged compounds allows the incoming R-olefin better accessibility to the zirconium center.

However, according to these studies, the presence or absence of a bridging group may not be as important as the nature of the substituents for controlling the comonomer

incorporation. For example, the substitute at the second position of bis(2-phenylindenyl)zirconium dichloride (**1**), bis(2-phenylethynylindenyl)zirconium dichloride (**2**), bis(2-cyclopentadienyl)zirconium dichloride (**3**) and bis(2-methylindenyl)zirconium dichloride (**4**) (Figure 2.15). Furthermore, it reported that 1-hexene insertion is in order of $1 > 2 \sim 4 > 3$. In conclusion, it suggested that having phenyl group close to the coordination site increases the selectivity for 1-hexene. Moreover, the similar copolymerization behavior of **2** and **4** suggests that any substituent larger than hydrogen is sufficient to improve the 1-hexene incorporation relative to **3**.

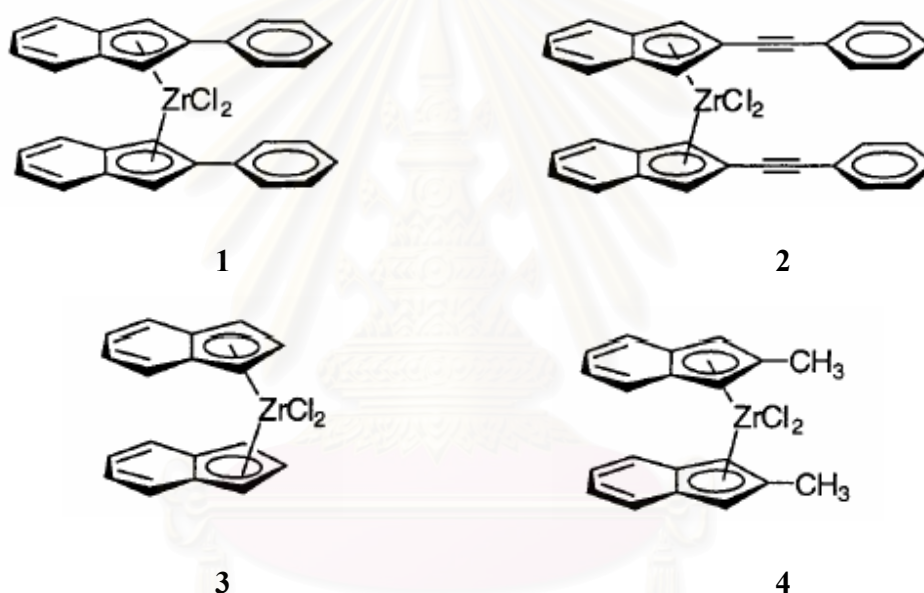


Figure 2.15 2-substitute catalyst, bis(2-Rindenyl)zirconium dichloride

Moreover the investigation on the difference in center metal atom has done by Dankova and Waymouth [46]. This study indicates that hafnium based metallocene systems incorporate α -olefin better than zirconium congeners. These result might be due to the either some subtle electronic influence of metal or metal's interaction with counter anion. On the others hand, hafnium complexes produced the activity lower than zirconium complexes. The lower productivity of hafnium might be rationalized by the higher hafnium-carbon bond strength.

2.4.2 Effect of cocatalysts and/or activators

The active species of metallocene complexes formed with a weak coordination between cationic metal complexes and the counter anionic compound. Unfortunately the counter anionic compound is very sensitive to air and impurities. Thus, the research in this field mostly is purposed to find the new kind of activators with the simple experiments. The most famous topic paid attention to the non-aluminoxane system activators, because the structure of aluminoxane still cannot be defined and hard to explain.

Akihiro Yano and coworkers [47] have investigated on ethylene polymerization with different activators. Ethylene polymerization was conducted with diphenylmethylenedicyclopentadienyl fluorenyl zirconium dichloride ($\text{Ph}_2\text{C}(\text{Cp})(\text{Flu})\text{ZrCl}_2$) activated with various activators such as methylaluminoxane MAO, tetrakis-(pentafluorophenyl)borates $\text{R-B}(\text{C}_6\text{F}_5)_4$, $\text{R} = \text{Me}_2\text{PhNH}$, Ph_3C , C_7H_7 , $\text{H}(\text{Et}_2\text{O})_n$, dimethylanilinium tetrakis pentafluoro-phenyl aluminate $\text{Me}_2\text{PhNHP-Al}(\text{C}_6\text{F}_5)_4$ and tris-pentafluorophenyl borane $\text{B}(\text{C}_6\text{F}_5)_3$ to study the correlation between catalyst performance for ethylene polymerization and cocatalysts at high temperature. The different activity was discovered and assigned to the relative coordinative abilities of the anions and tightness of the ion-pairing.

T. J. Marks et al. [48] have report on the effect of activator on the stereospecificity on propylene polymerization with different kind of activators (Mononuclear and polynuclear perfluoroaryl – borate, - aluminate and – gallate) with C_s -symmetric $[\text{Me}_2\text{C}(\text{Cp})(\text{fluorenyl})]\text{ZrMe}_2$ catalyst. These systems revealed a marked counteranion dependence of polymerization activity, product polymer syndiotacticity, and relative $[m]$ and $[mm]$ stereoerror abundance, with the polynuclear perfluoroaryl cocatalysts uniformly giving enhanced product polymer stereoregularity versus the neutral analogues.

On the one hand, not only the aluminoxane has effect to the polymerization behavior but the trialkylaluminum has the influence too. T. Shiono et al. [49] have studied on the effect of trialkylaluminum type to the characteristic of polymerization. For example, the addition of Oct_3Al and Et_3Al increased the propagation rate of living

polymerization with [t-BuNSiMe₂Flu]TiMe₂ / B(C₆F₅)₃ system at -50 °C.

2.4.3 Effect of Solvent medium

Olefins polymerization in slurry phase is important to accompany with the solvent medium. Each kind of solvent has own characteristic, such as, polarity, dielectric constant or molecular structure, etc. F. Forlini et al. [50,51] have reported the effect of solvent medium to the propylene/1-hexene polymerization with ethylene-bis-(indenyl)zirconium dichloride/MAO system. According to this study, the dielectric constant value of the solvent medium had large effect to the productivity of polymerization. On the other hands polymer compositions are similar. Evidently, activity and selectivity versus the more hindered comonomer are governed by the different factors: the solvent polarity, which as the enormous effect on activity has in fact the negligible effect on comonomer compositions.

The exceptional activity improvement due to the polar solvent is well known, which was accounted for by the fact that the increase of the dielectric constant should enhance the ionic dissociation. The shift of the equilibrium reaction versus the ionic solvent separated active species leads to a wider active center population and explains the high activity observed.

However, the solvent polarity also has the nucleophilic nature of solvent which could compete more with the α -olefins than with propylene, in the coordinate to the active site, due to steric reason.

K. Nishii et al. [52,53] have investigated on the solvent effect to the stereospecificity in propylene polymerization by the [t-BuNSiMe₂Flu]TiMe₂-based catalyst systems with dried-aluminoxane as cocatalyst at 0 °C. This study exhibited that if heptane was chosen to be a solvent medium, the obtain polypropylene gave the syndiotactic polypropylene. On the contrary, chlorobenzene as polymerization medium gave the atactic polypropylene. Furthermore, either heptane or chlorobenzene produces the living nature of polymerization. Thus, block syndiotactic-atactic polypropylene could be produced from this system.

In conclusion we could announce that, the monomer insertion behavior depend on the solvent polarity including the dielectric constant value.

CHAPTER III

EXPERIMENTAL

An enormous number of research article of metallocene catalytic system for olefins polymerization have been pressed in the journal for this decade. Mostly of the article tends to observe for the new kind of catalyst or the new type of cyclic polymerization. One main point of investigation is to study the polymer microstructure produced from metallocene catalyst. Not only the homogeneous polymerization was been investigated, but also the supported metallocene catalytic systems. Therefore, the effect of co-catalyst and activators in slurry phase process of ethylene based copolymerization on the productivity, polymer microstructure and polymer properties made with different kind of aluminoxane or organoborane compounds, including the solvent medium is presented on this work.

3.1 Objective

To study the influence of the co-catalyst and activators in homogeneous and heterogeneous metallocene systems on the catalytic activity and polymer properties during ethylene based copolymerization in slurry phase process.

3.2 Scope of investigation

- 3.2.1 Synthesize, prepare and characterize the catalyst and several types of aluminoxane and organoborane compounds
- 3.2.2 Comparison the effect of aluminoxane and organoborane compounds on the productivity and polymer properties of ethylene based copolymerization
- 3.2.3 Investigate the effect of solvent medium on the productivity and polymer properties on the ethylene based copolymerization
- 3.2.4 Study the effect of second monomer on the polymerization behavior and polymer properties in ethylene based copolymerization
- 3.2.4 Characterize the obtain polymer with conventional investigation instrument: Nuclear magnetic resonance spectroscopy (NMR), Gel permeation chromatography (GPC), and Differential scanning calorimeters (DSC)

3.3 Experimental

The detail of experimental in this present of study announce as the following

3.3.1 Material

The preparation and handling of the catalyst were operated in a nitrogen atmosphere with Schlenk techniques. The titanium complex was synthesized according to the literature and the literature [54]. The others chemicals are listed as followed

1. n-Buthyllithium 1.5M solution in hexane was purchased from Kanto fine Chemical and used without further purification.
2. Methyllithium 1 M solution in diethyl ether was purchased from Kanto fine Chemical and used without further purification.
3. Dichlorodimethylsilane (99%) was purchased from Aldrich Chemical Company, Inc and used without further purification.
4. tert-Butylamine (99+%) was purchased from Aldrich Chemical Company, Inc and used without further purification.
5. TiCl_4 (99+%) was purchased from MERCK and used without further purification.
6. MeMgBr 3M concentration soluble in diethyl ether was purchased from Aldrich Chemical Company, Inc and used without further purification.
7. Fluorene (99%) was purchased from Aldrich Chemical Company, Inc and used without further purification.
8. (1,2,3,4-methyl)-(1,3-cyclopentadiene) was purchased from Aldrich Chemical Company, Inc and used without further purification.
9. Hexane (95%) was donated from Shell (Public) Company, Inc. and purified by distilling over sodium under argon atmosphere before use.
10. Diethylether (99%) was purchased from Fluka Chemie, A.G., Switzerland. And purified by distilling over CaH_2 with at least 6 hour reflux under argon atmospheric before used.
11. Tetrahydrofuoran was purchased from Fluka Chemie, A.G., Switzerland. And purified by distilling over CaH_2 with at least 6 hour reflux under argon atmospheric before used.
12. Pentane was purchased from Fluka Chemie, A.G., Switzerland. And purified by distilling over over sodium under argon atmosphere before used.

13. Heptane was purchased from Fluka Chemie, A.G., Switzerland. And purified by distilling over sodium under argon atmosphere before used.

14. Chlorobenzene was purchased from Fluka Chemie, A.G., Switzerland. And purified by distilling over sodium under argon atmosphere before used.

15. Dichloromethane was purchased from Fluka Chemie, A.G., Switzerland. And purified by distilling over sodium under argon atmosphere before used.

16. Toluene was devoted from EXXON Chemical Ltd., Thailand. This solvent was dried over dehydrated CaCl_2 and distilled over sodium/benzophenone under argon atmosphere before use.

17. Modified-Methylaluminoxane (MMAO) 1.86 M in toluene was donated from Tosoh Akso, Japan and used without further purification.

18. Methylaluminoxane (MAO) 2.667 M in toluene was donated from Tosoh Akso, Japan and used without further purification.

19. Borane ($\text{B}(\text{C}_6\text{F}_5)_3$) was donated from Tosoh Akso, Japan and used without further purification.

20. Triphenylcarbonborate ($\text{Ph}_3\text{CB}(\text{C}_6\text{F}_5)_4$) was donated from Tosoh Akso, Japan and used without further purification.

21. Ethylene gas (99.96%) was devoted from National Petrochemical Co.,Ltd.Thailand and used as received.

22. 1-Hexene (99+%) was purchased from Aldrich Chemical Company, Inc. and purified by distilling over sodium under argon atmosphere before use.

23. 1-Octene (98%) was purchased from Aldrich Chemical Company, Inc. and purified by distilling over sodium under argon atmosphere before use.

24. 1-Decene ($\geq 97\%$) was purchased from Fluka Chemie A.G. Switzerland. and purified by distilling over sodium under argon atmosphere before use.

25. Hydrochloric acid (Fuming 36.7%) was supplied from Sigma and used as received.

26. Methanol (Commercial grade) was purchased from SR lab and used as received.

27. Sodium (99%) was purchased from Aldrich Chemical Company, Inc. and used as received.

28. Benzophenone (99%) was purchased from Fluka Chemie A.G. Switzerland. and used as received.

30. Calciumhydride (99%) was purchased from Fluka Chemie A.G. Switzerland. and used as received.

31. Ultra high purity argon gas (99.999%) was purchased from Thai Industrial Gas Co., Ltd., and further purified by passing through columns packed with molecular sieve 3 A, BASF Catalyst R3-11G, sodium hydroxide (NaOH) and phosphorus pentoxide (P_2O_5) to remove traces of oxygen and moisture.

3.3.2 Equipment

Due to the metallocene system is extremely sensitive to the oxygen and moisture. Thus, the special equipments were required to handle while the preparation and polymerization process. For example, glove box: equipped with the oxygen and moisture protection system was used to produce the inert atmosphere. Schlenk techniques (Vacuum and Purge with inert gas) are the others set of the equipment used to handle air-sensitive product.

3.3.2.1 Cooling system

The cooling system was in the solvent distillation in order to condense the freshly evaporated solvent.

3.3.2.2 Inert gas supply

The inert gas (argon) was passed through columns of BASF catalyst R3-11G as oxygen scavenger, molecular sieve 3×10^{-10} m to remove moisture. The BASF catalyst was regenerated by treatment with hydrogen at 300 °C overnight before flowing the argon gas through all the above columns. The inert gas supply system is shown in **Figure 3.1**.

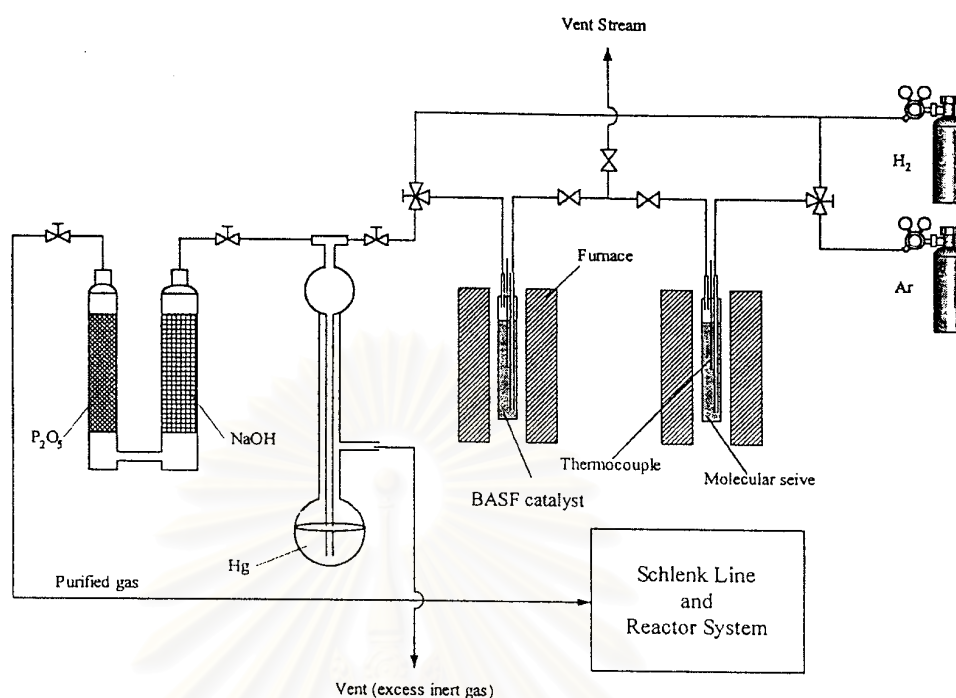


Figure 3.1 Inert gas supply system

3.3.2.3 Magnetic stirrer and heater

The magnetic stirrer and heater model RTC basis from IKA Labortechnik were used.

3.3.2.4 Reactor

A 100 ml glass flask connected with 3-ways valve was used as the copolymerization reactor for atmospheric pressure system and a 100 ml stainless steel autoclave was used as the copolymerization reactor for high pressure systems.

3.3.2.5 Schlenk line

Schlenk line consists of vacuum and argon lines. The vacuum line was equipped with the solvent trap and vacuum pump, respectively. The argon line was connected with the trap and the mercury bubbler that was a manometer tube and contain enough mercury to provide a seal from the atmosphere when argon line was evacuated. The Schlenk line was shown in **Figure 3.2**.

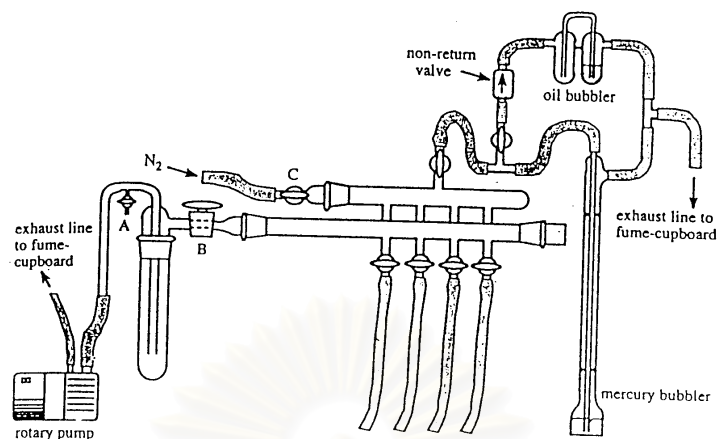


Figure 3.2 Schlenk line

3.3.2.6 Schlenk tube

A tube with a ground glass joint and side arm, which was three-way glass valve as shown in **Figure 3.3**. Sizes of Schlenk tubes were 50, 100 and 200 ml used to prepare catalyst and store materials which were sensitive to oxygen and moisture.



Figure 3.3 Schlenk tube

3.3.2.7 Vacuum pump

The vacuum pump model 195 from Labconco Corporation was used. A pressure of 10^{-1} to 10^{-3} mmHg was adequate for the vacuum supply to the vacuum line in the Schlenk line.

3.3.2.8 Polymerization line

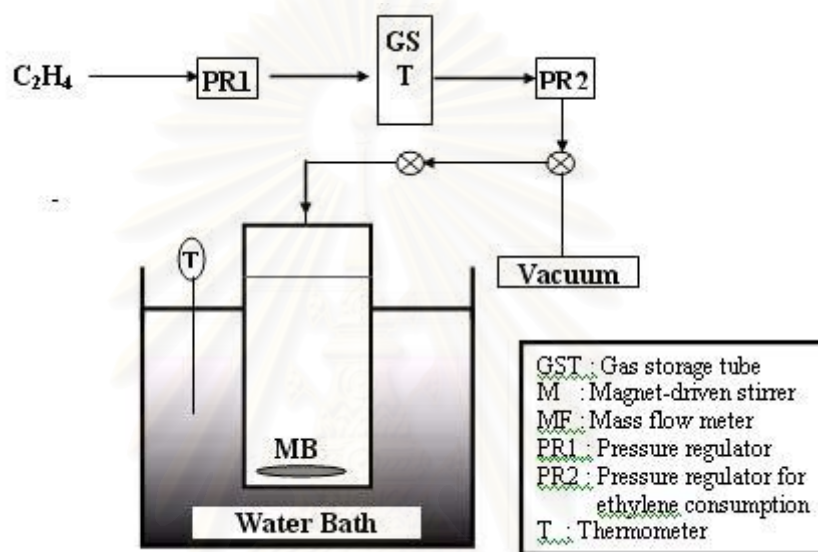


Figure 3.4 diagram of system in slurry phase polymerization

3.3.3 Catalyst synthesis

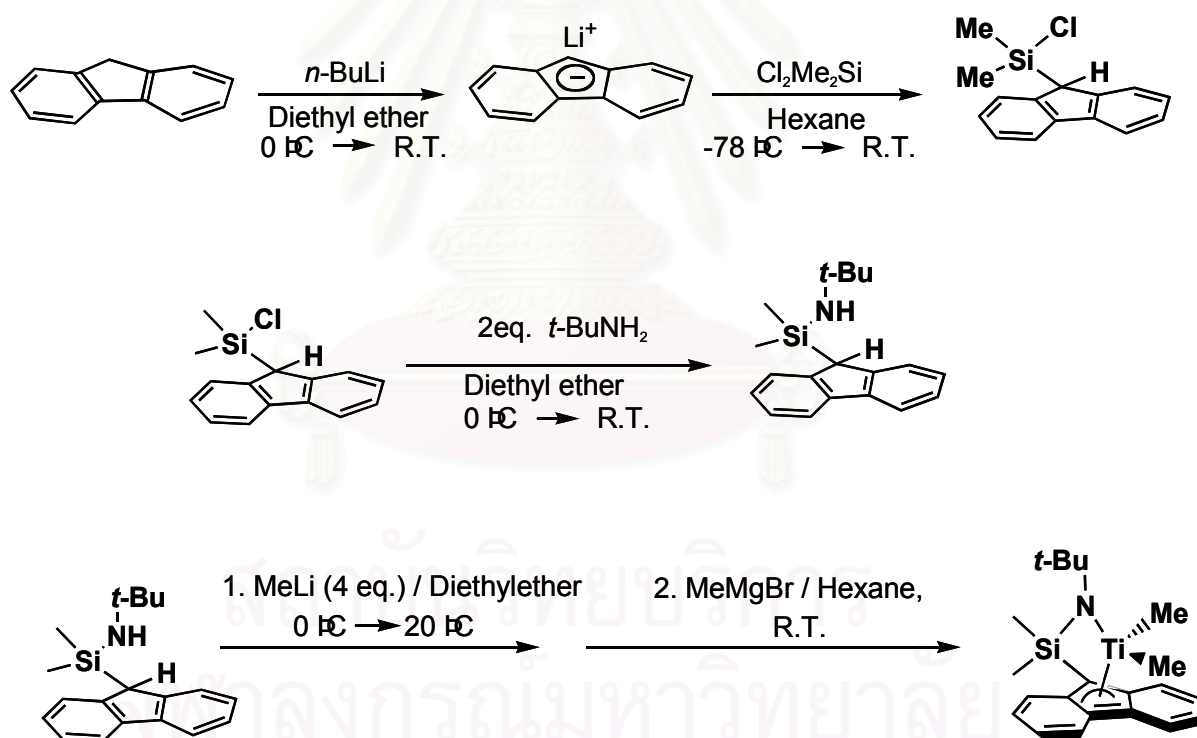
3.3.3.1 Synthesis of *t*-BuNHSiMe₂Flu

Firstly, The solution of fluorene (11.6 g, 70mmol) in diethylether (120 ml) was added n-butyllithium (1 equivalent to fluorene) at 0 °C within 1 hr and stirred for 3 hours and room temperature. After that the solution was evacuated to give Li(C₁₃H₉). Transfer the slurry solution to another flask that contain dichlorodimethylsilane (40 ml) soluble in hexane (100 ml) at -78 C, and stirred for overnight. The suspensions liquid was removed the excess silane compound in vacuo. After adding hexane and stir the solution, the not soluble solid was precipitate and the solvent was decanted. From the decanted solution we remove the solvent in vacuo again to obtain 9-chlorodimethylsilyl-fluorene.(16.2 g , 62 mmol) as off-white solid

Secondly, the solution of 9-chlorodimethylsilyl-fluorene (9.2 g, 36 mmol) in THF (100 ml) was added *t*-Butylamine (6 g 76 mmol) at 0 °C, and stirred overnight at room temperature. Solution was evacuated, washed with THF and decanted solvent was evacuated again to gave *t*-BuNHSiMe₂Flu as a yellow-orange oil.

3.3.3.2 Synthesis of [*t*-BuNMe₂SiFlu]TiMe₂ (catalyst 1)

Stirring the ligand *t*-BuNHSiMe₂Flu (1.56 g, 5.28 mmol) in Et₂O (100 ml) solution that was added Methyl lithium 4 equivalents slowly for 5 hours. And transfer this solution to another flask that contain the TiCl₄ (1 eq.) in pentane (100 ml) solution. The resulting solution was stirred overnight at room temperature. After that the solution was evacuated, washed, and stirred with hexane (130 ml). The decanted hexane solution was concentrate and cooled overnight at -30 C to recrystallize and give the yellow-orange crystal as [*t*-BuNMe₂SiFlu] TiMe₂ catalyst.



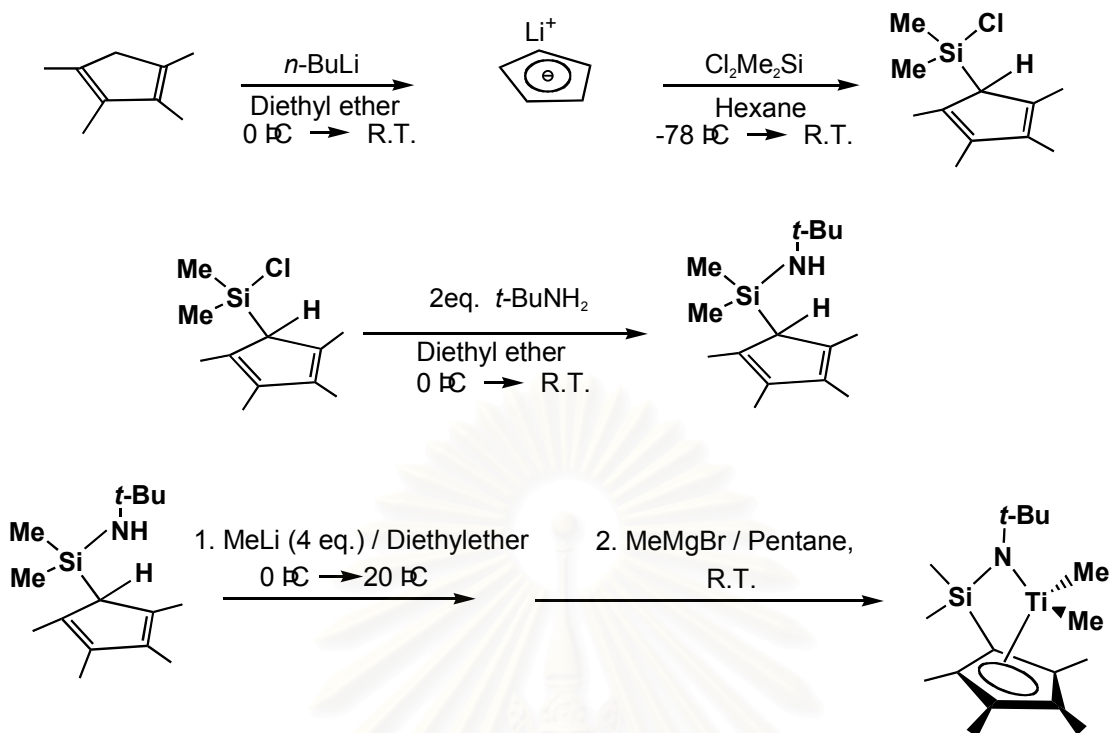
Scheme 3.1 Synthetic pathway of [*t*-BuNSiMe₂Flu]TiMe₂

3.3.3.3 Synthesis of *t*-BuNHMe₂SiClC₅HMe₄

To a solution of tetramethylcyclopentadiene (10 g, 82 mmol) in hexane (200 ml), n-butyllithium (58 ml of 1.5 M solution in hexane; 82 mmol) was added at 0 °C within 1 h. After stirring 3 h at room temperature, the solvent was removed under vacuum and washed with hexane several times to obtain Li(C₉H₁₃). To a solution of dichlorodimethylsilane (38 mL) in THF (100 mL), the suspension of the Li(C₉H₁₃) in THF (200 mL) was added at -78 °C. The resultant suspension was stirred for 8 h at room temperature. The solvent and excess dichlorodimethylsilane were removed under vacuum. Lithium chloride was precipitated with pentane and filtering it off followed by removal of solvent. The C₅HMe₄SiMe₂Cl was obtained as light yellow oil (14.26 g, 66 mmol). To a solution of C₅HMe₄SiMe₂Cl (14.26 g, 66 mmol) in THF (150 mL), 2 eq of *t*-butylamine was added at 0 °C over a period of 1 h. The reaction mixture was stirred for over night to obtain a yellow suspension. After removal of solvent, the product was extracted with pentane and filtered off. The solvent was removed and *t*-BuNHSiMe₂C₅HMe₄ was obtained as yellow oil (11.95 g, 45 mmol).

3.3.3.4 [*t*-BuNSiMe₂C₅Me₄]TiMe₂ (catalyst 2)

Stirring the ligand *t*-BuNHSiMe₂Flu (1.56 g, 5.28 mmol) in Et₂O (100 ml) solution that was added Methyl lithium 4 equivalents slowly for 5 hours. And transfer this solution to another flask that contain the TiCl₄ (1 eq.) in pentane (100 ml) solution. The resulting solution was stirred overnight at room temperature. After that the solution was evacuated, washed, and stirred with hexane (130 ml). The decanted hexane solution was concentrate and cooled overnight at -30 C to recrystallize and give the yellow-orange crystal as [*t*-BuNMe₂SiFlu] TiMe₂ catalyst.



Scheme 3.2 Synthetic pathway of $[\text{t-BuNSiMe}_2\text{C}_5\text{Me}_4]\text{TiMe}_2$

3.3.4 Preparation of d-MAO and d-MMAO

The dried MAOs were prepared according to the procedure reported previously [55,56].

100 ml of MAO solution in toluene was evacuated and washed with toluene (100 ml) for 3 times to remove the impurity. After that d-MAO was washed and dried with hexane to remove TMA in MAO to give d-MAO as white solid.

In the same method to MMAO, the solution was evacuated and washed with toluene (100 ml) for 3 times to remove the impurity. Then continue to wash with heptane to remove TMA and TIBA in MMAO to give d-MMAO as white solid.

3.3.5 Polymerization procedure

For the investigation the effect of activator, atmospheric pressure system was chosen to polymerize. Unfortunately, the activity is quite low. Thus we changed the system to the high pressure autoclave system. The polymerization procedures were reported as followed

3.3.5.1 Atmospheric pressure semibatch system

Polymerization was performed in a 100 ml glass reactor equipped with a magnetic stirrer and carried out as semi-batch method. First, the reactor was charged with MAO and 1-hexene in the certain amount was added. After the addition of solvent (toluene) the reactor was kept in the water bath for 30 min to reach at required reaction temperature. After that systems were changed from nitrogen to ethylene atmosphere system. When reaction medium was saturate with ethylene monomer, polymerizations were started by adding the 1 ml (20 μ mol) of catalyst solution. For the borane and borate system, polymerization was started by the successive additions of alkylaluminum, the borane or borate, and the complex to the monomer solution. Ethylene pressure and temperature were kept constant during polymerization, and the consumption rate of ethylene was monitored by mass flow meter. Polymerizations were conducted on the certain time and terminated with acidic methanol. The polymer obtained was precipitated in acidic methanol, filtered, adequately washed with methanol, and finally dried under vacuum at 60 °C for 6 h.

3.3.5.2 High pressure autoclave system

Polymerization was carried out in a 100-ml stainless steel autoclave reactor equipped with a magnetic stirrer. The solvent (toluene, heptane, chlorobenzene, and dichlorometahne) was introduced into the reactor (30 ml) followed by the desired amount of MMAO. The catalyst 1 in toluene (5 μ mol/ml) was added into the reactor to make the $[Al]_{MMAO}/[Ti]_{cat.1} = 1000$. The reactor was then immersed in liquid nitrogen. 1-hexene (3 ml \sim 0.018 mole) was added to the frozen reactor. Then, the reactor was adjusted to the polymerization temperatures (0°C and 70°C). Continuous feeding ethylene started the reaction. The pressure in the reactor was kept at 50 psi by continuous feeding the ethylene. Polymerization was conducted for 15 min, then

terminated with acidic methanol. The polymer obtained was precipitated, filtered, washed, and dried in ambience for three days before measuring the weight.

3.3.6 Characterization method

3.3.6.1 Gel Permeation Chromatography (GPC)

Molecular weight and molecular weight distribution of polymer (5 mg) were measured by GPC (Waters 150C) at 140 °C using *o*-dichlorobenzene as solvent and calibrated by polystyrene standards.

3.3.6.2 Nuclear magnetic resonance spectroscopy (NMR)

¹³C NMR spectra of polyethylene based polymer (50 mg) were recorded at 100 °C on a JEOL GX 500 spectrometer operated at 125.65 MHz in pulse Fourier transform mode with tetrachloroethane-*d*₂ as solvent. For ¹³C NMR, the pulse angle was 45°, and about 5000 scans were accumulated in a pulse repetition of 4.0 s and calculated according to the method of Randall [57]

3.3.6.3 Differential Scanning Calorimeter (DSC)

The melting temperature (*T*_m) and heat of fusion (ΔH_m) of copolymer were determined by Perkin-Elmer DSC 7 by using the polymer sample about 10 mg. The analyses were performed at heating rate of 20 °C/min in the temperature range 50-200 °C. The heating cycle was run twice. The first scan, samples were heated and cooled to room temperature. The second scan, sample were heated at the same rate, but only the result of the second scan were reported.

CHAPTER IV

EFFECT OF CO-CATALYSTS

Nowadays, polyethylene plays the major role in the plastic industry [58,59]. Density of polymer is one of the most important parameters for polymer properties. In order to dense polyethylene, ethylene- α -olefins were chosen to conduct with catalytic polymerization in order to obtain a new kind of linear low density polyethylene (LLDPE). Due to the catalyst abilities and co-catalyst, we can control the amounts of α -olefin insertion, short chain branching distribution and the triad distribution of copolymers. The different microstructure of copolymer will affect the polymer properties such as melting and glass transition temperatures, melt viscosity, and mechanical and optical properties, all of which define the type and useful range of application of these materials [60-63].

Marks et.al [64] have investigated polyethylene branching and α -olefin comonomer insertion enrichment concentrate on catalyst and co-catalyst nuclearity using many kinds of zirconium constrain geometry catalyst. They found that in single site polymerization system, the sequence of polymer insertion strongly depended on the bimetallic complexes of catalyst and co-catalyst that were employed in the system. As the part of the literature, they observed the differences of polymerization ability on norbornene polymerization [65] with [tert-BuNSiMe₂Flu]TiMe₂ (**1**) catalyst and methylaluminoxane and borate (Ph₃CB(C₆F₅)₄) were chosen to be activators. From this report it noted that catalyst**1**/methylaluminoxane and catalyst**1**/(Ph₃CB(C₆F₅)₄) systems were formed in different bimetallic active species

According to the chapter II, we have explained about the co-catalyst structure and its properties for the fundamental details. In this chapter, the result of polymerization of ethylene and ethylene/1-hexene polymerization with [t-BuNSiMe₂Flu]TiMe₂ (catalyst **1**) was applied to conducted the polymerization process with methylaluminoxane (MAO), modified-methylaluminoxane (MMAO), dried-methylaluminoxane (d-MAO), dried-modified-nethylaluminoxane (d-MMAO), borane (B(C₆F₅)₃) and borate (Ph₃CB(C₆F₅)₄) as the activators.

4.1 Ethylene/1-hexene polymerization results

The present study showed influences of various cocatalysts or activators on characteristics and catalytic behaviors of ethylene polymerization, 1-hexene polymerization and ethylene/1-hexene copolymerization in toluene as medium with $[t\text{-BuNSiMe}_2\text{Flu}]\text{TiMe}_2$ (**catalyst 1**) catalyst. Results of ethylene/1-hexene copolymerization with various activators such as MAO, d-MAO, MMAO, d-MMAO, and borate are shown in **Table 4.1**. It indicated that activities of every type of polymerization with d-MAO and d-MMAO exhibited the highest activities among any other activators. Enhanced activities arising from d-MAO and d-MMAO were attributed to less TMA and TIBA in the dried MAO and MMAO, respectively, considering result when MAO and d-MAO were used it was reported that the presence of TMA resulted in chain transfer reaction and also the excess of TMA in catalyst system would reduce the Ti(IV) species to inactive lower valence state[66]. Thus we can propose that activities of ethylene/1-hexene copolymerization with **catalyst 1**/aluminoxane system depended on the amounts of TMA present in the aluminoxane. Furthermore, when compared the results between MAO – d-MAO systems and MMAO – d-MMAO systems, it was obvious that TMA had stronger effect more than TIBA because in MAO systems polymerization activities decreased significantly compared to the MMAO systems.

Table 4.1 : Results of polymerization of ethylene/1-hexene polymerization with catalyst **1**^a

Polymer	Co-Catalyst	time (min)	Yield (g)	Activity ^b	M _n ^c	MWD ^c	N ^d
EH	MAO	15	0.27	53	0.15	1.39	180
EH	d-MAO	15	2.69	538	2.81	1.44	96
EH	MMAO	15	2.02	405	3.93	1.99	51
EH	d-MMAO	15	2.64	527	6.34	1.84	42
EH	Borate ^e	7	0.29	123	9.49	2.98	3
E	MAO	15	0.24	49	0.14	1.54	166
E	d-MAO	15	0.53	106	5.57	2.69	10
E	MMAO	15	0.68	135	- ^f	- ^f	- ^f
E	d-MMAO	15	0.55	109	15.1	3.25	3.6
E	Borate ^e	4	0.03	19	4.27	2.28	1
H	MAO	30	0.08	8	- ^g	- ^g	- ^g
H	d-MAO	30	0.71	71	1.36	1.85	52
H	MMAO	30	0.59	59	2.69	1.8	22
H	d-MMAO	30	0.62	62	1.77	1.82	35
H	Borate ^e	7	0.07	30	10.8	1.73	1

^aPolymerization conditions: Ti = 20 μmol, Al/Ti = 400, Solvent = toluene 30 ml, Temperature = 40°C. atmospheric pressure.

^bActivity = kg(polymer) mol⁻¹(Ti) hr⁻¹.

^cNumber of average molecular weight and molecular weight distributions were measured by GPC analysis using poly styrene as reference.

^dNumber of polymer chain calculated from yield and M_n

^eBorate compound (Ph₃CB(C₆F₅)₄) 20 μmol and using Oct₃Al 20 μmol as scavenger.

^fPolymer was not dissolve in Orthodichlorobenzene solution.

^gNot determined due to the polymer obtain cannot extract from the filtrate paper.

According to ethylene consumption profile in ethylene/1-hexene copolymerization systems as shown in **Figure 4.1** and in ethylene polymerization system as shown in **Figure 4.2** it indicated that deactivation of active species occurred in the borate system due to the unsuitable of polymerization temperatures of borate system at high temperature.

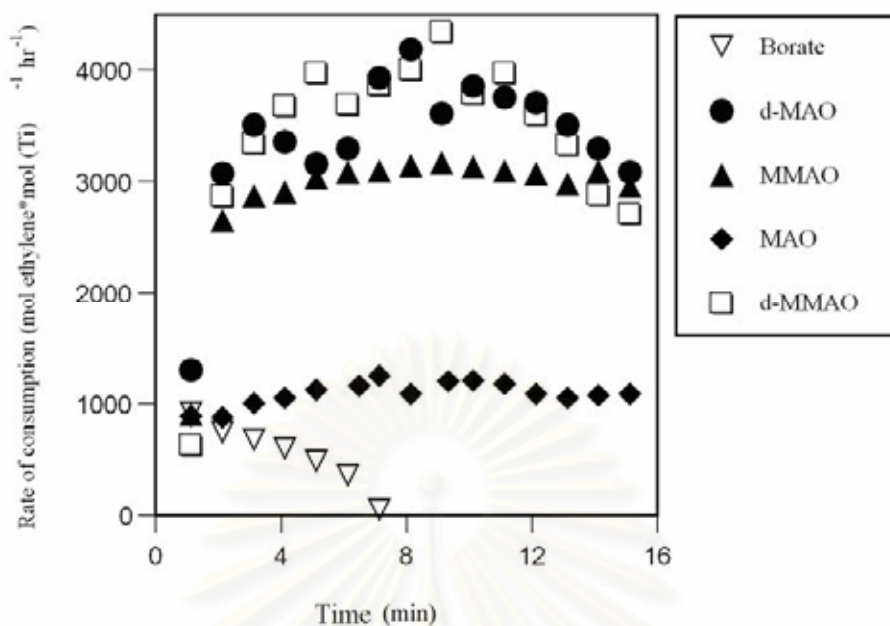


Figure 4.1 Ethylene rate consumption profile of ethylene/1-hexene copolymerization with **catalyst 1**/ activators

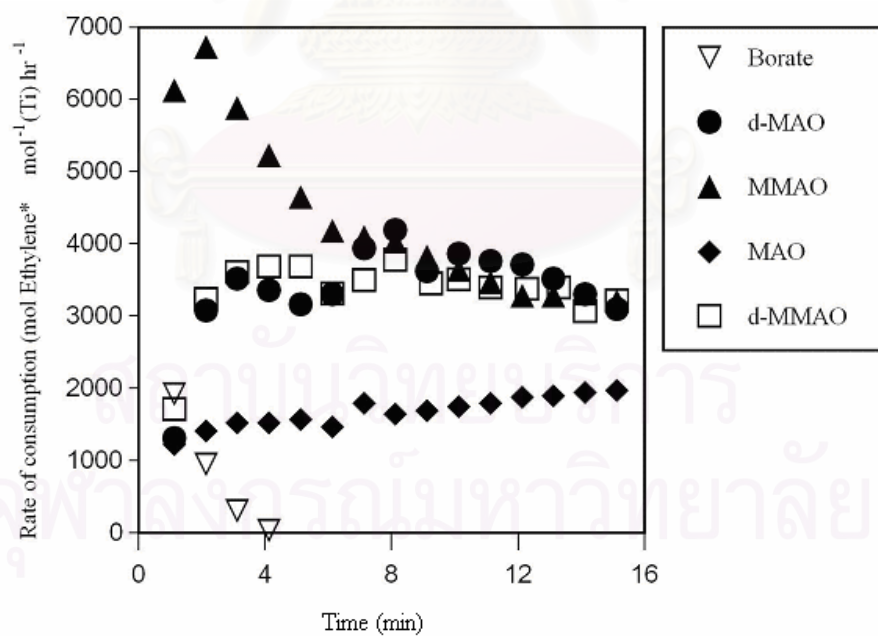


Figure 4.2 Ethylene rate consumption profile of ethylene polymerization with **catalyst 1**/ activators

On the other hand, MAOs and MMAOs systems exhibited the consistence in ethylene consumption rate when polymerization was conducted for several minutes. The consumption rate of ethylene when d-MAO, MMAO, and d-MMAO were employed in ethylene polymerization and ethylene/1-hexene copolymerization are relatively higher than that of when MAO was used as a cocatalyst. These results were evident of lower activities of ethylene polymerization and ethylene/1-hexene copolymerization. Precisely, with MMAO in the ethylene polymerization, showed the highest activity (**Table 4.1**). Moreover, the ethylene polymerization rate at initial was the highest as well. Unfortunately, it is probable due to the production large amounts of polyethylene increased the viscosity in the polymerization medium, toluene, thus prohibiting effective stirring which caused the apparent decrease in the polymerization rate and consequently led to the almost constant catalyst productivity during the several minutes.

Table 4.2: Triad distribution of ethylene/1-hexene copolymer

Co-Catalyst	HHH	EHH	EHE	EEE	HEH	HEE	%E	%H
d-MAO	0.18	0.31	0.10	0.11	0.15	0.15	40	60
MMAO	0.18	0.31	0.10	0.13	0.14	0.14	41	59
d-MMAO	0.14	0.33	0.10	0.15	0.14	0.15	43	57
Borate	0.33	0.36	0.05	0.04	0.15	0.07	26	74

Number average molecular weight (M_n) and molecular weight distribution (MWD) of produced polymer were also summarized in Table 1. Indeed, in the aluminoxane cocatalyst systems, ethylene/1-hexene copolymerizations and 1-hexene homopolymerizations did not exhibit the living nature of polymerization at this condition (40 °C, atmospheric pressure). Moreover, any kind of activators did not affect as seen in 1-hexene homopolymerization system, but the molecular weight distribution was independent with any aluminoxane type of cocatalysts. However, it essentially depended on types of cocatalyst. Surprisingly, in the ethylene homopolymerization systems, not only the molecular weight distribution depended on the cocatalysts, but also number average molecular weight. With MAO as cocatalyst the M_n value was very low due to the chain termination and chain transfer reaction occurred by TMA present in aluminoxane solution. On the other hand, for dried aluminoxane systems exhibit the highest value of M_n . This was probably because

chain transfer reaction and chain termination did not occur in dried aluminoxane system of ethylene homo-polymerization. Therefore, it was perhaps the living behavior of catalyst, was proceed since these systems were absence of TMA. From above, we can propose that chain transfer reaction and/or chain termination of bimetallic active species **catalyst 1**/dried-aluminoxane apparently after 1-hexene insertion.

4.2 Discussion of polymer microstructure

The characteristics of ^{13}C NMR spectra for all copolymers were similar. The triad distributions for all copolymer from ^{13}C NMR monomer insertion are shown in **Table 4.2**. The reactivity of ethylene and 1-hexene were calculated (see appendix D for more detail) using the same method and was shown in **Table 4.3**.

Table 4.3: Relative reactivity value of ethylene and 1-hexene

Co-Catalyst	r_E	r_H	$r_E r_H$
d-MAO	7.09	0.15	1.08
MMAO	7.91	0.16	1.24
d-MMAO	8.63	0.14	1.19
Borate	3.33	0.27	0.89

Based on the triad distribution of ethylene/1-hexene copolymers, we found that microstructure of copolymer obtained from aluminoxane system was slightly different in monomer incorporation, but found significantly when borated system was applied. We suspected that this difference was from the differences in the bimetallic complex active species between $[\text{aluminoxane}]^-[\text{catalyst}]^+$ and $[\text{Borate}]^-[\text{catalyst}]^+$ which had the electronic and geometric effects on the behaviors of co-monomer insertion in our systems, it's caused borate cocatalyst have higher of 1-hexene insertion in more than aluminoxane systems. Furthermore, from the reactivity of ethylene, it indicated that the highest reactivity of ethylene occurred with the presence of MMAO system. This result was similar to what we have found in the homopolymerization. Considering when use the MMAOs as cocatalyst the reactivity

of ethylene and 1-hexene are higher than the reactivities from MAOs system, it indicated that MMAOs cocatalyst not only increased the reactivity of ethylene but also increased the reactivity of 1-hexene at the same time.

In addition, when dried aluminoxanes were used, the reactivity of 1-hexene was found to significantly decrease compared with fresh ones (original MAO and MMAO). We suspected that absences of TMA and TIBA way reduce the probabilities of 1-hexene incorporation in copolymers.

As common, we know that the product value of reactivity of monomer will reflect the stereo regularity of polymer, such as, $r_1r_2 = 1$: alternating copolymer, $r_1r_2 > 1$: block copolymer, $r_1r_2 < 1$: random copolymer [3]. The copolymer produced from MMAO system was outstanding shown that its stereo regularity was a block type since it contained the highest triad of HHH, while the others are mostly contained EHH triad. We proposed that this structure came from the high reactivity of ethylene and 1-hexene of MMAO cocatalyst.

4.3 Summary

Type of activators strongly has strongly influence on the polymer microstructure the aluminoxane system gave less insertion of hexene comonomer than the comonomer produced from the borate system. Moreover, the deactivation of active species occurred for borate system while the aluminoxane system did not. In the view of molecular weight and molecular weight distribution, it should be noted that the molecular weight from borate system is higher than the aluminoxane systems. Unfortunately, it also has the boarder in molecular weight distribution also.

CHAPTER V

EFFECT OF SOLVENT MEDIUMS

In the present study, the effect of solvent mediums used in slurry polymerization of ethylene/1-hexene using the [t-BuNSiMe₂Flu]TiMe₂ catalyst (**catalyst 1**) was investigated. The solvent mediums such as heptane, chlorobenzene (CB), toluene, and dichloromethane (DCM) having different dielectric constant value (ϵ) were studied. The catalytic activities during polymerization were monitored and further discussed. The microstructure of polymer obtained was also investigated.

Based on this study, the catalytic polymerization was performed under slurry process using the solvent as a reaction medium. The different dielectric constant values (ϵ) of solvents were varied such as heptane ($\epsilon = 1.92$), toluene ($\epsilon = 2.38$), chlorobenzene ($\epsilon = 5.68$), and dichloromethane ($\epsilon = 8.93$). Effect of solvent on the catalytic activities and the microstructure were discussed as follows:

5.1 Effect of solvent on the catalytic activity

The catalytic activities based on polymer yields are shown in **Table 5.1**. For EH copolymerization at 70°C, it was found that with using toluene as the polymerization medium, activity was the highest followed by with heptane and chlorobenzene. No activity was observed when dichloromethane was employed. This indicated that the too high dielectric constant of solvent apparently resulted in such a low or no activity. Forlini et al. [50,51,67] also reported that the dielectric constant of solvent could alter the polymerization behaviors in other catalytic systems. The ethylene consumption rate during EH copolymerization at 70°C is shown in **Figure 5.1**. The similar trend for ethylene consumption was observed when heptane and chlorobenzene were employed. It indicated that the ethylene consumption gradually increased, then kept constant at the certain time. However, for toluene, the consumption rate of ethylene was high at the initial state, then decreased with time. This also indicated that no induction period was required when toluene was employed. In addition, the homopolymerization of ethylene and 1-hexene was also performed. For ethylene polymerization, the similar trend as seen for EH copolymerization can be observed as also shown in **Table 5.1** and **Figure 5.2**. There was no activity for 1-hexene

polymerization at the specified polymerization condition. In all cases, the polymerization did not proceed with the use of dichloromethane as a solvent medium.

Table 5.1 Polymerization results^a

Solvent	Polymer type	T	Yield	Activity ^b	Mn (10 ⁴) ^c	MWD ^c
Heptane	E ^d	70	0.75	1000	4.20	3.9
CB	E	70	0.50	400	0.56	3.3
Toluene	E ^d	70	1.13	1507	4.35	3.0
DCM	E	70	- ^e	- ^f	- ^f	- ^f
Heptane	E	0	0.13	107	- ^f	- ^f
CB	E	0	0.10	78	- ^f	- ^f
Toluene	E	0	0.08	63	- ^f	- ^f
DCM	E	0	- ^e	- ^f	- ^f	- ^f
Heptane	EH	70	3.08	2464	2.55	2.2
CB	EH	70	2.06	1648	2.11	5.1
Toluene	EH ^d	70	2.81	3747	4.68	2.1
DCM	EH	70	Trace	- ^f	- ^f	- ^f
Heptane	EH	0	0.89	712	- ^f	- ^f
CB	EH	0	0.13	108	- ^f	- ^f
Toluene	EH	0	0.13	104	- ^f	- ^f
DCM	EH	0	- ^e	- ^f	- ^f	- ^f

^aPolymerization conditions: Ti = 5 μmol , Al/Ti = 1000, 50 psig of ethylene pressure was applied.

^bActivity = $\text{kg}(\text{polymer}) \text{mol}^{-1}(\text{Ti}) \text{hr}^{-1}$.

^cNumber of average molecular weight and molecular weight distributions were measured by GPC analysis using polystyrene as reference.

^dUsing Ti = 3 μmol , Al/Ti = 1000

^ePolymerization did not proceed.

^fNot determined

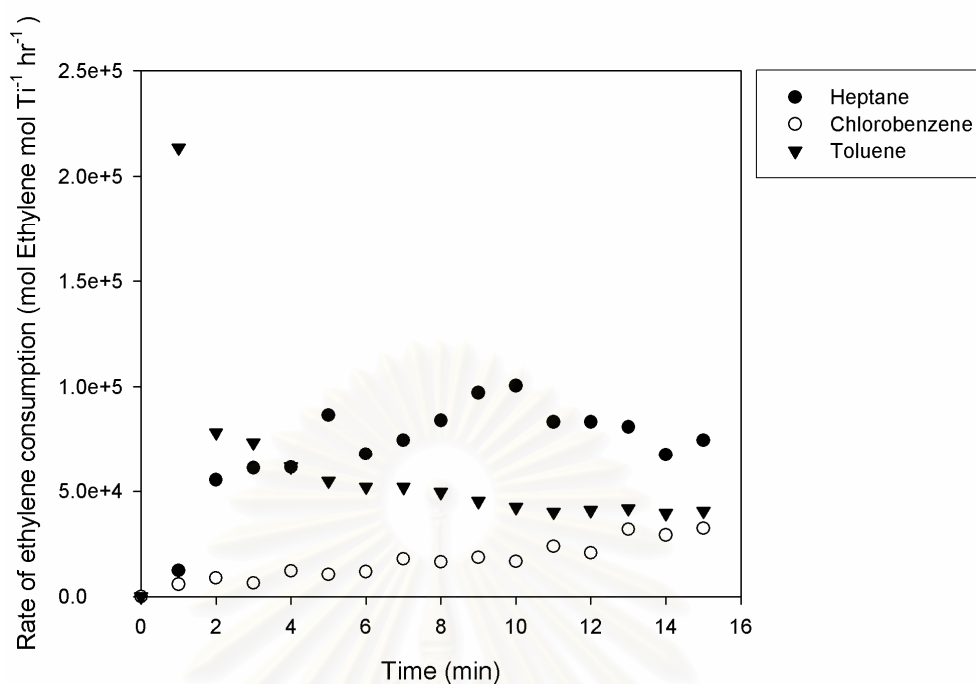


Figure 5.1 Ethylene consumption rate for ethylene/1-hexene copolymerization with various solvent mediums at 70°C

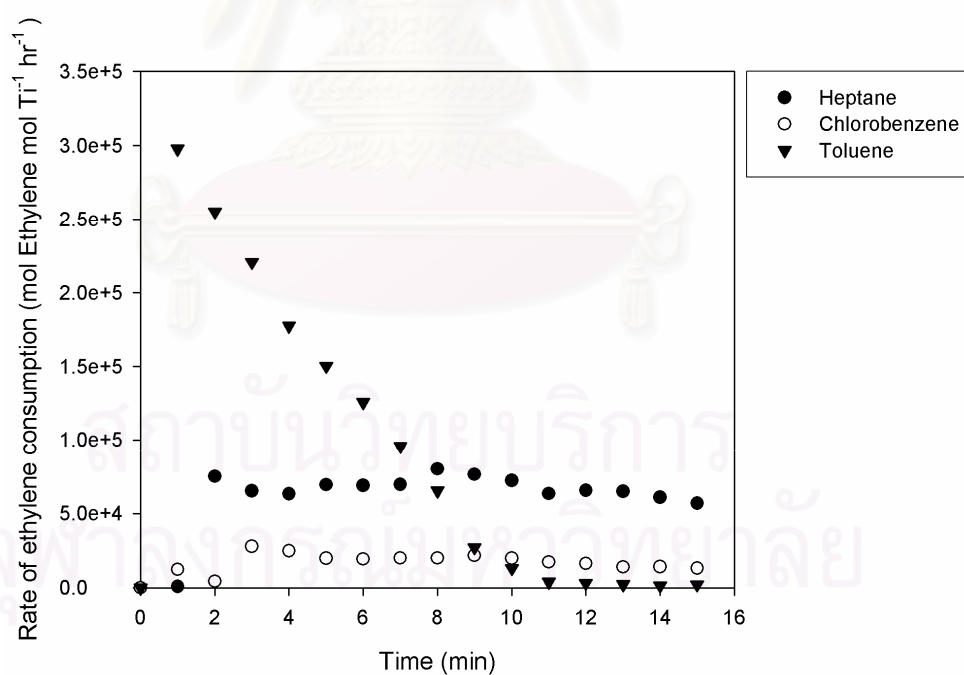


Figure 5.2 Ethylene consumption rate for ethylene polymerization with various solvent medium at 70 °C

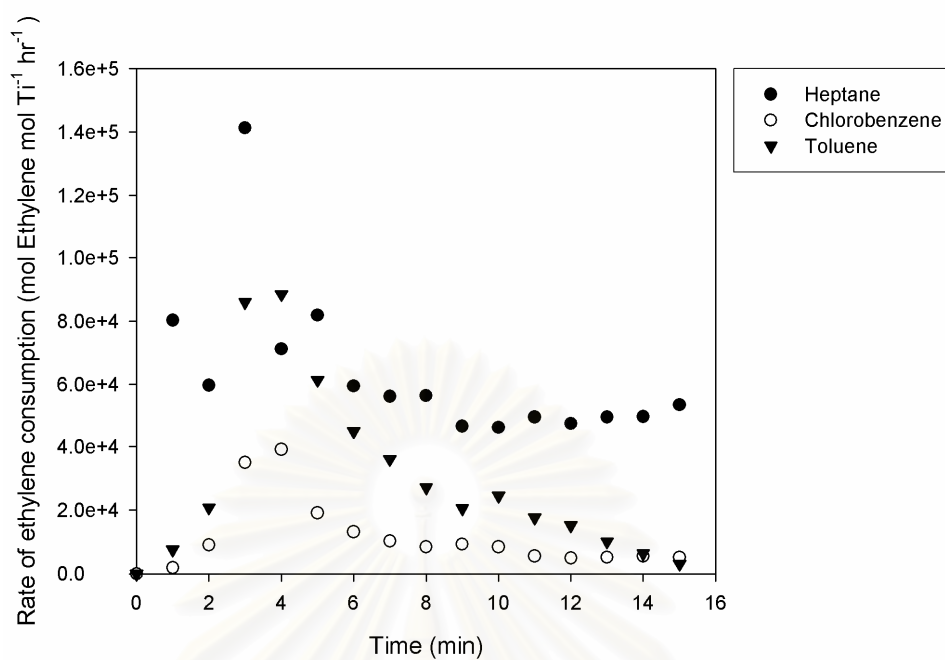


Figure 5.3 Ethylene consumption rate for ethylene/1-hexene copolymerization with various solvent mediums at 0°C

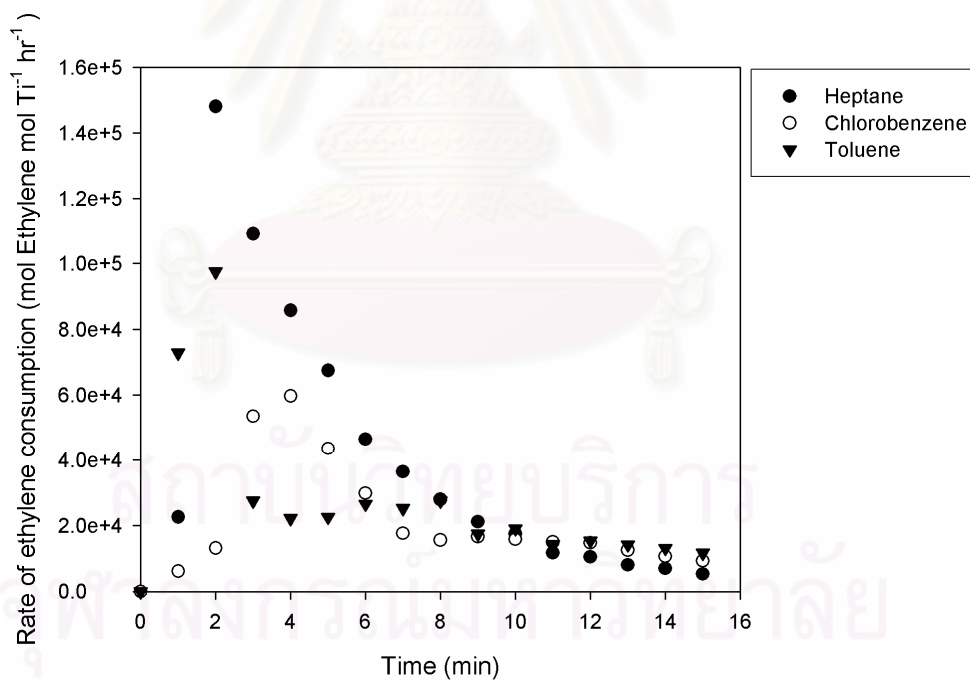


Figure 5.4 Ethylene consumption rate for ethylene polymerization with various solvent mediums at 0°C

Considering the EH copolymerization behaviors at 0°C, the catalytic activities regarding to different solvent mediums are also shown in **Table 5.1**. It can be observed that the activities were much lower (3 to 370 times) than those at 70°C. It indicated that using heptane resulted in the highest activity among other solvent mediums. The change in activity order compared to that at high temperature can be attributed to differences in solvent behaviors when temperature changed. The ethylene consumption rate during EH copolymerization at 0°C is shown in **Figure 5.3**. It can be seen that for all solvent mediums, the ethylene consumption increased until reaching a maximum point, then decreased with time. It also indicated that the highest consumption rate of ethylene was observed when heptane was employed. The homopolymerization of ethylene and 1-hexene was also performed. For ethylene polymerization, the similar trend as seen for EH copolymerization can be observed as also shown in **Table 5.1** and **Figure 5.4**. It should be noted that the resulted activities in **Table 5.1** were based the yields of polymer (or copolymer) obtained. Therefore, they needed to account for the amounts of 1-hexene insertion in the polymer yields as well. **Figures 5.1 to 5.3** showed on the ethylene consumption only during the EH polymerization without the consideration of 1-hexene incorporated. Thus, it was different. **Figures 5.2 and 5.4** revealed the ethylene consumption for ethylene homopolymerization at 70 and 0°C, respectively. Again, it differed from the activities based on yields as seen in **Table 5.1** probably due to the loss of low MW PE during filtration. There was no activity for 1-hexene polymerization at the specified polymerization condition as also seen at 70°C. It should be noted that the major factor to be considered besides the solvent polarity is the solubility of ethylene as a function of solvent and temperature. It is the concentration of the solvent, and not the concentration of ethylene in the gas phase above the solvent, which is directly to the rate of ethylene polymerization. Hence, the solubility of ethylene at 70 and 0°C in the various solvents measured in this study is illustrated in **Table 5.2**. Based on the solubility information as shown here, it indicates that there is no variation in solubility of ethylene in the various solvents. Thus, the solubility of ethylene was not responsible for a significant part of the differences in the measured activities in this present study. On the other hand, the different activities observed were attributed to the solvent polarity itself.

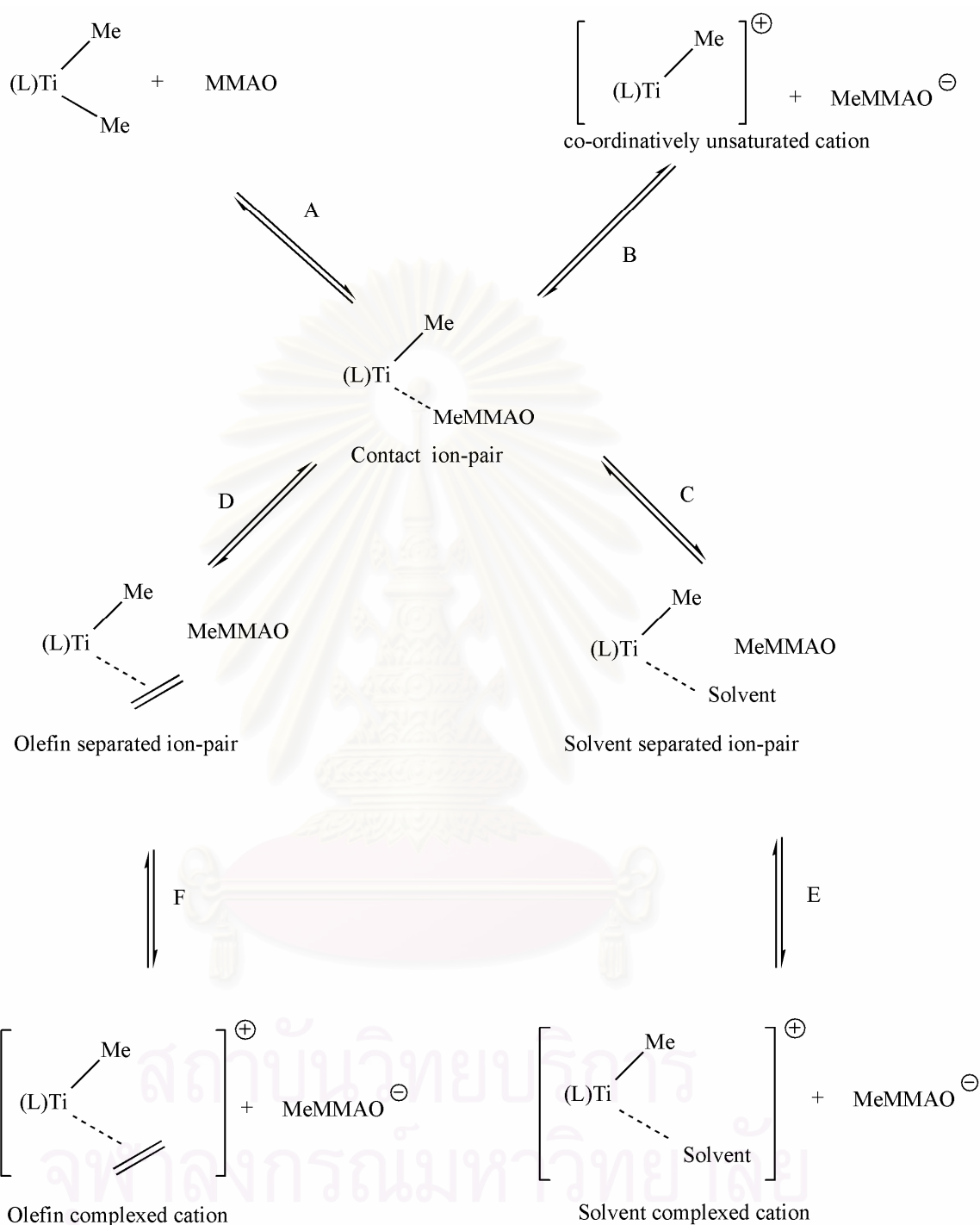
Table 5.2: Solubility of ethylene in different solvents obtained from this study

Solvent	Solubility	
	mol/l ^a	mol/l ^b
Heptane	0.811	1.086
Toluene	0.826	1.115
Chlorobenzene	0.809	1.099

^aT = 70 °C, ethylene pressure = 50 psi

^bT = 0 °C, ethylene pressure = 50 psi

In order to give a better understanding, the conceptual model of solvent effect was redrawn based on the work done by Ziegler group [68] as shown in **Scheme 5.1**. Based on this model, the possible reaction of the contact ion-pair is depicted, where L represents the ligand coordinated to Ti center atom and MMAO represents the cocatalyst used in this work. The activation of the catalyst containing dimethyl group by the cocatalyst (as a Lewis acid) can lead to the formation of a contact ion-pair as seen in pathway A. In some case, the cocatalyst can produce the reaction mixture with the contact ion pair, then dissociate into completely solvated cation and anion as shown in pathway B. Besides, a molecule of the solvent can interact with the cationic moiety pushing away the anion to form the solvent separated ion-pair as shown in pathway C. From pathway C, with the strongly coordinating solvent, the solvation of ion-pair can lead to the formation of the solvent complexed cation with the counter anion sufficiently far away as shown in pathway E. In addition, pathway D indicates the case when olefin insertion is present. With further insertion of olefin, the dissociation of ion-pair results to form the olefin complexed cation as seen in pathway F. With different solvent mediums, there are different coordination abilities. Therefore, those affect the relative population of the active species and models. In general, in non-polar solvent, the dominant species is the contact ion-pair whereas for the aromatic solvent, there are solvent separated ion-pair and solvent complexed cation. [50,51,68]



Scheme 5.1 Conceptual model of solvent effect redrawn based on the work by Ziegler group [68]

Based on the possible reaction of the contact ion-pair model, the following considerations regarding to the solvent effect can be proposed; (i) the polarity of solvent greatly affects the polymerization activity where the high polarity of solvent

gives high activity until the ion-pair becomes fully separated (at 70°C, $[\text{activity}]_{\text{toluene}} > [\text{activity}]_{\text{heptane}} > [\text{activity}]_{\text{dichlorobenzene}}$), (ii) at low temperature, heptane gives the highest activity since the interaction between cationic and solvent is less than the interaction between cationic and monomer. Therefore, the less polarity of solvent results in high polymerization activity.

5.2 Polymer microstructure

A quantitative analysis of triad distribution for all polymer samples was performed on the basis assignment of the ^{13}C NMR spectra of ethylene/1-hexene copolymer [57]. The triad distribution and reactivity ratios of monomer were shown in **Tables 5.3** and **5.4**, respectively. At 70°C, it showed that insertion of 1-hexene was the highest with chlorobenzene. Therefore, it was suggested that the higher dielectric constant of solvent resulted in the higher degree of 1-hexene insertion. It also indicated that the polymers obtained from all solvent mediums were block polymers ($r_E \cdot r_H > 1$). Considering the effect of solvent at 0°C as also shown in **Tables 5.3** and **5.4**, the similar trend for 1-hexene insertion was still observed where the chlorobenzene system showed the highest insertion of 1-hexene. In addition, the block polymer was still obtained in the chlorobenzene system whereas the toluene and heptane systems gave the alternating polymer ($r_E \cdot r_H < 1$). This was suggested that at low temperature, the gap between the cation and anion for the contact ion-pair (**Scheme 5.1**) could be enlarged only with the solvent having high dielectric constant value. Therefore, the high degree of 1-hexene insertion would be preferred resulting in increased reactivity ratio of 1-hexene (r_H) value.

Table 5.3 Triad distribution of copolymer obtained from ^{13}C NMR

Solvent/T	HHH	EHH	EHE	EEE	HEH	HEE
Toluene70	0.190	0.208	0.106	0.190	0.134	0.172
Heptane70	0.097	0.243	0.124	0.203	0.137	0.196
CB70	0.607	0.074	0.052	0.071	0.106	0.090
Toluene0	0.004	0.236	0.171	0.208	0.103	0.279
Heptane0	0.041	0.202	0.154	0.218	0.111	0.275
CB0	0.359	0.239	0.072	0.046	0.159	0.124

Table 5.4 Monomer incorporation and the reactivity ratio

Solvent/T	%E	%H	$r_E r_H$
Toluene70	50	50	1.76
Heptane70	54	46	1.14
CB70	27	73	5.17
Toluene0	59	41	0.60
Heptane0	60	40	0.80
CB0	33	67	1.21

Table 5.5 Melting temperature and % crystallinity of polymer produced

Polymer/solvent/T	T_m	% Crystallinity ^a
E(Toluene70)	132	62
E(Heptane70)	133	59
E(CB70)	124	64
EH(Toluene70)	- ^b	- ^c
EH(Heptane70)	-	-
EH(CB70)	-	-

^aCalculated from heat of crystalline formation based on HDPE

^bValue not be detected from the measurement

^cCan not be calculated without T_m

5.3 Thermal properties

The melting temperature (T_m) obtained from DSC of polymer obtained is shown in **Table 5.5**. The typical DSC scans for the crystalline as well as non-crystalline products are shown in **Figure 5.5**. (see scanned peak in appendix C) It can be observed that for ethylene polymerization the T_m ranged between 124 to 133°C. In general, T_m is proportional to the crystallinity of polymer. This was suggested that using the solvent having high dielectric constant value apparently resulted in decreased crystallinity of polymer. However, considering the copolymerization of ethylene/1-hexene, no T_m was observed in all systems. The non-crystalline polymers obtained were attributed to the high degree of 1-hexene insertion as mentioned before.

5.4 Summary

In this chapter, it clearly revealed that the different of solvent medium that we employed to the polymerization process exhibited the different results. The high polarity solvent gave the high polymerization activity, unfortunately too high dielectric constant solvent, the productivity could be reduced until not active. Moreover, the polarity of solvent medium not affects only the activity but also the polymer microstructure. Thus, suitable solvent should be prepared for the desired condition of LLDPE that we want to synthesize.

CHAPTER VI

EFFECT OF SECOND MONOMERS

Nowadays, several researchers have shown that the type of catalyst has an important effect on the structure and molecular weight of polymer [41-46]. However, very few comparable studies show how the type of comonomer influences the activity and polymer properties.

With the active species ion pair model which has investigated by Mary *et al.* [68] reported that the contact ion pair model of active species could altered to the olefin separated ion pair and further to olefin complex cation model. Changing the α -olefin type affect to the active species formation between cationic complex and counter anionic due to the steric of the copolymer propagate from each active species. A density functional study with the conductor-like screening model of the CGC catalyst/MAO on the initiation and the propagation state of ethylene polymerization was done by Yang *et al.* [69]. It reported that the distance for the monomer insertion was increased by the first monomer form the olefin coordinate model to ion pair. Thus, from these studies, we purposed that with the different type of monomer insert to the active species ion pair model caused the different behavior of ethylene/ α -olefin copolymerization behavior.

In the present chapter, we are communicating the result of polymerization of the temperature effect and the α -olefin monomer in ethylene/ α -olefin polymerization behaviors. Polymerizations were proceeded with [t-BuNSiMe₂Flu]TiMe₂ and modified-methylaluminoxane (MMAO) system by using heptane as solvent medium. Polymer properties and polymer microstructure were investigated to suggest the interpretation of solvent polarity effect on the comonomer composition and polymer distribution. Ethylene and ethylene/ α -olefin polymerization was conduct by using heptane as solvent medium. The temperature parameter which was chosen to study on this paper is 0 °C and 70 °C. Polymerization was done by catalyst1/MMAO system. The result and polymer characterization were described below.

6.1 Effect of α -olefin comonomer

According to the **Table 6.1**, it is clearly illustrated that the productivity of polymerization increased with the insertion of second α -olefin monomer both at 0 °C and 70 °C of polymerization. These phenomena are commonly well known as the second comonomer effect in copolymerization behavior [67]. At 70 °C of polymerization temperature, the copolymerization of ethylene/ α -olefin gave the highest activity with 1-octene play the role as α -olefin monomer. As we seen the ethylene consumption rate on the polymerization at 70 °C as shown in **Figure 6.1**, it exhibited that the highest consumption rate was found only when 1-octene monomer was chosen to incorporate the copolymerization. On the other hand, others system, either the copolymerization of ethylene/ α -olefin or the polymerization of polyethylene, it showed the same ethylene consumption behaviors. At the initial period of polymerization, the ethylene consumption gradually increased with time after that the consumption rates of ethylene remain almost constant. However, when 1-octene was applied as the second monomer, the ethylene consumption behavior was totally changed. The high rate of ethylene consumption was appear at the initial rate and then gradually decreased with time until reach the value same as the other systems did. From this evident, it should be noted that the active species of ion pair can be affected from the second monomer in polymerization. In this case the proper geometry and steric of 1-octene can generate the highest activity in ethylene/ α -olefin polymerization at 70 °C. Again, from **Table 6.1**, we found that the molecular weight of polymer was reduced when the copolymerization was conducted. Thus, it probably we can pronounced that on the copolymerization, the chain transfer of polymer occurred after the α -olefin insertion unit. Moreover, with the higher α -olefin monomer, we obtained the higher molecular weight of copolymer. This result can interpreted with the larger molecule of α -olefin can increased the gap between the cationic active species and counter anion more separated [68]. Thus, it is more easily to the monomer to raise the propagation rate of polymer chain before the chain was terminated. As we found that molecular weight of polymer was reduced with the present of α -olefin, but the molecular weight distribution of copolymer is narrower than the polyethylene polymerization system. With these result, we can said that the chain transfer to the α -olefin monomers affect to the molecular weight distribution of

polymer. Moreover, the molecular weight distribution of copolymer is independent from the second monomer unit as show in the **Table 6.1** MWD of copolymer did not change with the α -olefin unit.

Table 6.1 Polymerization results^a

polymer	Temp. (°C)	Yield(g)	Activity ^b	Mn ^c	MWD ^c	T _m ^d
E	70	0.75	1000	4.2	3.9	134
EH	70	3.08	2464	2.6	2.2	n/a
EO	70	3.52	2820	3.60	2.0	n/a
ED	70	2.31	1846	3.63	2.1	99
E	0	0.13	107	- ^e	- ^e	- ^e
EH	0	0.89	712	- ^e	- ^e	- ^e
EO	0	0.45	364	- ^e	- ^e	- ^e
ED	0	0.42	336	- ^e	- ^e	- ^e

^aPolymerization conditions: Ti = 5 μ mol, Al/Ti = 1000, 50 psig of ethylene pressure.

^bActivity = kg(polymer) mol⁻¹(Ti) hr⁻¹.

^cNumber of average molecular weight and molecular weight distributions were measured by GPC analysis using poly styrene as reference.

^dMeasure by DSC (°C)

^eNot determined due to low activiry

n/a = not available to detect

Polymerization result at 0 °C result was shown in **Table 6.1**. Again, the activity of copolymerization between ethylene and α -olefin is higher than ethylene polymerization. Thus it can conclude that the temperature did not affect the second monomer phenomena by using this catalyst with MMAO system. With the polymerization result, it revealed that the highest activity was found when 1-hexene was chosen to copolymerization. Moreover, the larger molecule of α -olefin caused the reduction of polymerization activity. This event was confirmed by the ethylene consumption rate profile of ethylene and ethylene/ α -olefin polymerization at 0 °C which demonstrated in **Figure 6.2**. It showed that polymerization behavior either ethylene polymerization or ethylene/ α -olefin copolymerization is independent from the second monomer unit. The tren Ethylene consumption rate rapidly increased with time at the initial period of polymerization until reach the maximum value. After that, rate of ethylene consumption gradually decreased with time until reach one value and keep constant. for ethylene consumption behavior show the same characteristic.

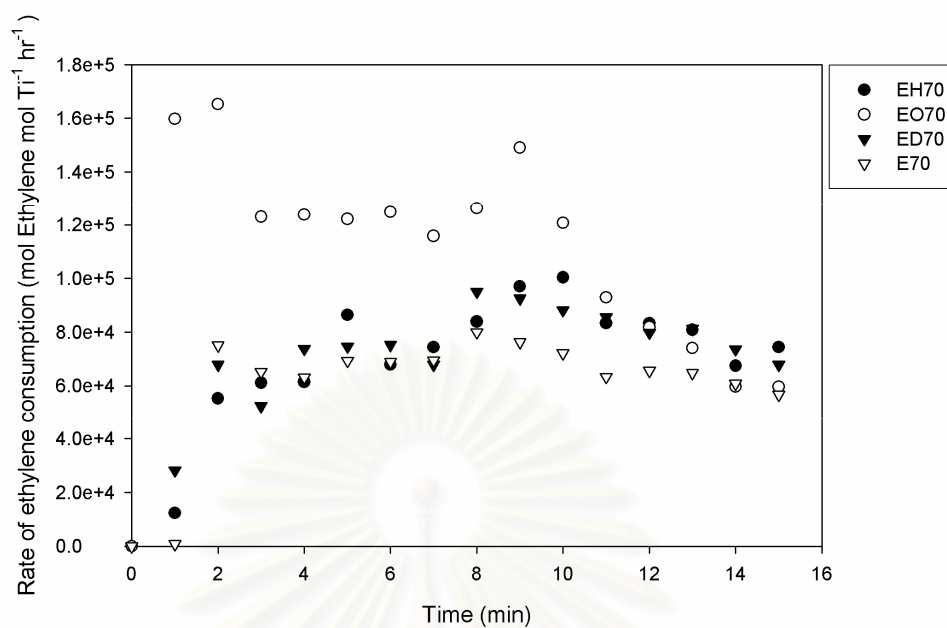


Figure 6.1 Ethylene rate consumption profile of ethylene/ α -olefin copolymerization and ethylene polymerization at 70 °C

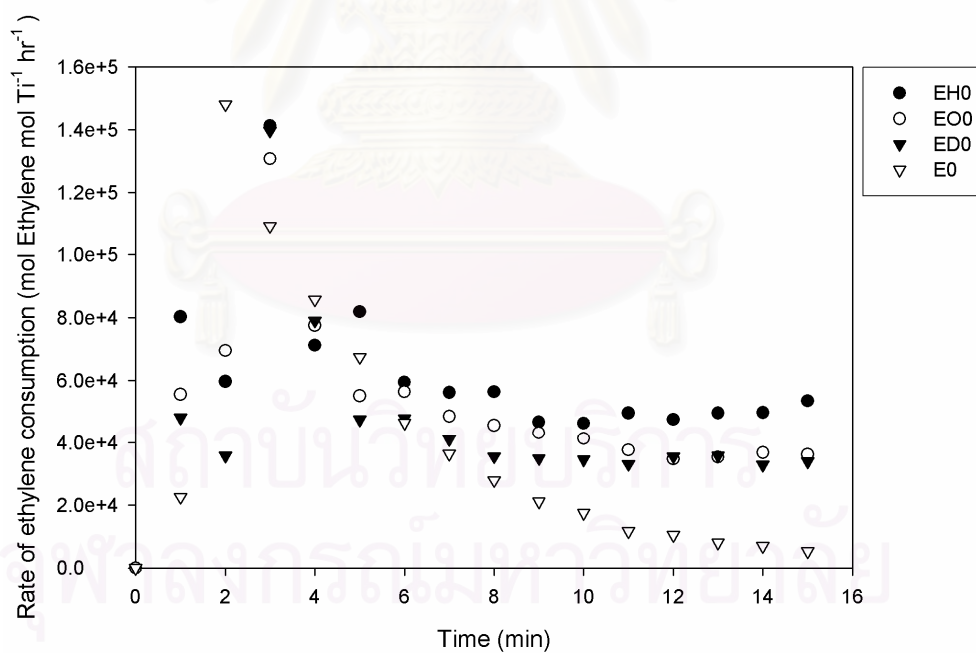


Figure 6.2 Ethylene rate consumption profile of ethylene/ α -olefin copolymerization and ethylene polymerization at 0 °C

From the ethylene consumption rate profile, it clearly showed that the rate of ethylene consumption in copolymerization system was higher than the homopolymerization system. This result we interpreted in term of the α -olefin insertion unit affect the ion pair model of polymerization. Thus, the higher activity came from the more easily of ethylene propagation and the α -olefin insertion unit also. However, due to the larger molecule of α -olefin unit could generate the bulky steric around the polymer chain; therefore, it caused the monomer insertion to the catalyst active species more difficult. Thus the activity decreased in order of 1-hexene > 1-octene > 1-decene.

Comparing the result of polymerization at 70 °C and 0 °C, it clearly exhibited temperature was the one important parameter in polymerization. The higher temperature increased the polymer activity due to the faster rate of propagation. Thus it causes activity increase. Moreover, α -olefin type did not influence the polymerization behavior as we noticed at 0 °C the polymerization behavior did not change with the size of α -olefin applied. Because of, at 0 °C the motive of each molecule in solvent medium was low. Thus the type of monomer insertion to the active species did not show a significant change in polymerization behavior. On the other hand, at 70 °C polymerization pattern affected by the olefin sizes as we seen, the highest activity was obtained when 1-octene comonomer was employed. This phenomenon could interpret via the active species formation was interfered by the α -olefin insertion unit. Because the insertion of α -olefin increased the space between the cationic active species and counter anion, therefore the increased of activity of 1-octene copolymerization compare with 1-hexene copolymerization was discovered. However, it is not always that the larger molecule of monomer gave the higher activity of polymerization. Ethylene/1-decene polymerization was performed, showed that the activity was less than ethylene/1-octene copolymerization, but it still higher than copolymerization with 1-hexene. Thus, it should be noted that, the larger molecule of α -olefin monomer can cause the active species ion pair to form the olefin complex cation. Moreover with the separation of ion pair, it required energy of formation to form the active species complexes. Therefore, the activity of polymerization decreased with the larger space between complex cation and counter anion. [69]

6.2 Polymer microstructure

A quantitative analysis of triad distribution for all copolymer samples was performed on the basis assignment of the ^{13}C -NMR spectra of ethylene/1-hexene copolymer [57]. Triad distribution and product reactivity ratio of monomer were shown in **Table 6.2 and 6.3**.

According to the monomer incorporation in the polymer chain distribution data, the polymerization result at 70 °C showed that the insertion of α -olefin copolymer influenced polymer microstructure. Copolymerization between ethylene and 1-hexene gave the highest insertion of α -olefin unit, and the amount of α -olefin insertion decreased with the increasing of carbon atoms in the α -olefin monomer. It indicated that for the large molecule of α -olefin, the monomer activity decreased. Thus, we can announced that with the larger molecule of α -olefin, it could generate the higher activity as we discuss above, on the other hands the monomer insertion to the polymer backbone was decreased too. Next focus on the copolymer structure, it showed that the copolymerization with this titanocene catalyst/ MMAO system by using heptane as solvent medium, the obtained copolymer gave the random-block structure. Comparing the result from the different monomer, it clearly showed that 1-decene gave the highest block structure in among of other α -olefin employed. From this evidence, it could be confirmed that with the higher alkene monomer, ethylene monomer played more important role on the polymer chain propagation step therefore, the blockier of copolymer structure was increased. Thus, the polymer microstructure of ethylene/1-decene showed the highest content of ethylene monomer and also the highest of [EEE] triad distribution too. Moreover, with the decreasing of ethylene insertion unit, comparing the result between ethylene/1-octene and ethylene/1-hexene copolymer, the triad distribution of [EEE] was decreased with the lower molecule of α -olefin monomer too. On the similar way, the triad distribution of [CCC] unit decreased with the increasing of the carbon atom number of α -olefin monomer.

Table 6.2 Triad distribution of copolymer

Batch	CCC	ECC	ECE	EEE	CEC	CEE
EH70	0.097	0.243	0.124	0.203	0.137	0.196
EO70	0.064	0.136	0.119	0.362	0.086	0.233
ED70	0.025	0.106	0.096	0.558	0.064	0.150
EH0	0.041	0.202	0.154	0.218	0.111	0.275
EO0	0.000	0.078	0.147	0.384	0.068	0.323
ED0	0.007	0.078	0.110	0.526	0.046	0.234

Again, the triad distribution and copolymer composition result from ethylene/ α -olefin polymerization was showed in **Table 6.2 and 6.3** respectively. It should be noted that, the α -olefin incorporation in the main chain of copolymer was decreased as the larger of α -olefin monomer applied. Furthermore, the copolymer microstructure showed the random-alternating copolymer with the polymerization at 0 C. However, it could be noted that the alternating structure was decreased in order of 1-hexene > 1-octene > 1-decene. This phenomenon can be interpreted in the term of monomer activity, it could say that 1-decene monomer is the slowest activity in the insertion step and 1-octene monomer is faster while the 1-hexene monomer is fastest. Thus, when 1-decene monomer was employed for the copolymerization the block of ethylene unit was not be interfered from the insertion of 1-dencene monomer. Therefore, the alternating structure was reduced.

Table 6.3 Monomer incorporation and its structure

Batch	%E	%C	r_{EC}
EH70	54	46	1.14
EO70	68	32	1.67
ED70	77	23	2.36
EH0	60	40	0.60
EO0	77	23	0.59
ED0	80	20	0.88

Comparing the result of copolymerization at 0 and 70 °C in the view of polymer microstructure, it should be noted that, the temperature was not affect on the α -olefin incorporation trend. Both polymerization conditions showed the decreasing of α -olefin insertion in the polymer main chain as the larger atom of α -olefin used in processes. However, it also clearly exhibited that the polymer microstructure are totally difference. All of the polymers which conduct from high temperature system showed the random-block structure. On the other hand, the polymers that produced from low temperature system gave the random-alternating structure. It was probably due to the different of monomer activity improving by changing of temperature. Since, the rising temperature caused the higher activity of ethylene monomer than the α -olefin monomer. Thus, ethylene monomer had more chance to produce the [EEE] triad with the less interfere from the α -olefin unit and the blockier of copolymer was obtained. Finally, it conclude that the temperature of polymerization was not affect to the trend of monomer incorporation whereas the significantly change in polymer microstructure was observe with changing of the polymerization temperature.

6.3 Thermal analysis of polymer

According to the **Table 6.1**, the melting temperatures of each polymer that produced from the different α -olefin incorporated were reported. For ethylene polymerization, we found that the melting temperature about 134 °C that commonly for polyethylene polymer [71, 72]. On the other hand, it clearly revealed that the melting temperature of polyethylene produced from ethylene/ α -olefin copolymerization system was disappeared except in the case of ethylene/1-decene copolymerization. This phenomenon was attributed to the high amounts of α -olefin contained in the copolymer resulted in decreased crystallinity for polyethylene [70]. However, comparing the result of polymerization at 70 °C and 0 °C, it showed that at the low temperature of polymerization although the insertion of α -olefin is less, but the polymer microstructure is alternating, the synthesized polymer was not showed the crystalline melting temperature. Thus, it can be concluded that ethylene/ α -olefin copolymer produced from these systems did not have any crystalline phases unless it was copolymerized with 1-decene at the high enough temperature to produce the ethylene block sequence length in polymer backbone.

6.4 Summary

LLDPE can be synthesized from the ethylene and α -olefin. Various size of α -olefin employed to polymerize in this chapter reveal that the different of α -olefin will affect on both activity and also the polymer microstructure of the LLDPE. As we seen that highest activity was found when 1-octene applied to the system and followed with 1-hexene and 1-decene. Therefore, we can conclude that the steric of the monomer influence the active species formation and further to the insertion of the monomer. Thus, the different of monomer gave the different result of LLDPE properties at the final.



สถาบันวิทยบริการ
จุฬาลงกรณ์มหาวิทยาลัย

CHAPTER VII

EFFECT OF CATALYST STRUCTURE

Several groups [73-80] have studied ethylene copolymerizations with a variety of α -olefins (C₃–C₁₈) using Group 4 metallocene catalysts with methylaluminoxane (MAO). Among the observations from this earlier work was that *ansa*-metallocenes with one or two atoms as bridging groups were more effective for incorporating comonomers than the unbridged metallocenes.[73-80] An even greater tendency for the incorporation of higher α -olefins is evident for the syndiospecific catalyst system, Me₂C(Cp)(Flu)ZrCl₂ (Cp = cyclopentadiene, Flu = fluorene)/MAO. In summary, the comonomer reactivity and intramolecular properties of ethylene-based copolymers may be tuned by investigating the role played by (a) π -ligands—the bridge connecting the two cyclopentadienyl (Cp) ligands and the substituents on the Cp rings; (b) σ – ligands—chlorine, alkyl, amide, or binaphetol; and (c) polymerization parameters such as [Al]/[Ti] ratio, polymerization temperature, cocatalytic system, and solvent.

In the present work, we are communicating the result of polymerization of the solvent polarity along with temperature effect on the ethylene polymerization and also ethylene/1-hexene polymerization behaviors. Polymerizations were proceeded with [t-BuNSiMe₂Flu]TiMe₂ (**Flu catalyst**) and [t-BuNSiMe₂(C₅Me₅)]TiMe₂ (**CGC catalyst**) with modified-methylaluminoxane (MMAO) as cocatalyst on the different dielectric constant solvents such as heptane, toluene, chlorobenzene. Polymer properties and polymer microstructure were further investigated to suggest the interpretation of solvent polarity effect on the comonomer composition and distribution

Based on this study, the catalytic polymerization was investigated under slurry process using the solvent as a reaction medium. The different dielectric constant values (ϵ) of solvents were varied such as heptane ($\epsilon = 1.92$), toluene ($\epsilon = 2.38$), and chlorobenzene ($\epsilon = 5.68$). And also the steric effect of the catalyst was studied by changing the ligand. Effect of solvent and catalyst structure on the catalytic activities and the microstructure were discussed as follows:

7.1 Effect of solvent on the catalytic activity

The catalytic activities based on polymer yields are shown in **Table 7.1**. For EH copolymerization at 70°C with **CGC catalyst**, it was found that the highest activity was found in chlorobenzene solvent and follow with the toluene and heptane respectively. This indicated that the higher dielectric constant of solvent can give the higher result of polymer activity for **CGC/MMAO** system. Forlini et al. [50,51] also reported that the dielectric constant of solvent could alter the polymerization behaviors in other catalytic systems by using $\text{Et}(\text{Ind})_2\text{ZrCl}_2$ catalyst for propylene/1-hexene copolymerization. From this study it also reported that the activity of polymerization depended on the solvent polarity in the same trend. The ethylene consumption rate during EH copolymerization at 70°C is shown in **Figure 7.1**. The similar trend for ethylene consumption was observed when heptane and toluene were employed. It indicated that the ethylene consumption gradually decreased, then kept constant at the certain time. However, for chlorobenzene, the consumption rate of ethylene was increased at the initial state, after that, it decreased with time to the constant value. This also indicated that no induction period was required when heptane and toluene were employed for catalyst **2/MMAO** systems. In addition, the homopolymerization of ethylene and 1-hexene was also performed. For ethylene polymerization, the similar trend as seen for EH copolymerization can be observed as also shown in **Table 7.1** and **Figure 7.2**. There was no activity for 1-hexene polymerization at the specified polymerization condition.

Considering the EH copolymerization behaviors at 0°C, the catalytic activities regarding to different solvent mediums are also shown in **Table 7.1**. It can be observed that the activities were much lower (10 to 500 times) than those at 70°C. It indicated that using heptane resulted in the highest activity among other solvent mediums. The change in activity order compared to that at high temperature can be attributed to differences in solvent behaviors when temperature changed. The ethylene consumption rate during EH copolymerization at 0°C is shown in **Figure 7.3**.

Table 7.1 Polymerization results with CGC/MMAO system^a

Solvent	polymer	T	Yield (g)	Activity ^b	Mn (10 ⁴) ^c	MWD ^c
Heptane	EH	70	0.98	3909	6.59	2.18
CB	EH	70	2.36	9438	6.72	2.48
Toluene	EH	70	2.19	8778	9.09	2.17
Heptane	E	70	0.27	1073	24.49	3.21
CB	E	70	0.38	1538	18.69	3.75
Toluene	E	70	0.31	1254	13.90	3.11
Heptane	H	70	- ^e	- ^e	- ^e	- ^e
CB	H	70	- ^e	- ^e	- ^e	- ^e
Toluene	H	70	- ^e	- ^e	- ^e	- ^e
Heptane	EH	0	0.04	146	- ^d	- ^d
CB	EH	0	0.01	42	- ^d	- ^d
Toluene	EH	0	0.03	105	- ^d	- ^d
Heptane	E	0	0.03	138	- ^d	- ^d
CB	E	0	0.07	264	- ^d	- ^d
Toluene	E	0	0.05	192	- ^d	- ^d
Heptane	H	0	- ^e	- ^e	- ^e	- ^e
CB	H	0	- ^e	- ^e	- ^e	- ^e
Toluene	H	0	- ^e	- ^e	- ^e	- ^e

^aPolymerization conditions: Ti = 3 μmol , Al/Ti = 1000, 50 psig of ethylene pressure was applied.

^bActivity = $\text{kg}(\text{polymer}) \text{mol}^{-1}(\text{Ti}) \text{hr}^{-1}$.

^cNumber of average molecular weight and molecular weight distributions were measured by GPC analysis using polystyrene as reference.

^dNot determined

^ePolymerization did not proceed.

Noticely, let focus on the ethylene polymerization at 0°C. It indicated that the polymerization activity was also follow by the order of the dielectric constant values. On ther other hands, the trend of activity for ethylene/1-hexene copolymerization is not in the trend of solvent polarity. This phenomena was attribut to the interfere of 1-hexene in the system.

It can be seen that for all solvent mediums, the ethylene consumption increased until reaching a maximum point, then decreased with time. It also indicated that the highest consumption rate of ethylene was observed when chlorobenzene was employed.

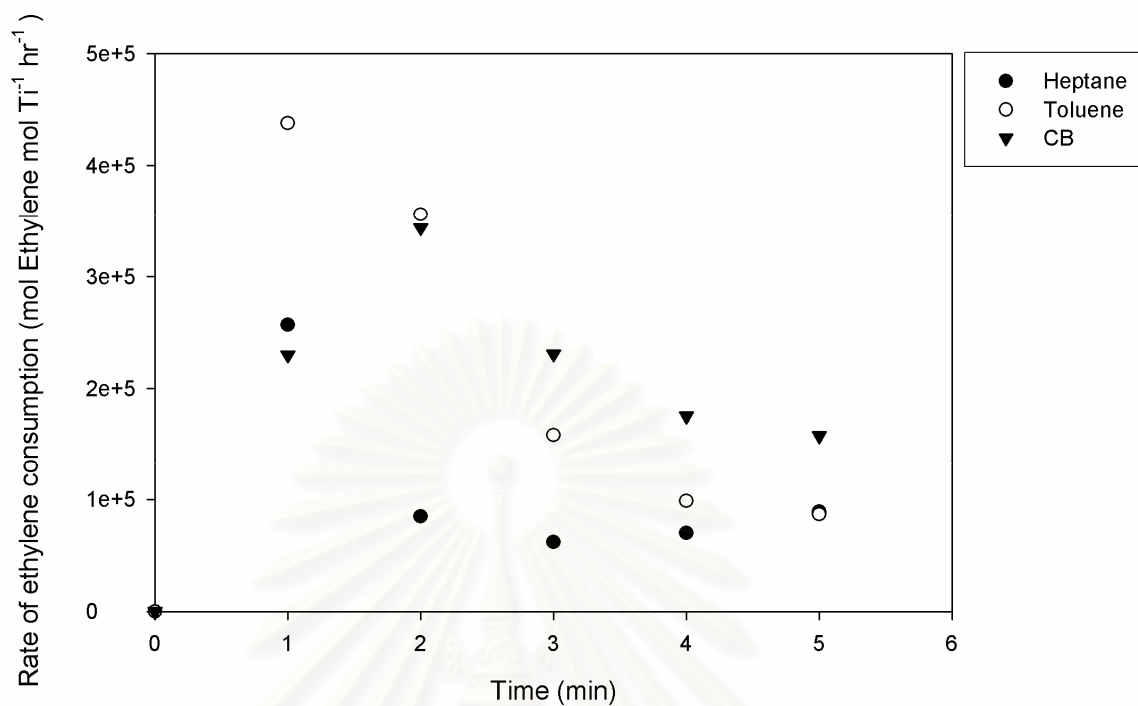


Figure 7.1 Ethylene rate consumption profile of ethylene/1-hexene copolymerization with various solvent of CGC/MMAO at 70 °C

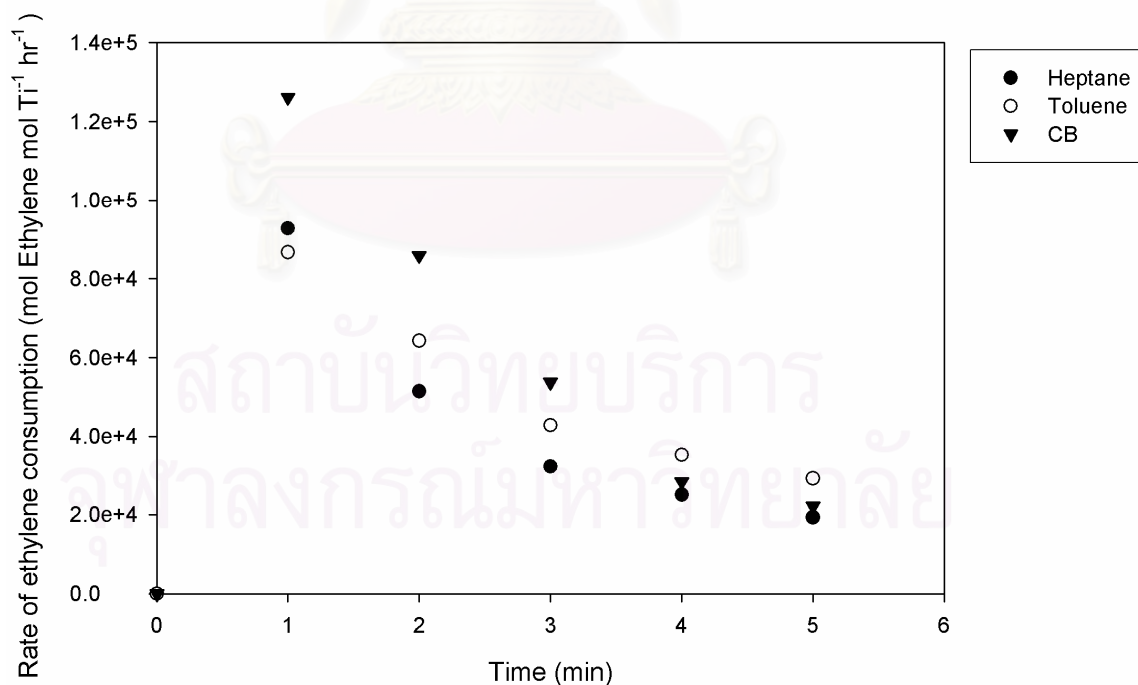


Figure 7.2 Ethylene rate consumption profile of ethylene polymerization with various solvent of CGC/MMAO at 70 °C

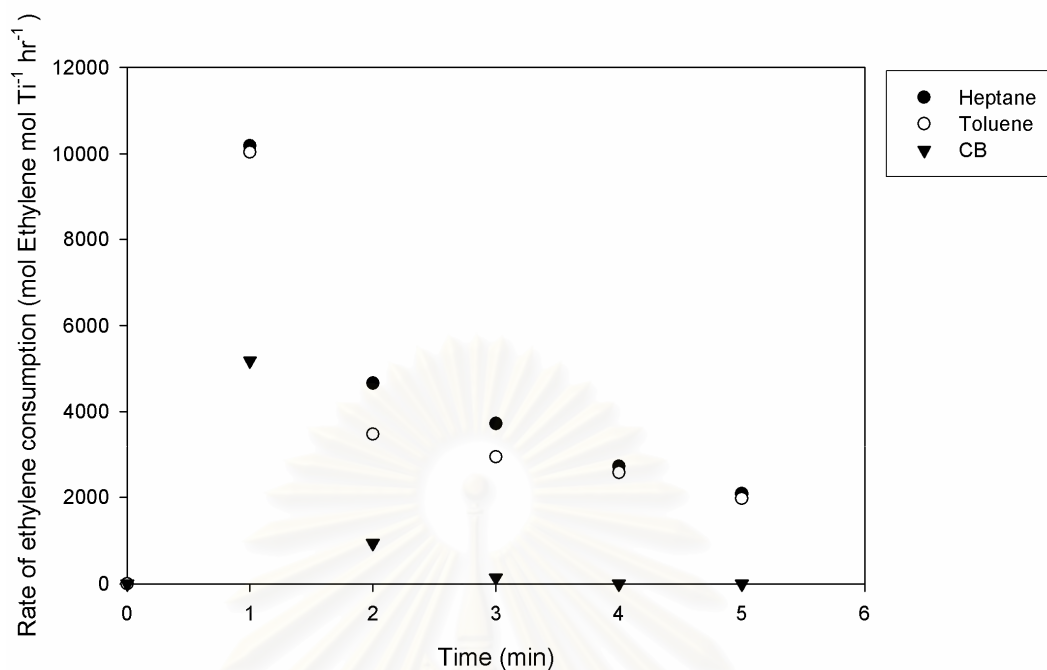


Figure 7.3 Ethylene rate consumption profile of ethylene/1-hexene copolymerization with various solvent of CGC/MMAO at 0 °C

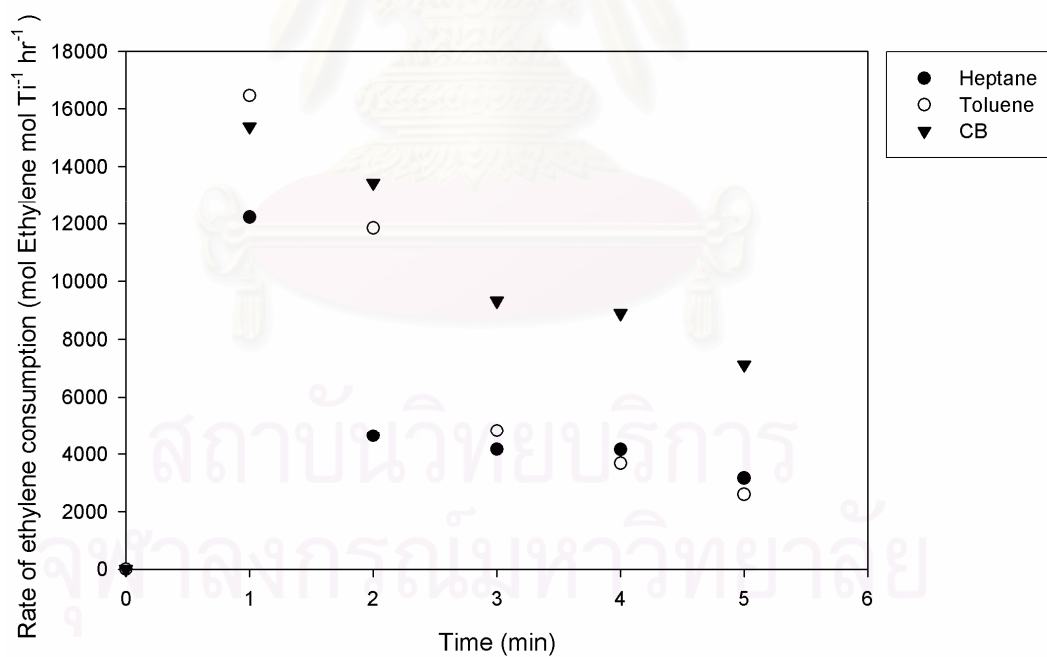


Figure 7.4 Ethylene rate consumption profile of ethylene polymerization with various solvent of CGC/MMAO at 0 °C

Table 5.1 (Repeated) Results for Flu catalyst^a

Solvent	Polymer type	T	Yield	Activity ^b	Mn (10 ⁴) ^c	MWD ^c
Heptane	E ^d	70	0.75	1000	4.20	3.9
CB	E	70	0.50	400	0.56	3.3
Toluene	E ^d	70	1.13	1507	4.35	3.0
Heptane	E	0	0.13	107	- ^f	- ^f
CB	E	0	0.10	78	- ^f	- ^f
Toluene	E	0	0.08	63	- ^f	- ^f
Heptane	EH	70	3.08	2464	2.55	2.2
CB	EH	70	2.06	1648	2.11	5.1
Toluene	EH ^d	70	2.81	3747	4.68	2.1
Heptane	EH	0	0.89	712	- ^f	- ^f
CB	EH	0	0.13	108	- ^f	- ^f
Toluene	EH	0	0.13	104	- ^f	- ^f

^aPolymerization conditions: Ti = 5 μmol , Al/Ti = 1000, 50 psig of ethylene pressure was applied.

^bActivity = $\text{kg}(\text{polymer}) \text{mol}^{-1}(\text{Ti}) \text{hr}^{-1}$.

^cNumber of average molecular weight and molecular weight distributions were measured by GPC analysis using polystyrene as reference.

^dUsing Ti = 3 μmol , Al/Ti = 1000

^ePolymerization did not proceed.

^fNot determined

From our previous study on the solvent effect of **Flu catalyst**/MMAO systems on the ethylene/1-hexene copolymerization system that was reported in chapter 5. Comparing the result of catalytic activity, it revealed the completely different trend of activity value. According to the previous polymerization results on **Table 5.1**, the highest activity was observed with toluene solvent. On the other hands, if the titanocene catalyst ligand has been changed from **Flu catalyst** derivative to cyclopentadienyl (Cp^*) (**CGC catalyst**), the copolymerization activity trend was altered. With the **CGC catalyst**/MMAO the trend of productivity value exhibited in the same trend as the solvent polarity. Surprisingly, from the result of copolymerization at 0 °C, both systems show the similar trend of catalytic activity. This phenomenon can be explained due to the competition of 1-hexene monomer to the solvent mediums are play more important roles than the active species formation of the catalyst.

Based on the possible reaction of the contact ion-pair model of the **CGC catalyst**, the following discussion regarding to the solvent effect can be proposed; (i) the polarity of solvent greatly affects the polymerization activity where the high polarity of solvent gives high activity until the ion-pair becomes fully separated (at 70°C, [activity]_{dichlorobenzene} > [activity]_{toluene} > [activity]_{heptane}), (ii) at low temperature, heptane gives the highest activity since the interaction between cationic and solvent is less than the interaction between cationic and monomer [69]. Therefore, the less polarity of solvent results in high polymerization activity.

7.2 Effect of solvent on the properties of polymer

A quantitative analysis of triad distribution for all polymer samples was performed on the basis assignment of the ¹³C NMR spectra of ethylene/1-hexene copolymer [57]. The triad distribution and reactivity ratios of monomer were shown in **Tables 7.3** and **7.4**, respectively. At 70°C, it showed that insertion of 1-hexene was the highest with chlorobenzene in both catalytic systems. Therefore, it was suggested that the higher dielectric constant of solvent resulted in the higher degree of 1-hexene insertion. It also indicated that the polymers obtained from all solvent mediums were block polymers ($r_E \cdot r_H > 1$) for the fluorine system, whereas for CGC/MMAO system the ethylene/1-hexene copolymer obtained in random microstructure. Considering the effect of solvent at 0°C as also shown in **Tables 7.3 and 7.4**, the different trend for 1-hexene insertion was still observed where the heptane system showed the highest insertion of 1-hexene and follow with toluene due to the competition of solvent polarity to the monomer at the high dielectric constant solvent for the CGC/MMAO system. On the other hand, for the fluorine system the insertion of α -olefin monomer was altered with the higher insertion of solvent polarity. In addition, the block polymer was still obtained in the high polarity solvent system both the 2 catalytic systems, whereas the toluene and heptane systems gave the alternating polymer ($r_E \cdot r_H < 1$) in fluorenyl system and only heptane in CGC catalyst system.

Table 7.2 Triad distribution of copolymer obtained from ^{13}C NMR

Solvent/T/Catalyst	HHH	EHH	EHE	EEE	HEH	HEE
Hep/70/CGC	0.191	0.039	0.073	0.107	0.196	0.394
Tol/70/CGC	0.163	0.148	0.055	0.042	0.176	0.416
CB/70/CGC	0.168	0.234	0.053	0.047	0.171	0.327
Hep/70/Flu	0.097	0.243	0.124	0.203	0.137	0.196
Tol/70/Flu	0.19	0.208	0.106	0.19	0.134	0.172
CB/70/Flu	0.607	0.074	0.052	0.071	0.106	0.09
Hep/0/CGC	0.000	0.214	0.111	0.405	0.066	0.240
Tol/0/CGC	0.023	0.060	0.065	0.645	0.038	0.168
CB/0/CGC ^a	-	-	-	-	-	-
Hep/0/Flu	0.041	0.202	0.154	0.218	0.111	0.275
Tol/0/Flu	0.004	0.236	0.171	0.208	0.103	0.279
CB/0/Flu	0.359	0.239	0.072	0.046	0.159	0.124

^aPolymerization did not proceed, thus it did not have polymer for investigation

This was suggested that at low temperature, the gap between the cation and anion for the contact ion-pair could be enlarged only with the solvent having high dielectric constant value. However, for the **CGC catalyst/MMAO** system, it showed that the insertion of 1-hexene is reduced from the high electric constant. Thus, it should be noted that for this system the interaction of solvent polarity to monomer was stronger than to the catalyst active species [69]. On the other hand, the high degree of 1-hexene insertion would be preferred resulting in increased reactivity ratio of 1-hexene (r_H) value for the Flu/MMAO system.

สถาบันวิทยบริการ
จุฬาลงกรณ์มหาวิทยาลัย

Table 7.3 Comparative monomer incorporation and the reactivity ratios

Solvent/T/Catalyst	%E	%H	$r_E r_H$
Toluene/70/CGC	63	37	0.94
Heptane/70/CGC	70	30	1.08
CB70/1/CGC	54	46	0.9
Toluene/0/CGC	85	15	3.29
Heptane/0/CGC	71	33	0.91
CB/0/CGC ^a	n.d.	n.d.	n.d.
Toluene/70/Flu	50	50	1.76
Heptane/70/Flu	54	46	1.14
CB/70/Flu	27	73	5.17
Toluene/0/Flu	59	41	0.60
Heptane/0/Flu	60	40	0.80
CB/0/Flu	33	67	1.21

^aPolymerization did not proceed, thus it did not have polymer for investigation

Table 7.4 Melting temperature and % crystallinity of polymer produced

Polymer/solvent/T/Catalyst	T_m	% Crystallinity ^a
E/Toluene/70/CGC	120	34
E/Heptane/70/CGC	133	48
E/CB/70/CGC	133	42
E/Toluene/70/Flu	132	62
E/Heptane/70/Flu	133	59
E/CB/70/Flu	124	64

^aCalculated from heat of crystalline formation based on HDPE

สถาบันวิทยบริการ
จุฬาลงกรณ์มหาวิทยาลัย

7.3 Thermal properties

The melting temperature (T_m) obtained from DSC of polymer obtained is shown in **Table 7.5**. It can be observed that for ethylene polymerization the T_m ranged between 120 to 133°C. In general, T_m is proportional to the crystallinity of polymer. This was suggested that using the solvent having high dielectric constant value apparently resulted in decreased crystallinity of polymer. Comparing the result with the Fluorenyl catalyst system, it was found that the polyethylene produce from the Fluorenyl system had higher crystallinity than obtain from the CGC catalytic system. Therefore, it should be proposed that polyethylene produced from the CGC catalytic system could generate the branching of polyethylene more than Fluorenyl catalytic system.

7.4 Summary

Catalyst structures are one of the most important parameter that we applied to design the conducted polymer. With the difference of ancillary of the catalyst will affect to the steric on the active species formation. As the result, polymer properties that obtain from different catalytic system gave the different result such as crystallinity of polyethylene and also the molecular weight of polymer as reported in this chapter.

CHAPTER VIII

CONCLUSIONS AND RECOMMENDATIONS

8.1 Conclusions

8.1.1 Effect of cocatalyst

In conclusion, we observed that the differences in cocatalysts used for polymerization of ethylene homopolymerization, 1-hexene homopolymerization and ethylene/1-hexene copolymerization, affected on the polymer properties and polymer microstructure. Increasing in productivity with dried aluminoxane were discovered attributing to the absence of TMA and TIBA in MAO and MMAO, respectively. This could reduce the chain transfer and/or chain termination in polymerization reaction. In addition, for ethylene homopolymerization systems, it showed some possibility of living nature of ethylene polymerization since it indicated high molecular weight and appropriate value number of active center. Therefore, with the MMAO system, activities of polymerization slightly decreased suggesting that TIBA that contained in MMAO system did not have strong effects as TMA present in typical MAO. Moreover, when borate compound was chose at high temperatures, it clearly exhibited deactivation of active species was occurred at polymerization temperature 40 °C both in ethylene homopolymerization and ethylene/1-hexene copolymerization. On the other hand, the bulky and steric effect of borate compound enhanced the insertion of 1-hexene in copolymerization of catalyst 1 system. Furthermore, we found that comonomer insertion of 1-hexene was independent from aluminoxane types which we used to study in this paper. In contrast, triad distribution of copolymers produced from MMAO was different from other aluminoxanes due to the highest of reactivity both ethylene and 1-hexene.

8.1.2 Effect of solvent medium

In summary, the catalytic activity during ethylene/1-hexene copolymerization with the Ti complex (catalyst 1)/MMAO can be altered within different solvent mediums employed. In order to give a better explanation, the contact ion-pair model under the typical polymerization condition was applied. At low polymerization temperature (0°C), activities increased with increasing the dielectric constant value of

solvent, except for dichloromethane (no activity). However, at high polymerization temperature (70°C), it was found that too high dielectric constant value of solvent resulted in low activity due to the fully separated ion-pair formed. It should be mentioned that the solvent having high dielectric constant value gave the high degree of 1-hexene insertion resulting in enhanced reactivity ratio of 1-hexene (r_H). There was no significant effect of solvent on the thermal properties of polymer obtained

8.1.3 Effect of second monomer

With the different kinds of α -olefin, it can cause the system to generate different active species type after the insertion of monomer occurred. Therefore, the polymerization behaviors of ethylene/ α -olefin polymerization with titanocene/MMAO system depend on the α -olefin applied to the copolymerization. The highest activity on copolymerization was observed when ethylene/1-octene copolymerization was conducted at high temperature. It could interpret by term of the distance between cationic and anionic of contact ion pair. The most suitable distance gave the highest activity because that distance referred to the more easily of monomer insertion and also not to high requirement of complexation energy to generate the active species. Thus, at 70 °C, copolymerization of 1-hexene gave the lower activity since the space is not open enough where as the lower activity observed from 1-decene copolymerization came from it need high complexation energy to form the active species. However, polymerization system at 0 °C showed the different behavior, α -olefin type is not affect the polymerization behavior. It follow the trend that higher alkene gave the less activity due to its less active. On the view of polymer microstructure and monomer incorporation, it clearly showed that the higher alkene gave the less incorporation in polymer backbone and independence with the polymerization temperature. On the other hand, temperature has the significant effect on the polymer microstructure. Copolymer obtain from 70 °C polymerization gave the block structure while the copolymer from 0 °C polymerization gave the alternating structure. These results were attributed to be the monomer activities of two monomers were affect from the different temperature not similar. Therefore, the alternating structure did not give any crystalline melting temperature. Furthermore, with the high insertion of α -olefin, the obtained copolymer also did not show the melting temperature too.

8.1.4 Effect of catalyst structure

In summary, the catalytic activity during ethylene/1-hexene copolymerization with the Ti complex (**CGC catalyst**)/MMAO can be altered within different solvent mediums employed. At high polymerization temperature (70°C), it was found that high dielectric constant value of solvent resulted in higher activity due to the separation of the ion-pairs. Comparing the result with the (**Flu catalyst**)/MMAO system. It revealed that the trend of activity and solvent polarity were difference between these 2 systems. Thus, we could announce that the activity of polymerization not only depended on the solvent polarity but also the catalyst structure too. Moreover, it should be mentioned that polyethylene produced from the CGC system had more branching than Fluorenyl system, Thus it should be noted that crystallinity of polymer depend on the catalyst structure applied to the system.

8.2 Recommendation

Relative monomer reactivity ratio of ethylene/ α -olefin copolymerization should be investigation in depth analysis. Further understanding of catalyst reactivity to ethylene (r_E) and comonomer (r_C) are important to understanding the active species properties.

Solvent medium that have larger different in the structure, such as, high steric of solvent compare to the low steric also the one topic of interested for research because the steric hindrance also one important parameter to the insertion step of monomer to the active species ion pairs.

Addition of alkylaluminum such as (TMA,TEA,TIBA or DEAC) can be the variable to the polymerization process due to it can enhanced the propagation rate of polymer but it also can be a chain transfer reagent of the active species. On this study the effect of alkyl aluminum are not fully investigated. Therefore, the polymerization systems perform with alkylaluminum was attributed to the further research.

Changing from the homogeneous system to the heterogeneous system is the most interesting topic for recommendation. Because with the supported system the catalyst will be immobilized on support, thus the formation of active species was interfered by the steric effect of support. Therefore, the result of polymerization behaviors should be altered by changing type of support.

REFERENCES

- [1] Soga, K. and Shiono, T. Ziegler-Natta catalysts for olefin polymerizations. **Progress in Polymer Science** 22(1997): 1503 – 1546.
- [2] Robinson, S. **Chemistry & Industry** 12(2001): 377 - 378.
- [3] Krentsel B. A., Kissin, Y. V., Kleiner V. J., Stotskaya L. L. **Polymers and Copolymers of Higher α -Olefins**. Cincinnati. Hanser/Gardner Publications: 1997.
- [4] Bert, K.E.; Crossland, R.; Ford, H; Gardner, A.K. Polyethylene. 1933-83 **Proceeding of the Golden Jubilee Conference, The plastic and Rubber Institute, London** (1983): B1.1 -B1.31.
- [5] Staub, R.B. Polyethylene 1933-83 **Proceeding of the Golden Jubilee Conference, The plastic and Rubber Institute, London** (1983): B5.4.1 -B5.4.14.
- [6] Phillip Townsend Associates **Newsletter for Plastics and Chemical Industries**, June 2001, Vol. 56.
- [7] Buckalew, L.; Schumacher, J.W. **Chemical Economics Handbook-SRI International**, Plastics and Resins August 580(2000): 1321.
- [8] Reddy S.S. and Sivaram S. Homogeneous metallocene-methylaluminoxane catalyst systems for ethylene polymerization **Progress in Polymer Science** 20(1995): 309-367.
- [9] Ziegler, K., H. Breil, H. Martin, and E. Holzkamp. **German patent 973,626**, issued April (1960),14.
- [10] Natta, G., P. Pino, P. Corradini, F. Danusso, E. Mantica, G. Mazzanti and G. Moraglio. **Journal of American Chemical Society** 77(1995): 1708-1710.
- [11] Huang, J. and Rempel, G.L. Ziegler-Natta catalysts for olefin polymerization: Mechanistic insights from metallocene systems. **Progress in Polymer Science** 20(1995) 459-526.
- [12] Hamielec, A.E. and Soares, J.B.P. Polymerization reaction engineering – Metallocene catalysts. **Progress in Polymer Science** 21(1996): 651-706.
- [13] Richards, C.T. **Plastic Rubber Composites Processing and Applications**, 27(1)(1998): 3-7.

- [14] Helmut G. Alt and Alexander Koppl.. Effect of the Nature of Metallocene Complexes of Group IV Metals on Their Performance in Catalytic Ethylene and Propylene Polymerization. **Chemical Review** 100(2000): 1205-1221.
- [15] Johnson, J.C. **Metallocene Technology**. Newjersey: Noys Data Co.1973.
- [16] Laucher, J.W. and Hoffmann, R. Structure and Chemistru of bis(cyclopentadienyl)-ML_n complex. **Journal of american chemical society** 98(1976): 1729 – 1749.
- [17] Gupta, V.K., Satish, S. andBhardwaj. Metallocene Complexes of Group 4 Elements in the Polymerization of Monoolefins. **Journal of Molecular Science –Reviews in Macromolecular Chemistry and Physics**.C34,No.3(1994), 439-514.
- [18] Pasynkiewicz S. Aluminoxanes-Synthesis, Structure, Complexes , and Reactions. **Polyhedron** 9(1990): 429-453.
- [19] Chien J. C. ,Wang B. P.. Supported Catalysts for stereospecific Polymerization of Propylene. **Journal of Polymer Science: Part A: Polymer Chemistry** 14(8) (1976): 1915-1932.
- [20] Sinn H. Proposal for structure and effect of methylaluminumoxane Based on Mass Balances and Phase separation Experiement. **Macromolecular Symposia** 97(1995): 27-52.
- [21] Corradini, P. and Guerra, G., Models for the stereospecificity in homogeneous and heterogeneous Ziegler-Natta polymerizations. **Progress in Polymer Science** 16(1991): 239.
- [22] Resconi, L., Abis, L. and Franciscono, G. 1-Olefin polymerization at bis(pentamethylcyclopentadienyl)zirconium and -hafnium centers: enantioface selectivity. **Macromolecules**. 25(1992): 6814-6817.
- [23] Cavallo, L., Corradini, P., Guerra, G. and Vacatello, M. On the effects of methyl substituents on chelating ligands in models for homogeneous isospecific Ziegler-Natta catalysis. **Polymer** 32(1991): 1329-1335.

- [24] Ciardelli, F., Altomare, A. and Carlini, C. Chiral discrimination in the polymerization of α -olefins by Ziegler-Natta initiator systems. **Progress in Polymer Science** 16(1991): 259-277.
- [25] Ewen J. A. Mechanisms of stereochemical control in propylene polymerizations with soluble Group 4B metallocene/methylalumoxane catalysts **Journal of The American Chemical Society**. 106(1984): 6355-6364.
- [26] Herfert, N. and Fink, G. Hemiisotactic Poly(Propylene) Through Propene Polymerization with the $iPr[3-MeCpFlu]ZrCl_2/MAO$ Catalyst System: A Kinetic and Microstructural Analysis. **Makromolekulare Chemie Macromolecular Symposia** 66(1993): 157-178.
- [27] Ewen J. A., Elder M. J. Metallocene/polypropylene structural relationships: implications on polymerization and stereochemical control mechanisms. **Makromol. Chem. Macromol. Symp.** 48/49(1991): 253-295.
- [28] Kaminsky, W., Ahlers, A., and Moller-Lmdenhof, N., Asymmetric Oligomerization of Propene and 1-Butene with a Zirconocene/Alumoxane Catalyst, **Angewandte Chemie International Edition in English** 28(1989): 1216.
- [29] Eshuis, J., Tan, Y., Teuben, J., and Renkema, J. Catalytic olefin oligomerization and polymerization with cationic group IV metal complexes $[Cp_2^*MMe(THT)]^+[BPh_4]^-$, M = Ti, Zr and Hf. **Journal of molecular catalysis** 62(1990): 277 – 287.
- [30] Chen, J.C.W. and Wang, B. Metallocene-methylaluminoxane catalysts for olefin polymerization. V. Comparison of Cp_2ZrCl_2 and $CpZrCl_3$ **Journal of Polymer Science Part A: Polymer Chemistry** 28(1990) 15-38.
- [31] Tsutsui, T., Mizuno, A., and Kashiwa, N. The microstructure of propylene homo- and copolymers obtained with a Cp_2ZrCl_2 and methylaluminoxane catalyst system **Polymer** 30(1989): 428-431.
- [32] Tsutsui, T., Mizuno, A., and Kashiwa, N. Effect of hydrogen on propene polymerization with ethylenebis(1-indenyl)zirconium dichloride and methylaluminoxane catalyst system. **Macromolecular Rapid Communications** 11(1990): 565-570.

- [33] Resconi, L., Piemontesi, F., Franciscano, G., Abis, L., and Fiorani, T., Olefin polymerization at bis(pentamethylcyclopentadienyl)zirconium and -hafnium centers: chain-transfer mechanisms **Journal of The American Chemical Society**. 114(1992): 1025-1032.
- [34] Kaminsky, W., Ahlers, A. and Steiger, R. Stereospecific polymerization by metallocene/aluminoxane catalysts **Journal of Molecular Catalysis A: Chemical** 74(1992): 109-119.
- [35] Fischer, D., Junglin, S., and Malhaupt, D. Donor- and acceptor-modified metallocene-based homogeneous Ziegler-Natta catalysts **Makromolekular Chemistry Macromolekular Sympopia**. 66(1993): 191-202.
- [36] Newburg, N.R. Bis-(Cyclopentadienyl)-Titaniumdichloride-alkylaluminum complexes as catalysts for the polymerization of ethylene **Journal of the American Chemical Society** 79(1957): 5072-5073.
- [37] Sinn, H. and Kaminsky, W. Ziegler-Natta-Catalysis. **Advance Organometallics Chemistry** 18(1980): 99-149.
- [38] Devore, D.D., Neithamer, D.R., Lapointe, R.E., and Mussell, R.D. **U.S. Patent 5,625,087**. 1997.
- [39] Yamamoto, K., Wakatsuki, K., Hozumi, H., and Furusawa, A. **Eur.Pat.Appl. 708,117**. 1996.
- [40] Sarah E. Reybuck, Robert M. Waymouth. Investigation of Bridge and 2-Phenyl Substituent Effects on Ethylene/ α -Olefin Copolymerization Behavior with 1,2'-Bridged Bis(indenyl)zirconium Dichlorides. **Macromolecule** 37(2004): 2342-2347.
- [41] Alexander Koppl, Andrea I. Babel, Helmut G. Alt. Homopolymerization of ethylene and copolymerization of ethylene and 1-hexene with bridged metallocene/methylaluminoxane catalysts: the influence of the bridging moiety **Journal of Molecular Catalysis A: Chemical** 153(2000): 109-119.
- [42] I.Kim, S.Y. Kim, M. H. Lee, Y.K. Do, M.S. Won. Ethylene/1-hexene copolymerizations by syndioselective metallocenes: Direct comparison of $\text{Me}_2\text{C}(\text{Cp})(\text{Flu})\text{ZrMe}_2$ with $\text{Et}(\text{Cp})(\text{Flu})\text{ZrMe}_2$. **Journal of Polymer Science Part A: Polymer Chemistry** 37(1999): 2763-2772.

- [43] Mahesh K. M., Adam P. Cole, and Robert M. Waymouth, Synthesis, Structure, and Ethylene/ α -Olefin Polymerization Behavior of (Cyclopentadienyl)(nitroxide)titanium Complexes **Organometallics** 23(2004): 836-845.
- [44] Akihiro Y., Saiki H., Tosiyuki K., Makoto S., Morihiko S., Akira A. Ethylene/1-hexene copolymerization with Ph₂C(Cp)(Flu)ZrCl₂ derivatives: correlation between ligand structure and copolymerization behavior at high temperature **Macromolecular Chemistry and Physics** 200(1999): 1542-1553.
- [45] S. E. Reybuck, A. Meyer, and Robert M. Waymouth. Copolymerization Behavior of Unbridged Indenyl Metallocenes: Substituent Effects on the Degree of Comonomer Incorporation **Macromolecule** 35(2002): 637-643.
- [46] Michaela Dankova and Robert M. Waymouth. High Comonomer Selectivity in Ethylene/Hexene Copolymerization by Unbridged Indenyl Metallocenes. **Macromolecule** 36(2003): 3815-3820.
- [47] Akihiro Y., Saiki H., Satoru Y., Akira A., Influence of activators on ethylene polymerization with diphenylmethylidene-(cyclopentadienyl)(fluorenyl) zirconium dichloride catalysts at high temperature **Journal of Molecular Catalysis A: Chemical** 148(1999): 77-86.
- [48] M. C. Chen, John A. S. Roberts, and T. J. Marks. New Mononuclear and Polynuclear Perfluoroarylmatalate Cocatalysts for Stereospecific Olefin Polymerization **Organometallics** 23(2004): 932-935.
- [49] T. Shiono, S. Yoshida, H. Hagihara, T. Ikeda, Additive effects of trialkylaluminum on propene polymerization with (*t*-BuNSiMe₂Flu)TiMe₂-based catalysts **Applied Catalysis A: General**, 200(2000): 145-152.
- [50] F. Forlini, I. Tritto, P. Locatelli, M.C. Sacchi, F. Piemontesi. ¹³C NMR studies of zirconocene-catalyzed propylene/1-hexene copolymers: in-depth investigation of the effect of solvent polarity. **Macromolecular Chemistry and Physics** 201(2000) 401-408.
- [51] F. Forlini, E. Princi, I. Tritto, M.C. Sacchi, F. Piemontesi, ¹³C NMR Study of the Effect of Coordinating Solvents on Zirconocene-Catalyzed Propene/1-Hexene Copolymerization **Macromolecular Chemistry and Physics** 203 (2002) 645-652.

- [52] K. Nishii, T. Matsumae, E. O. Dare, T. Shiono, T. Ikeda. Effect of Solvents on Living Polymerization of Propylene with [t-BuNSiMe₂Flu]TiMe₂-MMAO Catalyst System **Macromolecular Chemistry and Physics**. 205(2004): 363-369.
- [53] K. Nishii, T. Shiono, T. Ikeda, A Novel Synthetic Procedure for Stereoblock Poly(propylene) with a Living Polymerization System **Macromolecular Rapid Communications** 25(2004): 1029-1032.
- [54] Hagihara H., T. Shiono, T. Ikeda, Living Polymerization of Propene and 1-Hexene with the [t-BuNSiMe₂Flu]TiMe₂/B(C₆F₅)₃ Catalyst **Macromolecule** 31(1998): 3184-3188.
- [55] T. Hasan, A. Ioku, K. Nishii, T. Shiono, T. Ikeda. Syndiospecific Living Polymerization of Propene with [t-BuNSiMe₂Flu]TiMe₂ Using MAO as Cocatalyst. **Macromolecules** 34(2001): 3142-3145.
- [56] A. Ioku, T. Shiono, T. Ikeda. Supporting effect of methylaluminoxane on propene polymerization with monocyclopentadienylalkyltitanium derivatives **Applied Catalysis A: General**, 226(2002): 15-22.
- [57] James C. Randall. A Review of High Resolution Liquid ¹³C Nuclear Magnetic Resonance Characterization of Ethylene-Based polymers, **Macromolecular Chemistry and Physics** C29(1989): 201.
- [58] Krentsel B. A., Kissin, Y. V., Kleiner V. J., Stotskaya L. L. **Polymers and Copolymers of Higher α -Olefins**. Cincinnati. Hanser/Gardner Publications: 1997.
- [59] Odian, G. **Principles of Polymerization**, (New York, John Wiley & Sons, , (1991).
- [60] Simanke A. G., Galland G. B., Quijada R. Mauler R. S., Influence of the comonomer content on the thermal and dynamic mechanical properties of metallocene ethylene/1-octene copolymers **Polymer** 40 (1999): 5489-5495.
- [61] Kaminsky W. Zirconocene catalysts for olefin polymerization. **Catal Today** 20 (1994) 257-271.

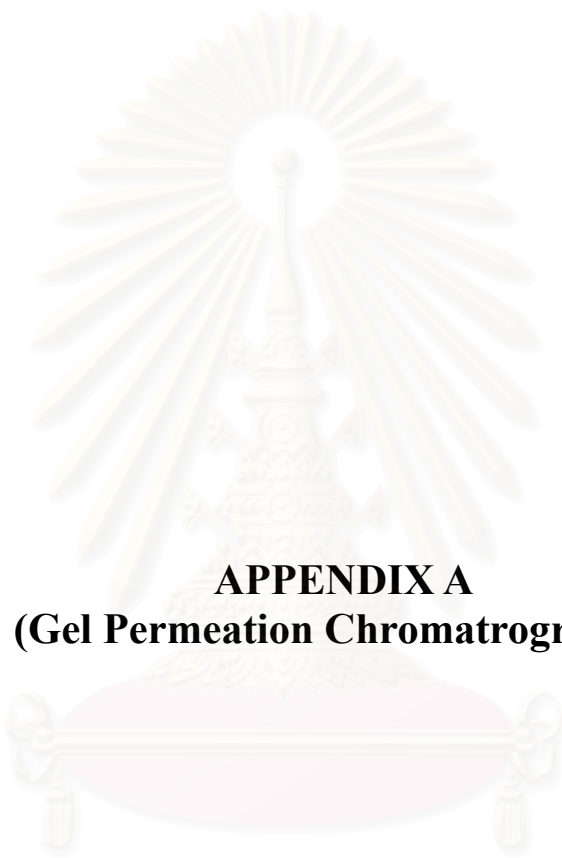
- [62] Gupta, V.K., Satish, S. and Bhardwaj. Metallocene Complexes of Group 4 Elements in the Polymerization of Monoolefins. **Journal of Molecular Science –Reviews in Macromolecular Chemistry and Physics** C34, No.3(1994), 439-514.
- [63] Bochmann M. Cationic Group IV Metallocene Complexes and Their Role in Polymerisation Catalysis: The Chemistry of Well-defined Ziegler Catalysts **Journal of Chemical Society Dalton Trans** (1996) 255-270.
- [64] T.J.Marks, L.L.Sands, A.L. Rheingold, Catalyst/Cocatalyst Nuclearity Effects in Single-Site Polymerization. Enhanced Polyethylene Branching and α -Olefin Comonomer Enchainment in Polymerizations Mediated by Binuclear Catalysts and Cocatalysts via a New Enchainment Pathway **Journal of The American Chemical Society** 124 (2002) 12725-12741.
- [65] Hasan T., Shiono T., Ikeda T. Highly Efficient Ti-Based Catalyst Systems for Vinyl Addition Polymerization of Norbornene **Macromolecule** 37 (2004) 7432-7443.
- [66] E.O.Dare, G.A.Olatunji, D.S.Ogunniyi, Polymerization behavior of propene with [*t*-BuNSiMe₂Flu]TiMe₂: effects of solvents and cocatalysts **European Polymer Journal**, 40 (2004) 2333-2341.
- [67] F. Forlini, Z.Q. Fan, I. Tritto, P. Locatelli, Metallocene-catalyzed propene/1-hexene copolymerization: Influence of amount and bulkiness of cocatalyst and of solvent polarity **Macromolecular Chemistry and Physics** 198 (1997) 2397-2408.
- [68] M.S.W. Chan, K. Vanka, Cory C. Pye, T.Ziegler. Density Functional Study on Activation and Ion-Pair Formation in Group IV Metallocene and Related Olefin Polymerization Catalysts. **Organometallics** 18 (1999) 4624-4636.
- [69] S. H. Yang, J. Huh, Won Ho Jo. Effect of Solvent Polarity on the Initiation and the Propagation of Ethylene Polymerization with Constrained Geometry Catalyst/MAO Catalytic System: A Density Functional Study with the Conductor-Like Screening Model. **Macromolecule** 38(2005):1402-1409.
- [70] Bunjerd Jongsomjit, Sutti Ngamposri, and Piyasan Praserttham, Application of Silica/Titania Mixed Oxide-Supported Zirconocene Catalyst for Synthesis of Linear Low-Density Polyethylene, *Industrial engineering and chemistry research* 44(2005): 9059-9063

- [71] Liu S., Yu G. and Huang B., **Journal of applied polymer science** 66(1997): 1715-1720
- [72] Gray A.P., **Thermochim Acta**1 (1970):563
- [73] Herfert, N.; Montag, P.; Fink, G.m Elementary processes of the Ziegler catalysis, 7. Ethylene, α -olefin and norbornene copolymerization with the stereorigid catalyst systems $iPr[FluCp]ZrCl_2/MAO$ and $Me_2Si[Ind]2ZrCl_2/MAO$ **Macromolecular Chemistry** 194(1993): 3167-3182.
- [74] Fink, G.; Herfert, N. Elementary processes of the Ziegler catalysis, 6. Ethylene, α -olefin and norbornene copolymerization with the stereorigid catalyst systems $iPr[FluCp]ZrCl_2/MAO$ and $Me_2Si[Ind]2ZrCl_2/MAO$ **Macromolecular Chemistry** 193(1992): 1359-1367.
- [75] Koivumaki, J.; Fink, G.; Seppala, J. V. Copolymerization of Ethene/1-Dodecene and Ethene/ 1-Octadecene with the Stereorigid Zirconium Catalyst System $iPr[FluCp]ZrCl_2/MAO$ and $Me_2Si[Ind]2ZrCl_2/MAO$: Influence of the Comonomer Chain Length **Macromolecules** 27(1994): 6254-6258.
- [76] Seppala , J. V.; Koivumaki, J.; Liu, X. Co- and terpolymerization of ethylene with 1-butene and 1-decene by using Cp_2ZrCl_2 -methylaluminumoxane catalyst **Journal of Polymer Science Part A: Polymer Chemistry** 31 (1993) : 3447-3452.
- [77] Koivumaki, J.; Seppala , J. V. **Journal of Polymer Science Part A: Polymer Chemistry** 26(1993) :5535.
- [78] Koivumaki J.; Seppala , J. V. Copolymerization of ethylene and 1-hexadecene with Cp_2ZrCl_2 -methylaluminumoxane catalyst **Polymer** 34(1993) : 1958
- [79] Pietikainen, P.; Seppala , J. V. Low Molecular Weight Ethylene/Propylene Copolymers. Effect of Process Parameters on Copolymerization with Homogeneous Cp_2ZrCl_2 Catalyst **Macromolecules** 27(1994) :1325-1328.
- [80] Koivumaki, J. Copolymerization of ethylene and 1-octadecene with the Cp_2ZrCl_2/MAO and Cp_2HfCl_2/MAO catalyst systems **Polymer Bulletins** 34 (1995): 413-418.
- [81] N.Inataragamjon, T.Shiono, B.Jongsomjit, P.Prasertham. Elucidation of solvent effects on the catalytic behaviors for $[t-BuNSiMe_2Flu]TiMe_2$ complex during ethylene/1-hexene copolymerization. **Catalysis Communications** 7(2006) 721-727.



APPENDICES

สถาบันวิทยบริการ
จุฬาลงกรณ์มหาวิทยาลัย



APPENDIX A
(Gel Permeation Chromatography)

สถาบันวิทยบริการ
จุฬาลงกรณ์มหาวิทยาลัย

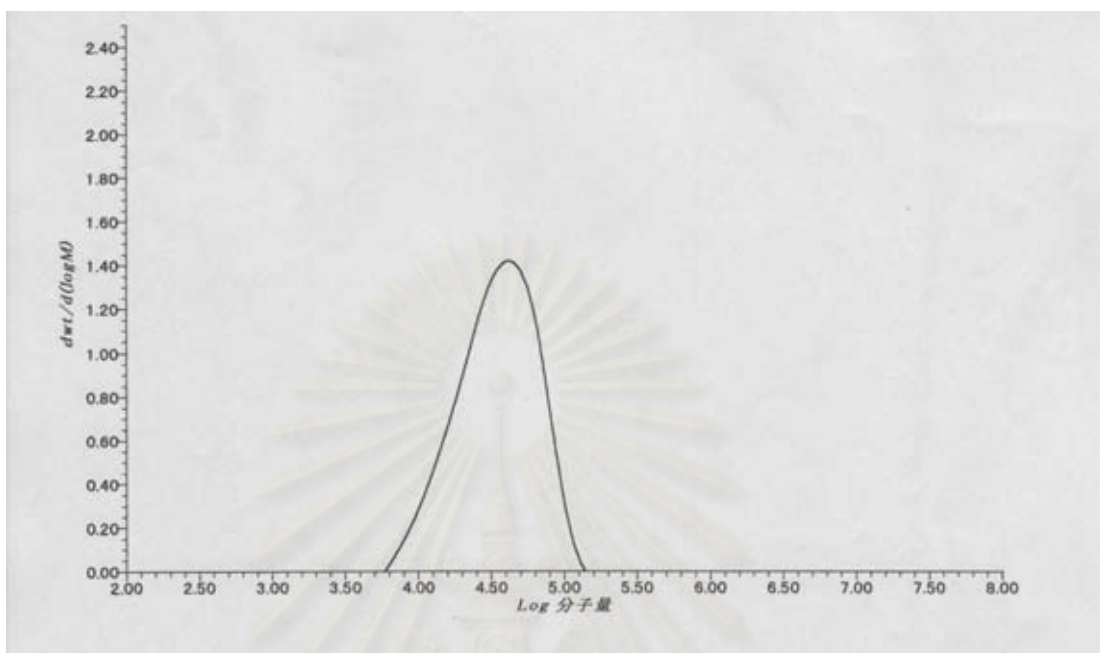


Figure A1 : GPC curve of ethylene/1-hexene copolymerization with catalyst1/d-MAO at 40 °C

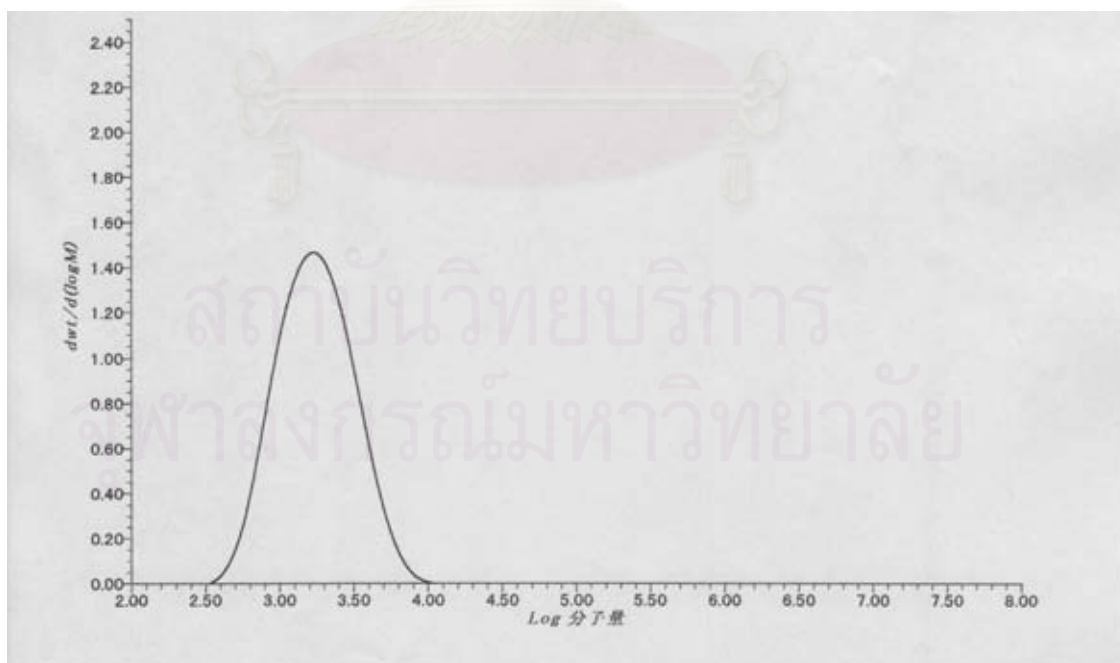


Figure A2 : GPC curve of ethylene/1-hexene copolymerization with catalyst1/MAO at 40 °C

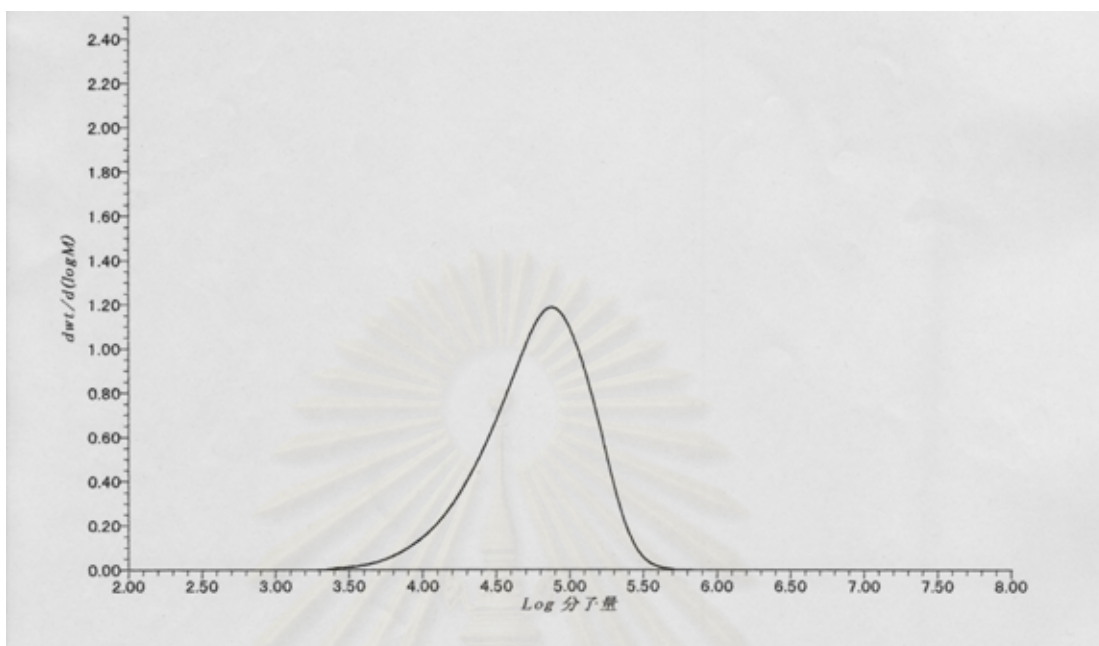


Figure A3 : GPC curve of ethylene/1-hexene copolymerization with catalyst1/MMAO at 40 °C

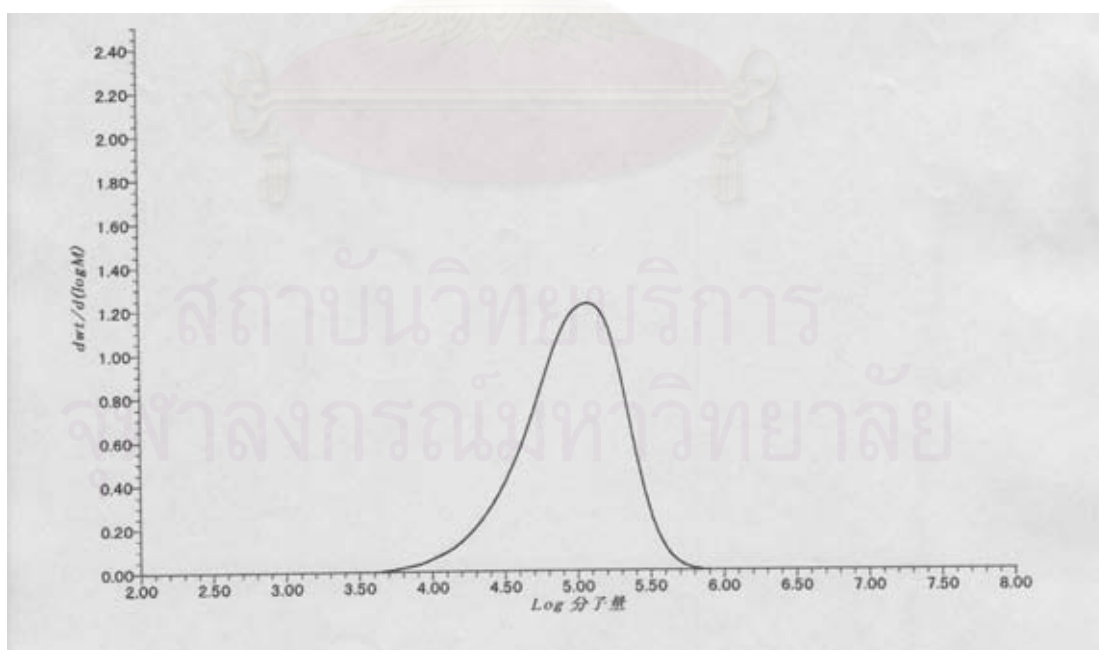


Figure A4 : GPC curve of ethylene/1-hexene copolymerization with catalyst1/d-MMAO at 40 °C

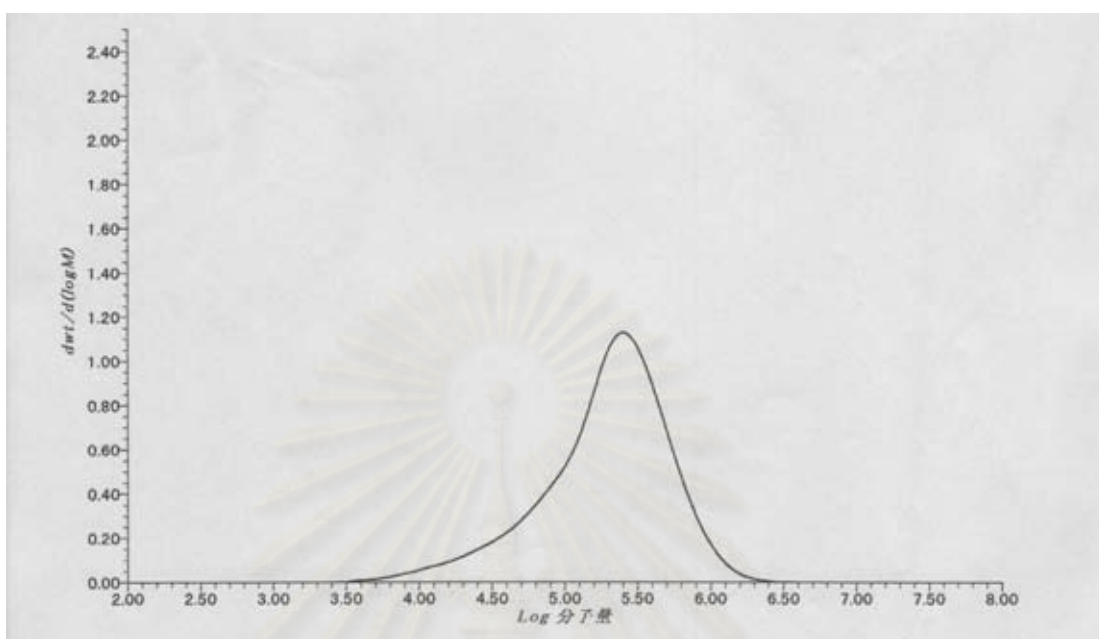


Figure A5 : GPC curve of ethylene/1-hexene copolymerization with catalyst1/Borate at 40 °C

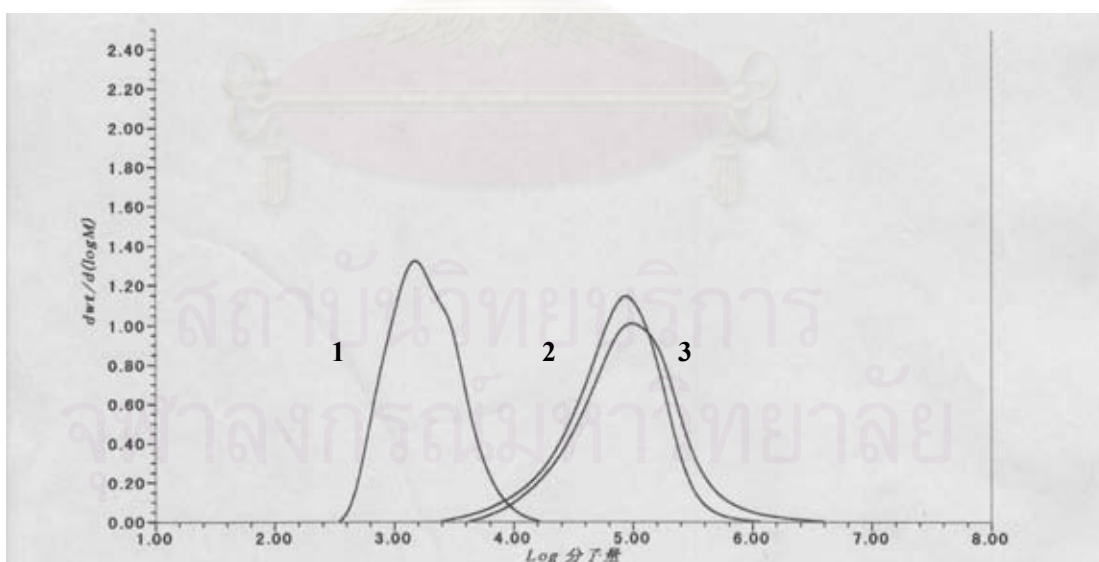


Figure A6 : GPC curve of ethylene polymerization with catalyst1 1. MAO 2. d-MAO 3. Borate cocatalyst at 40 °C

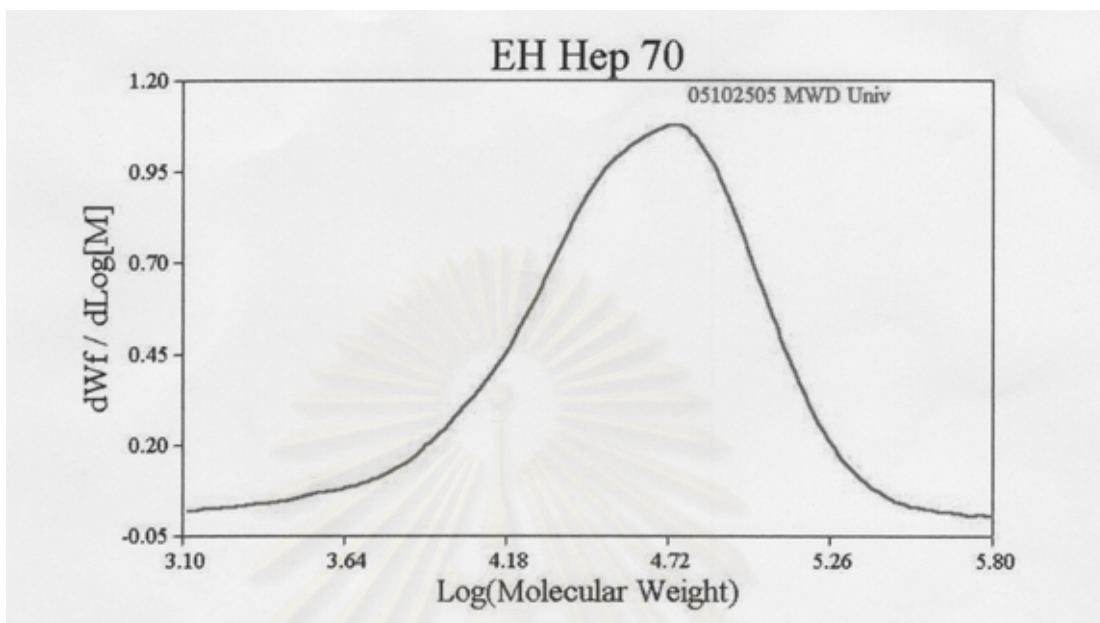


Figure A7 : GPC curve of ethylene/1-hexene copolymerization with catalyst1/MMAO in heptane at 70 °C

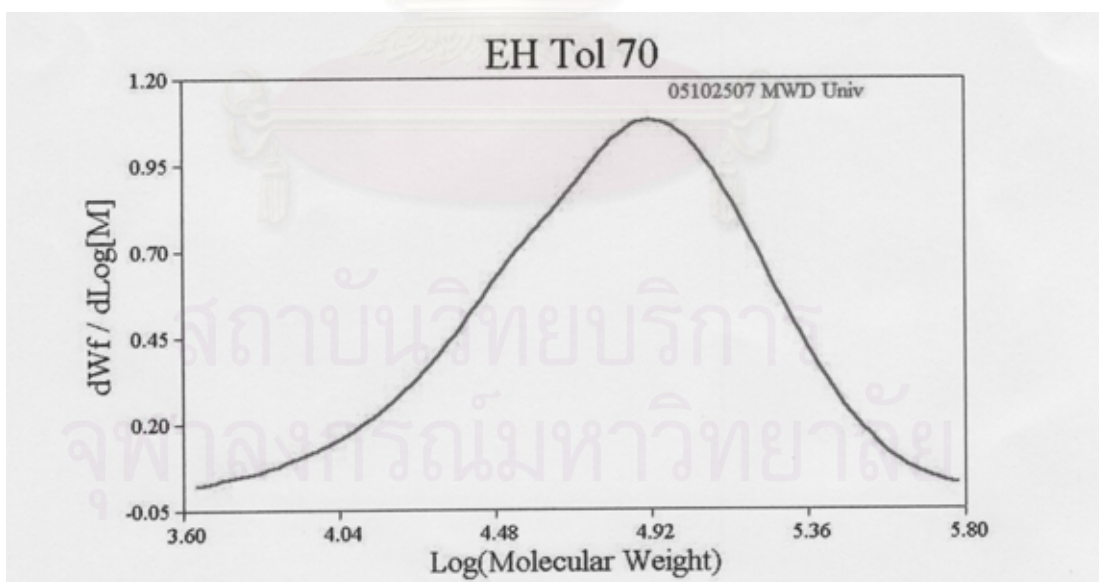


Figure A8 : GPC curve of ethylene/1-hexene copolymerization with catalyst1/MMAO in toluene at 70 °C

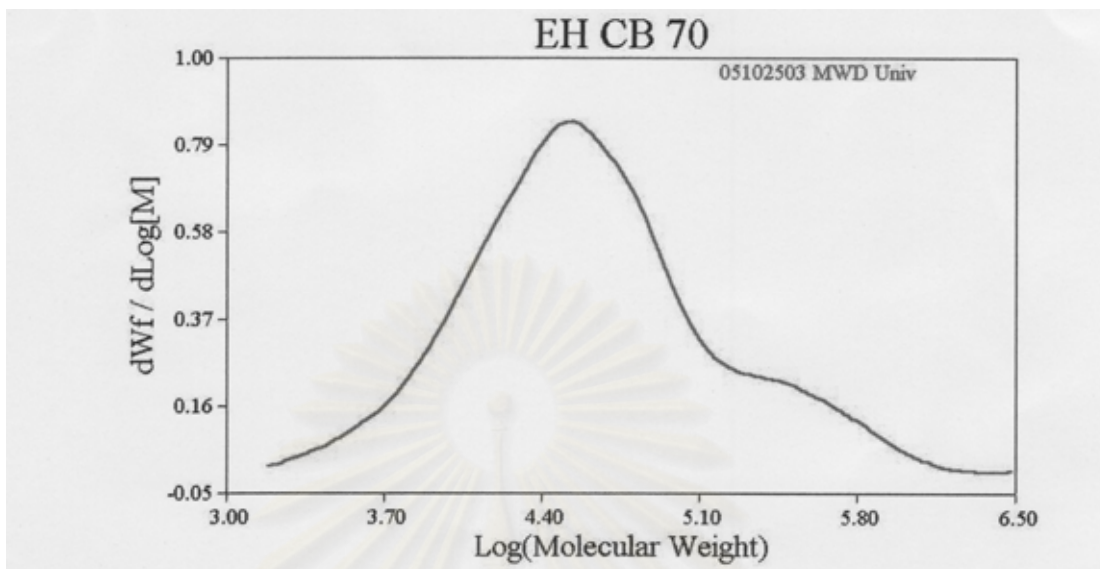


Figure A9 : GPC curve of ethylene/1-hexene copolymerization with catalyst1/MMAO in chlorobenzene at 70 °C

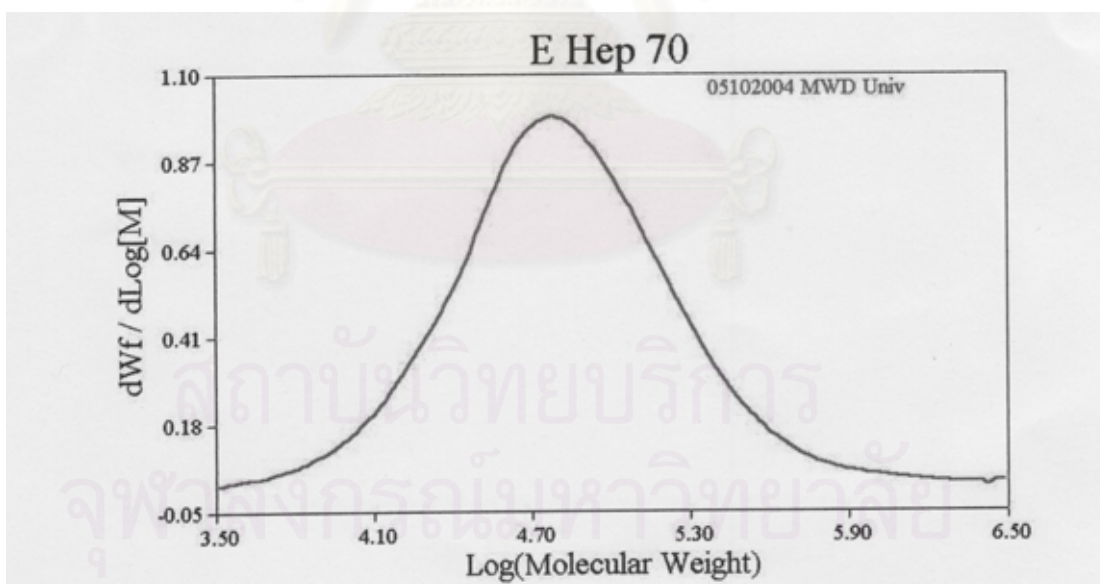


Figure A10 : GPC curve of ethylene polymerization with catalyst1/MMAO in heptane at 70 °C

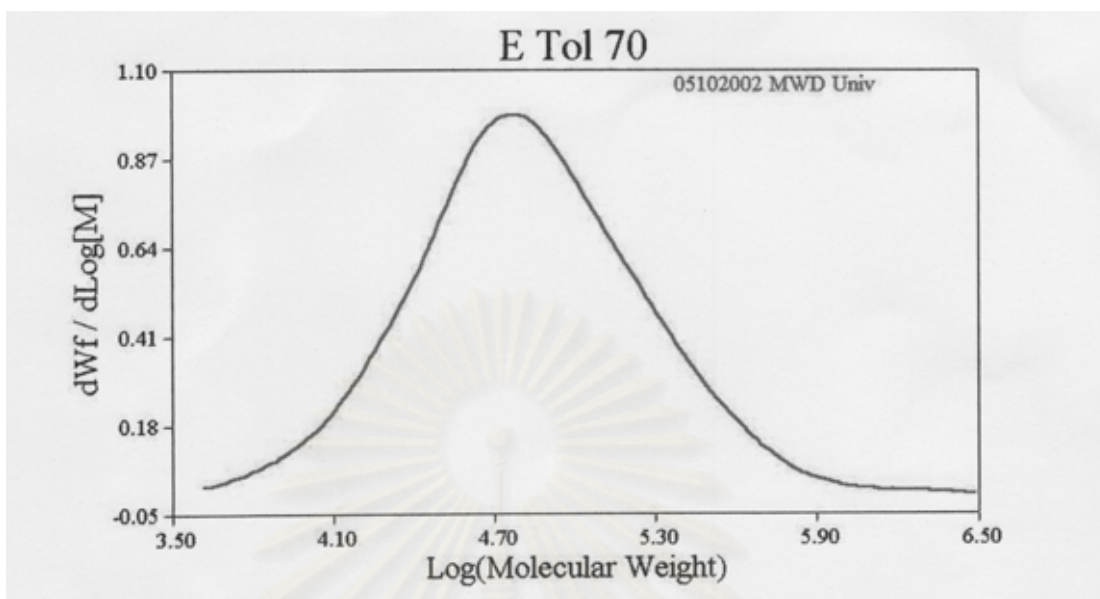


Figure A11 : GPC curve of ethylene polymerization with catalyst1/MMAO in toluene at 70 °C

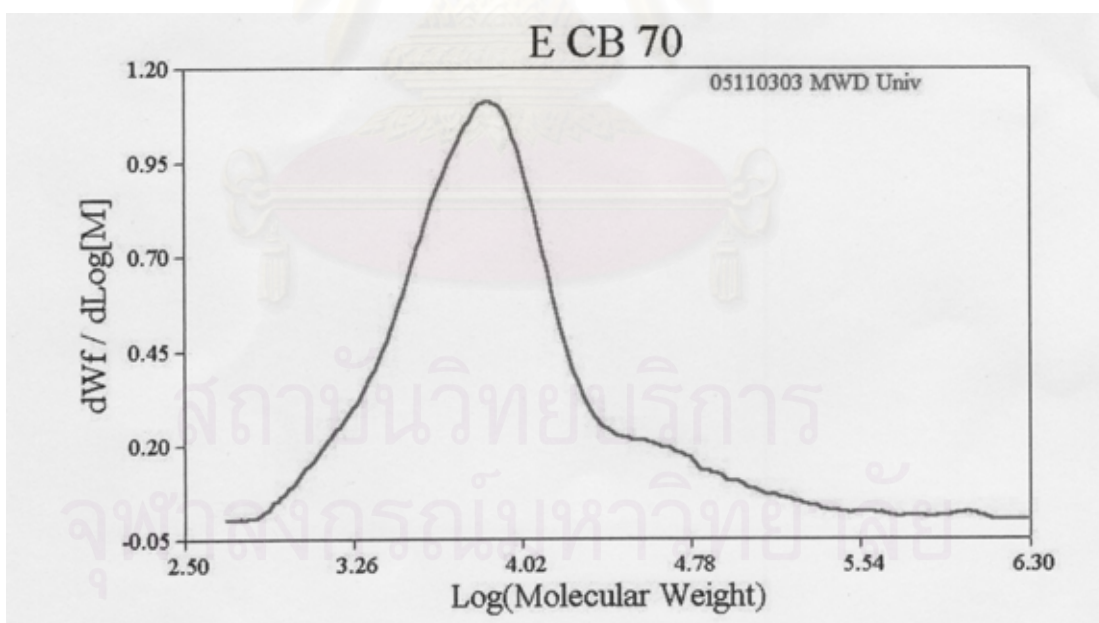


Figure A12 : GPC curve of ethylene polymerization with catalyst1/MMAO in chlorobenzene at 70 °C

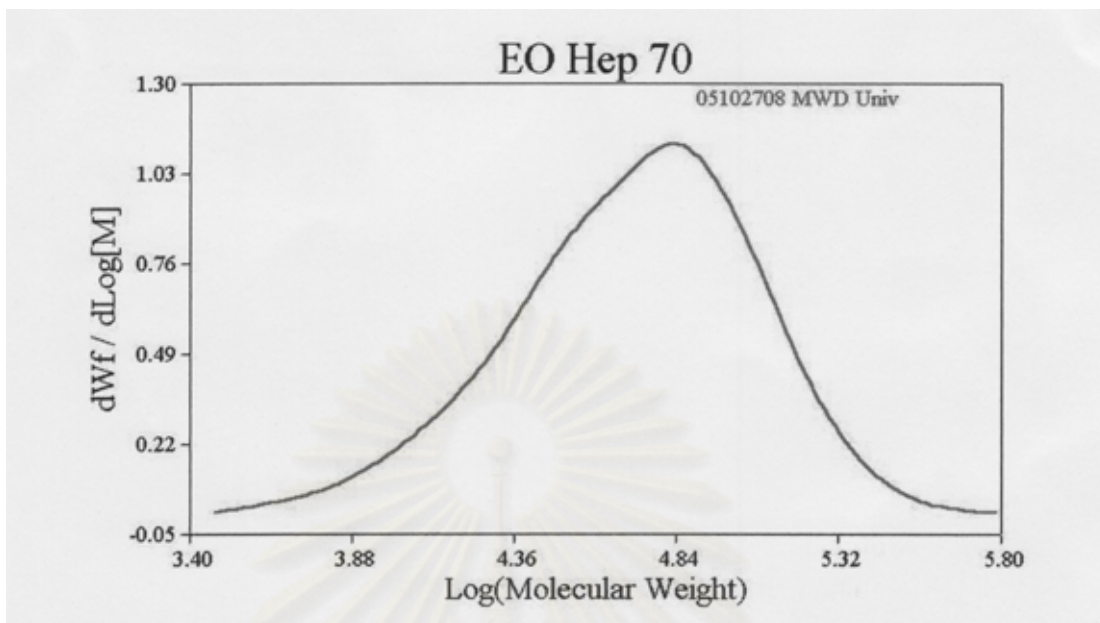


Figure A13 : GPC curve of ethylene/1-octene copolymerization with catalyst1/MMAO in heptane at 70 °C

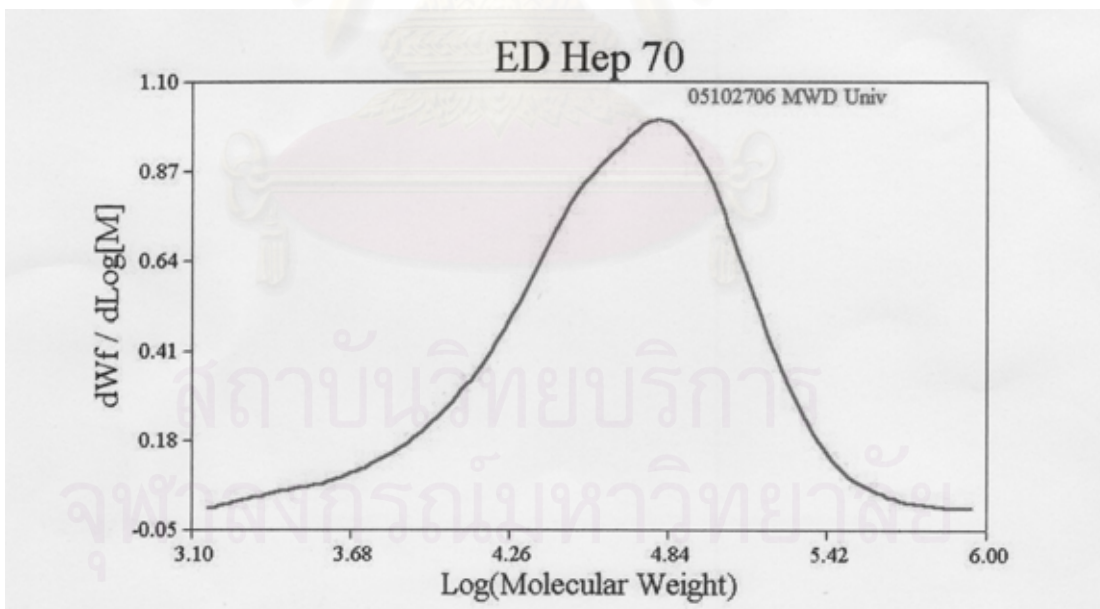


Figure A14 : GPC curve of ethylene/1-decene copolymerization with catalyst1/MMAO in heptane at 70 °C

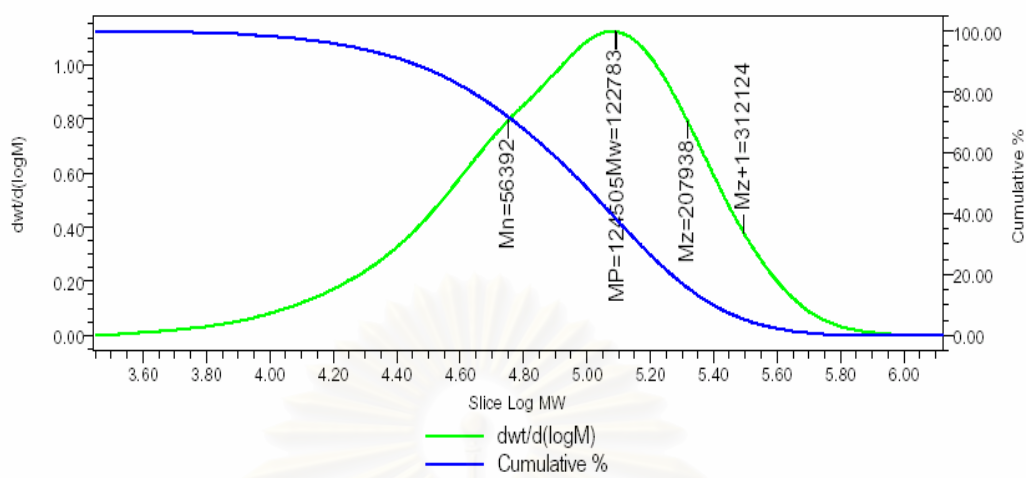


Figure A15 : GPC curve of ethylene/1-hexene copolymerization with catalyst2/MMAO in heptane at 70 °C

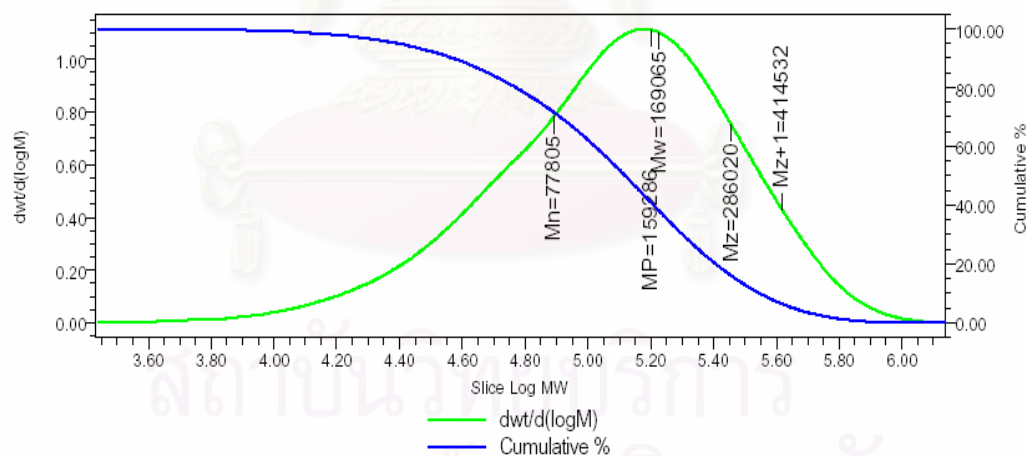


Figure A16 : GPC curve of ethylene/1-hexene copolymerization with catalyst2/MMAO in toluene at 70 °C

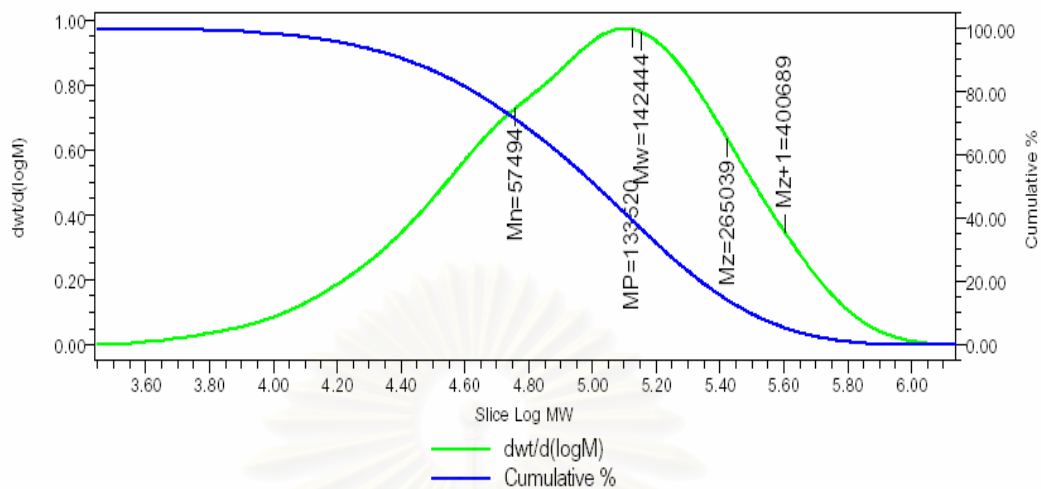


Figure A17 : GPC curve of ethylene/1-hexene copolymerization with catalyst2/MMAO in chlorobenzene at 70 °C

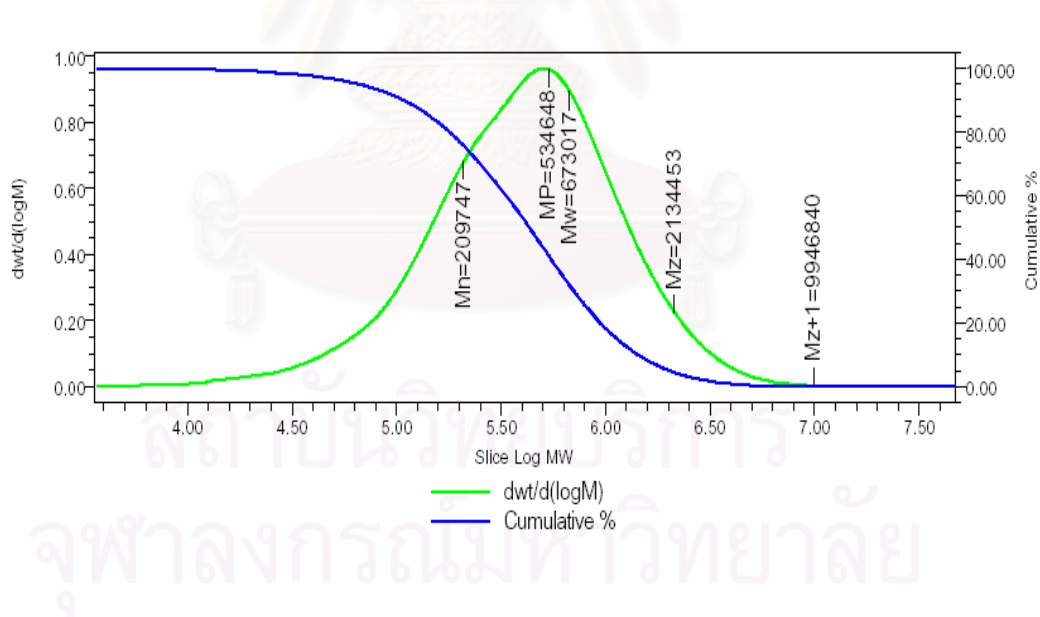


Figure A18 : GPC curve of ethylene polymerization with catalyst2/MMAO in heptane at 70 °C

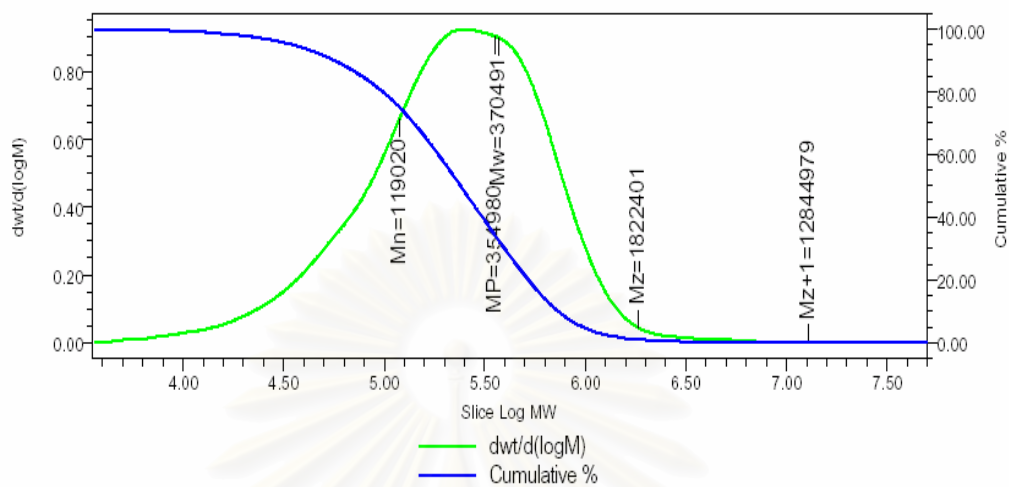


Figure A19 : GPC curve of ethylene polymerization with catalyst2/MMAO in toluene at 70 °C

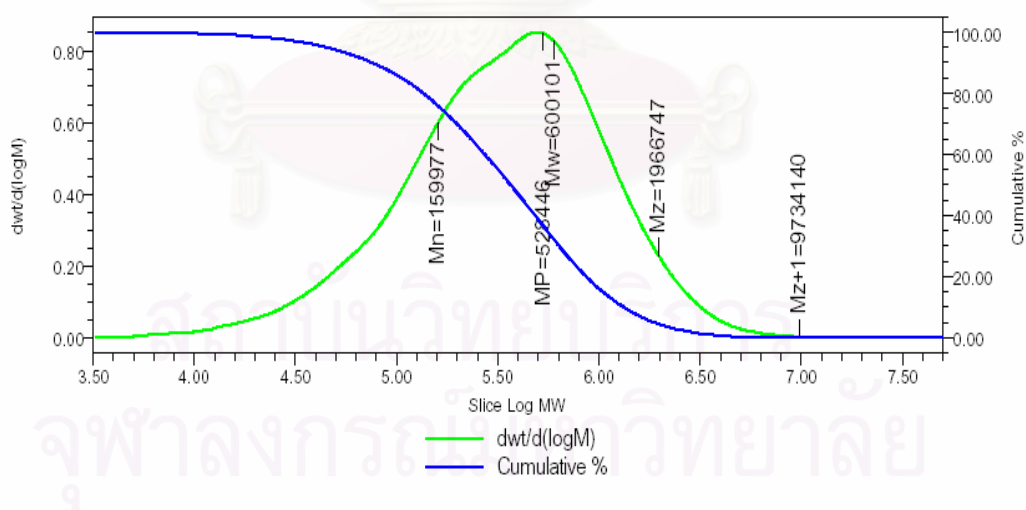


Figure A20 : GPC curve of ethylene polymerization with catalyst2/MMAO in chlorobenzene at 70 °C



APPENDIX B
(Nuclear Magnetic Resonance)

สถาบันวิทยบริการ
จุฬาลงกรณ์มหาวิทยาลัย

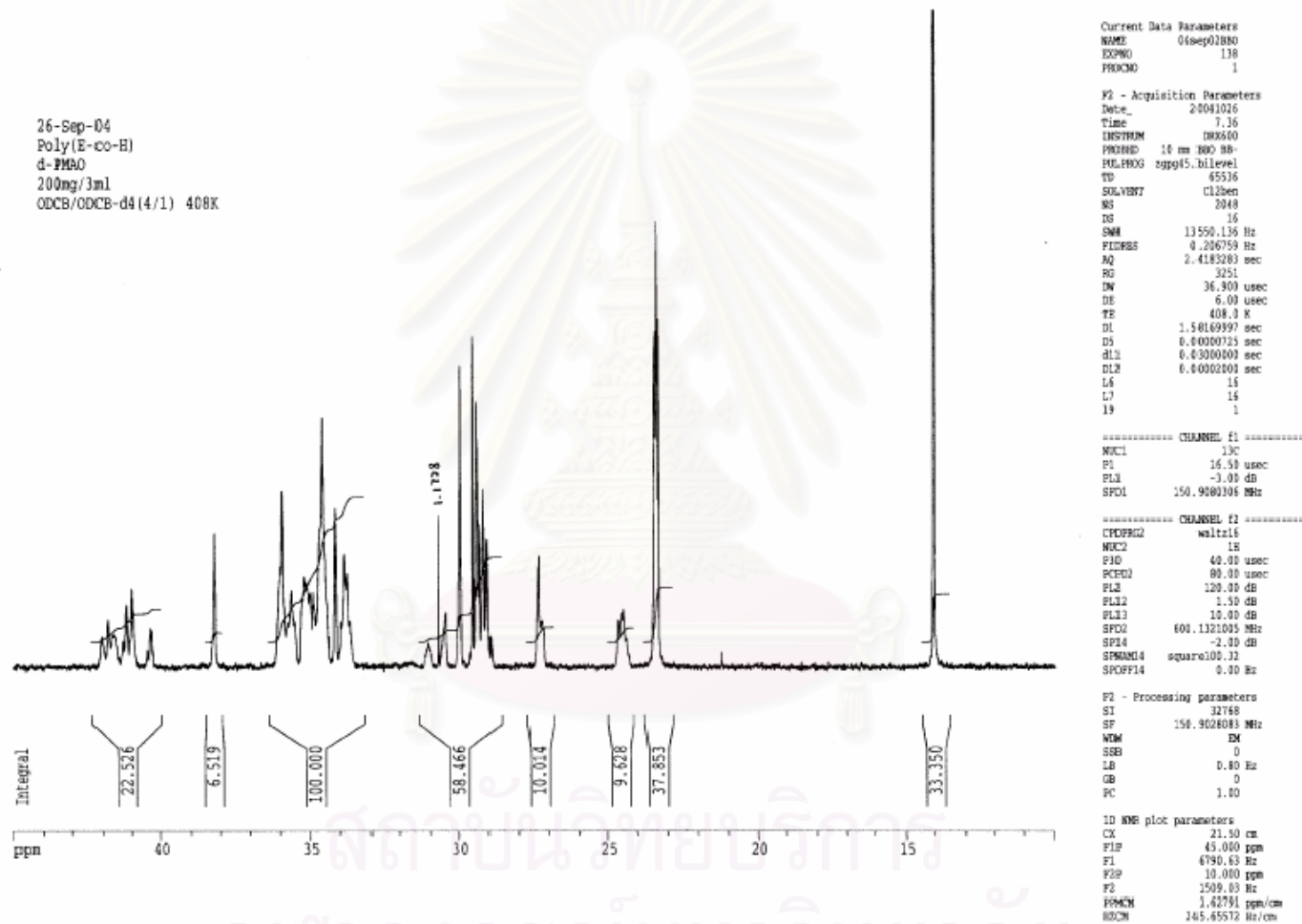


Figure B1 : ^{13}C -NMR spectrum of ethylene/1-hexene copolymer with catalyst 1/d-PMAO system at 40 °C

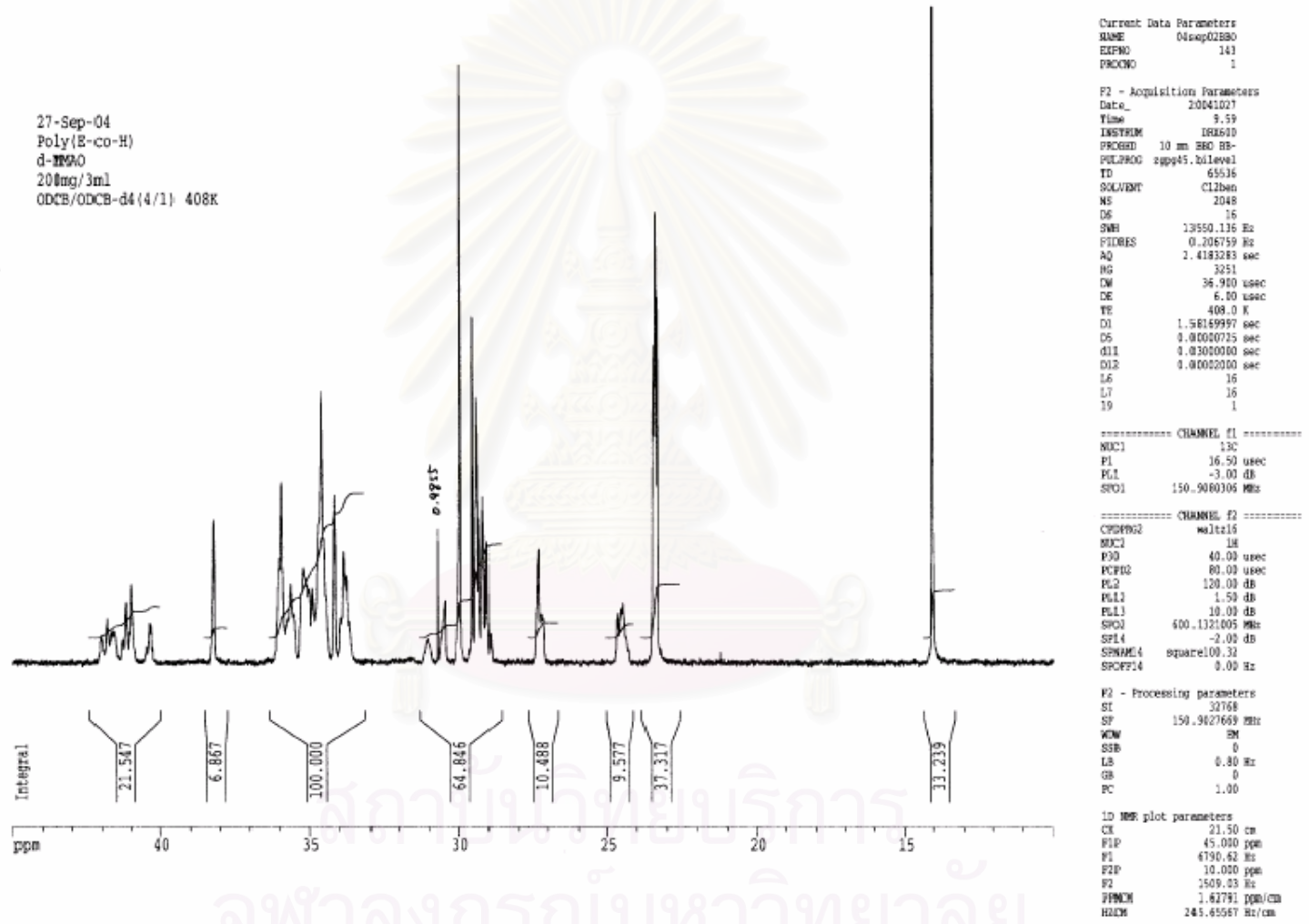


Figure B2 : ^{13}C -NMR spectrum of ethylene/1-hexene copolymer with catalyst 1/d-MMAO system at 40 °C

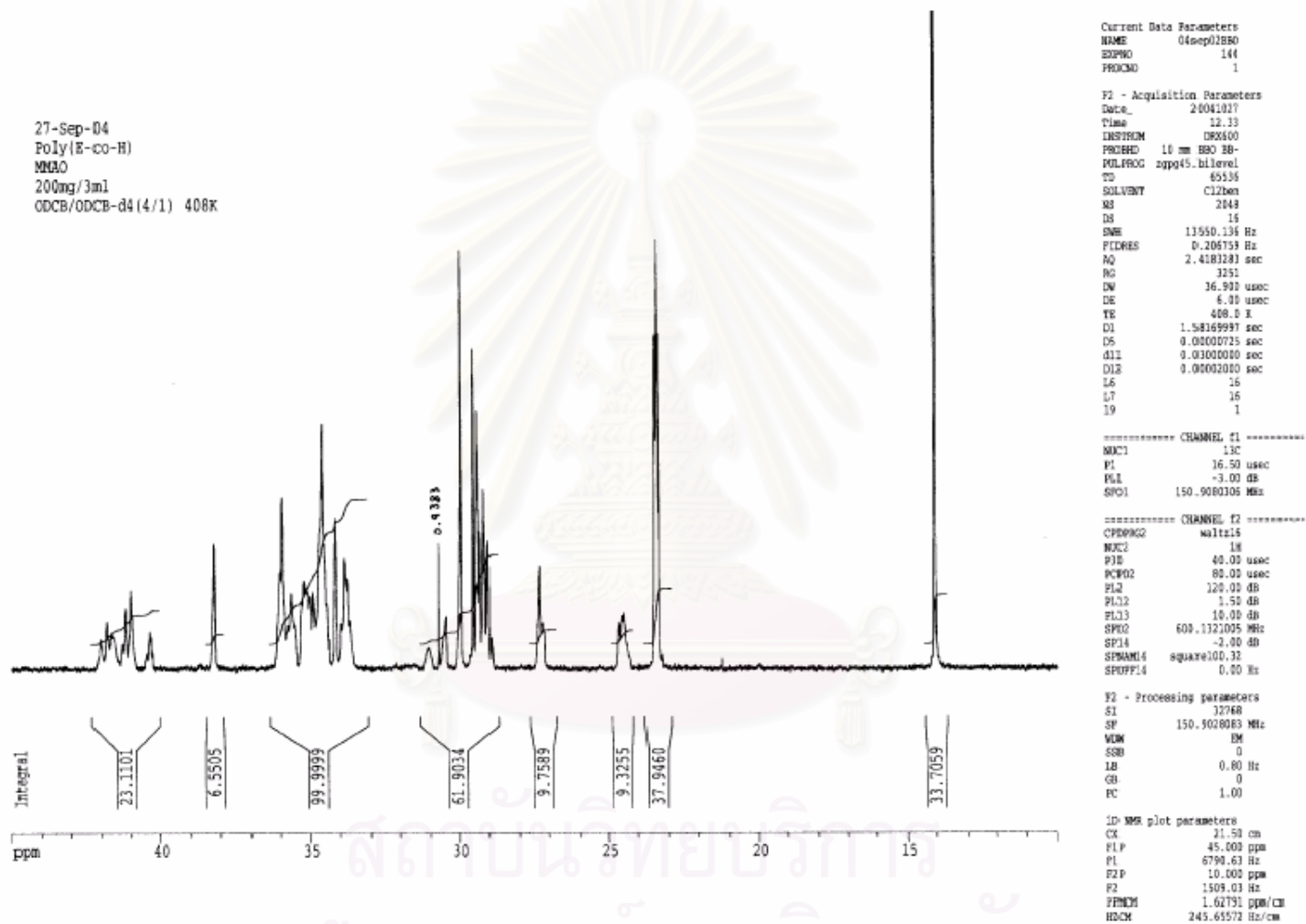


Figure B3 : ^{13}C -NMR spectrum of ethylene/1-hexene copolymer with catalyst 1/MMAO system at 40 °C

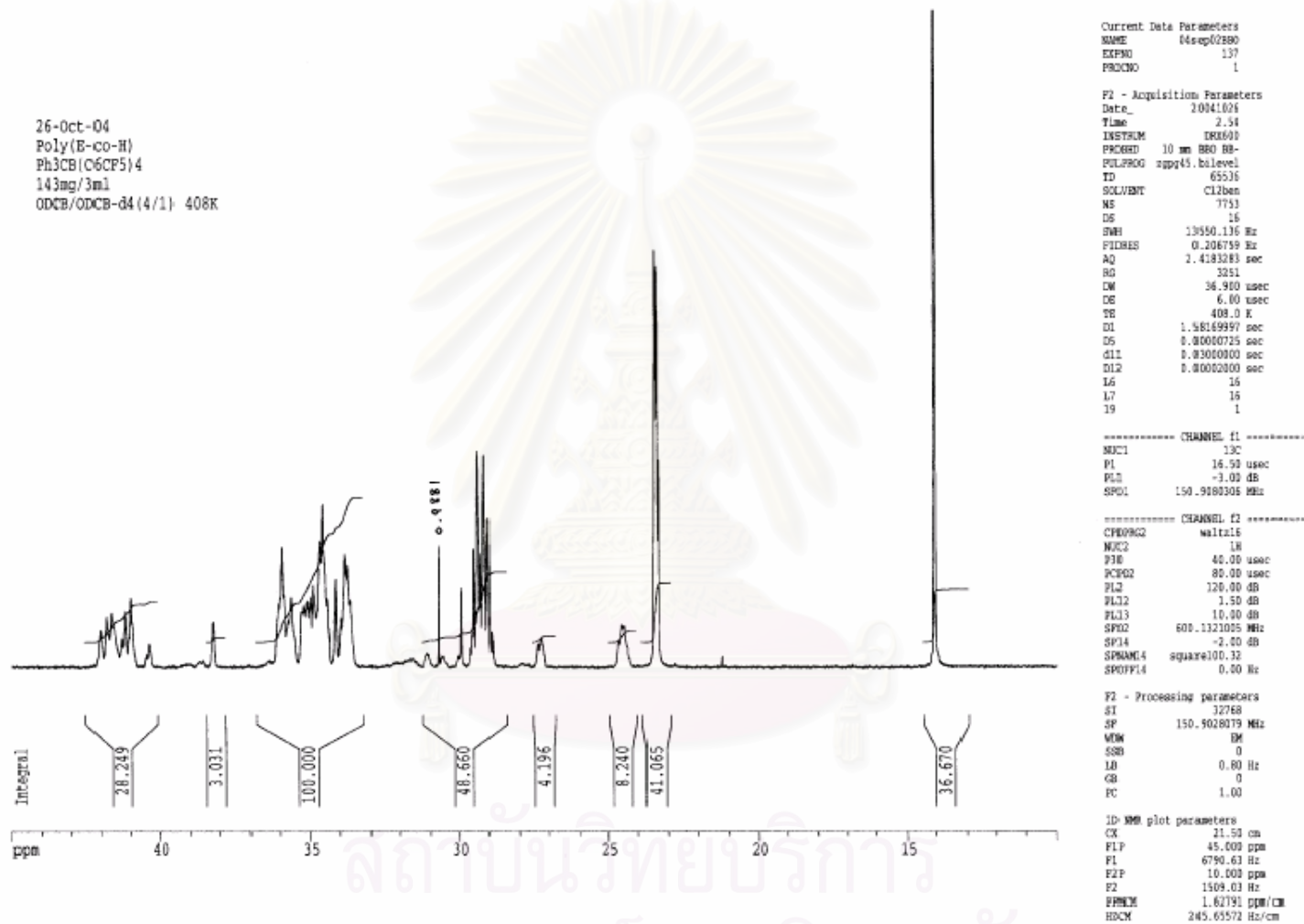


Figure B4 : ^{13}C -NMR spectrum of ethylene/1-hexene copolymer with catalyst 1/Borate system at 40 °C

Department of Science Service
Chemistry Division
Lab no.: YD 596
Name of sample: EHC7 70
Instrument: Avance DFX-400
Solvent: CDCl3 at 70c
Operator: Nongnaphat D.
Date: 22-08-2005

Current Data Parameters
NAME 13EDCB
EXPNO 4
PROCNO 1

F2 - Acquisition Parameters
Date_ 500000
Time 18.48
INSTRUM dpx400
PROBHD 5 mm QNP 1H
PULPROG zgdc
TD 131072
SOLVENT CDCl3
NS 10920
DS 0
SWH 25125.629 Hz
FIDRES 0.191693 Hz
AQ 2.6083827 sec
RG 4096
DW 19.900 usec
DE 7.14 usec
TE 304.0 K
d11 0.0300000 sec
PL12 19.00 dB
CPDPRG2 waltz16
PCPD2 106.00 usec
SFO 400.1317746 MHz
NUC1 13C
PL2 120.00 dB
D1 3.00000000 sec
P1 6.80 usec
DE 7.14 usec
SFO 100.6242995 MHz
NUC1 13C
PL1 -6.00 dB

F2 - Processing parameters
SI 65536
SF 100.6127069 MHz
WDW EM
SSB 0
LB 2.00 Hz
GB 0
PC 1.00

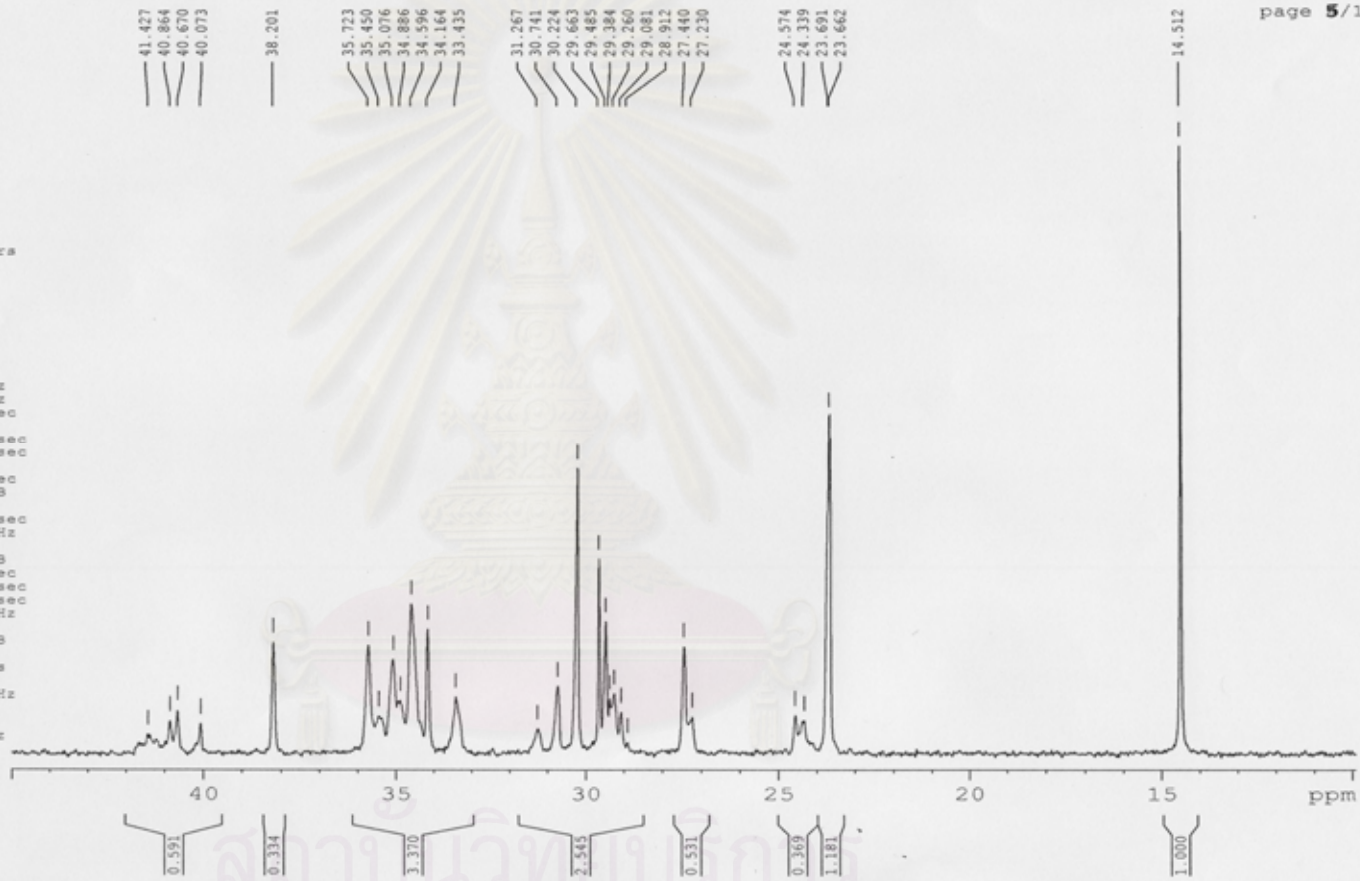


Figure B5 : ¹³C-NMR spectrum of ethylene/1-hexene copolymer with catalyst 1/MMAO in heptane at 70 °C

Department of Science Service
 Chemistry Division
 Lab no. YD 595
 Name of sample: EMTol 70
 Instrument : Avance DPX-400
 Solvent : CDCl3 at 70c
 Operator : Nongnaphat D.
 Date : 22-08-2005

Current Data Parameters
 NAME 13EDCS
 EXPNO 8
 PROCNO 1

F2 - Acquisition Parameters
 Date_ 500000
 Time 10.03
 INSTRUM dpx400
 PROBHD 5 mm QNP 1H
 PULPROG zgpg30
 TD 131072
 SOLVENT CDCl3
 NS 5766
 DS 0
 SWH 25125.629 Hz
 FIDRES 0.191693 Hz
 AQ 2.6083827 sec
 RG 8192
 DW 19.900 usec
 DE 7.14 usec
 TE 304.0 K
 d11 0.0300000 sec
 FL12 19.00 dB
 CPDPRG2 waltz16
 PCPD2 106.00 usec
 SFO2 400.1317746 MHz
 NUC2 13C
 PL2 120.00 dB
 D1 3.0000000 sec
 S1 6.80 usec
 DE 7.14 usec
 SFO1 100.6242993 MHz
 NUC1 13C
 PL1 -6.00 dB

F2 - Processing parameters
 SI 65536
 SF 100.6127069 MHz
 WDW EM
 SSB 0
 LB 2.00 Hz
 GB 0
 SC 1.00

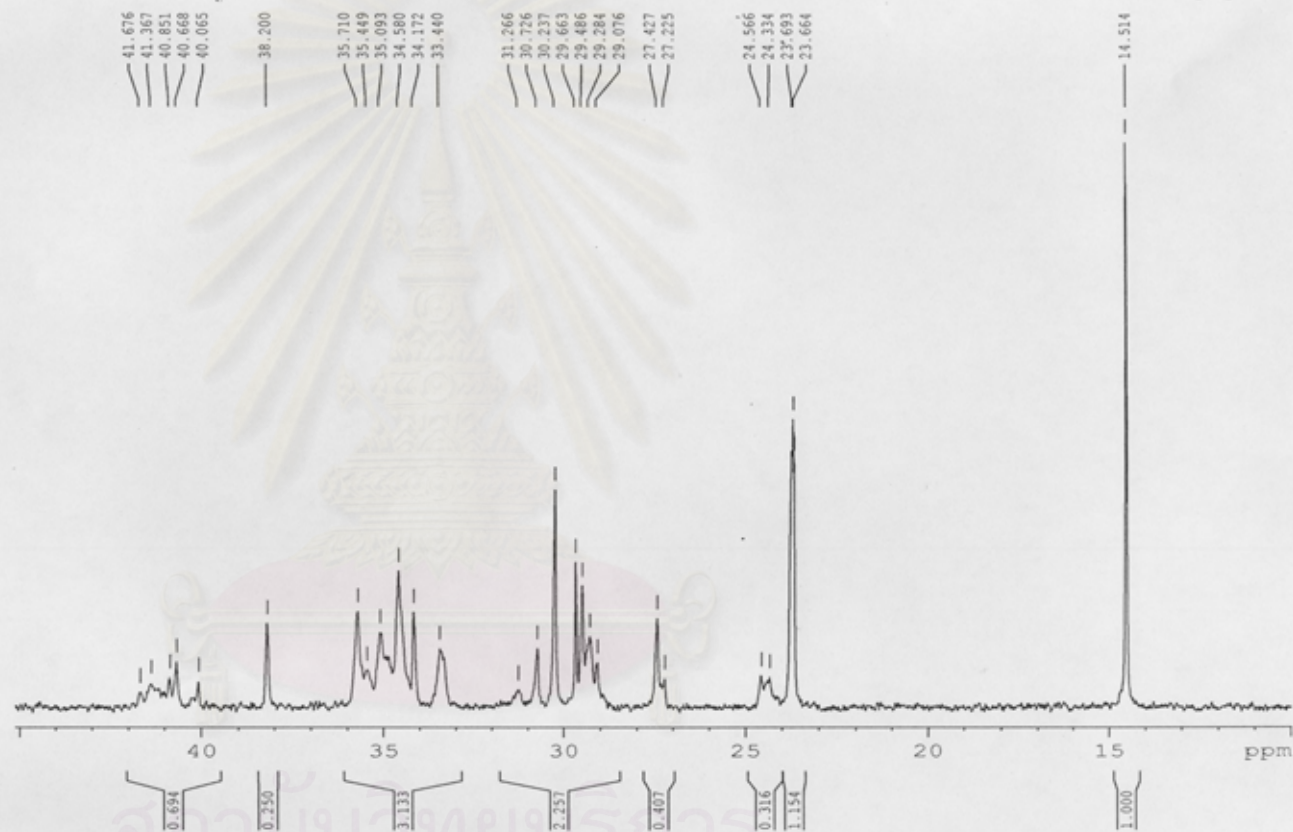


Figure B6 : ¹³C-NMR spectrum of ethylene/1-hexene copolymer with catalyst 1/MMAO in toluene at 70 °C

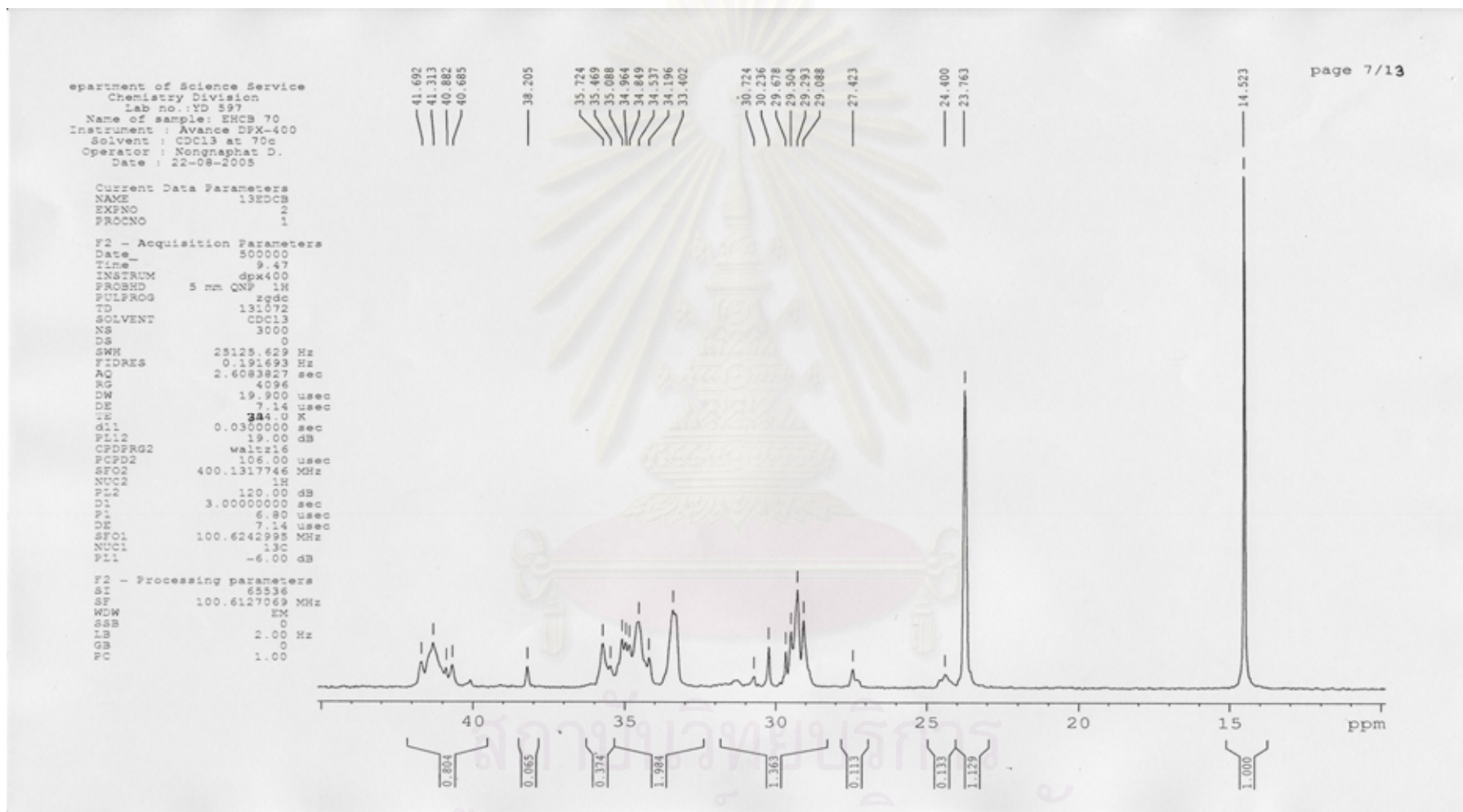


Figure B7 : ^{13}C -NMR spectrum of ethylene/1-hexene copolymer with catalyst 1/MMAO in chlorobenzene at 70 °C

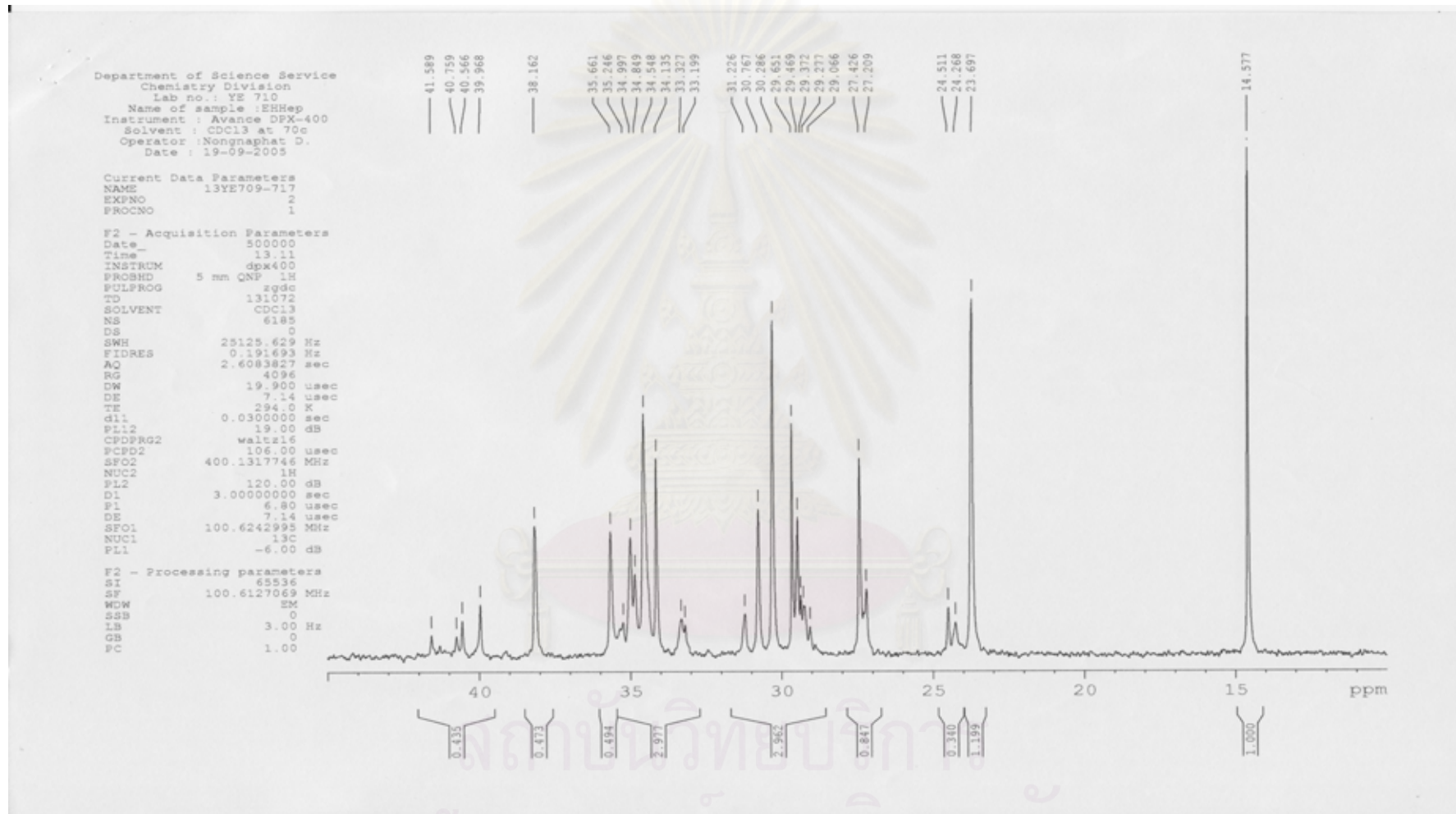


Figure B8 : ^{13}C -NMR spectrum of ethylene/1-hexene copolymer with catalyst 1/MMAO in heptane at 0 °C

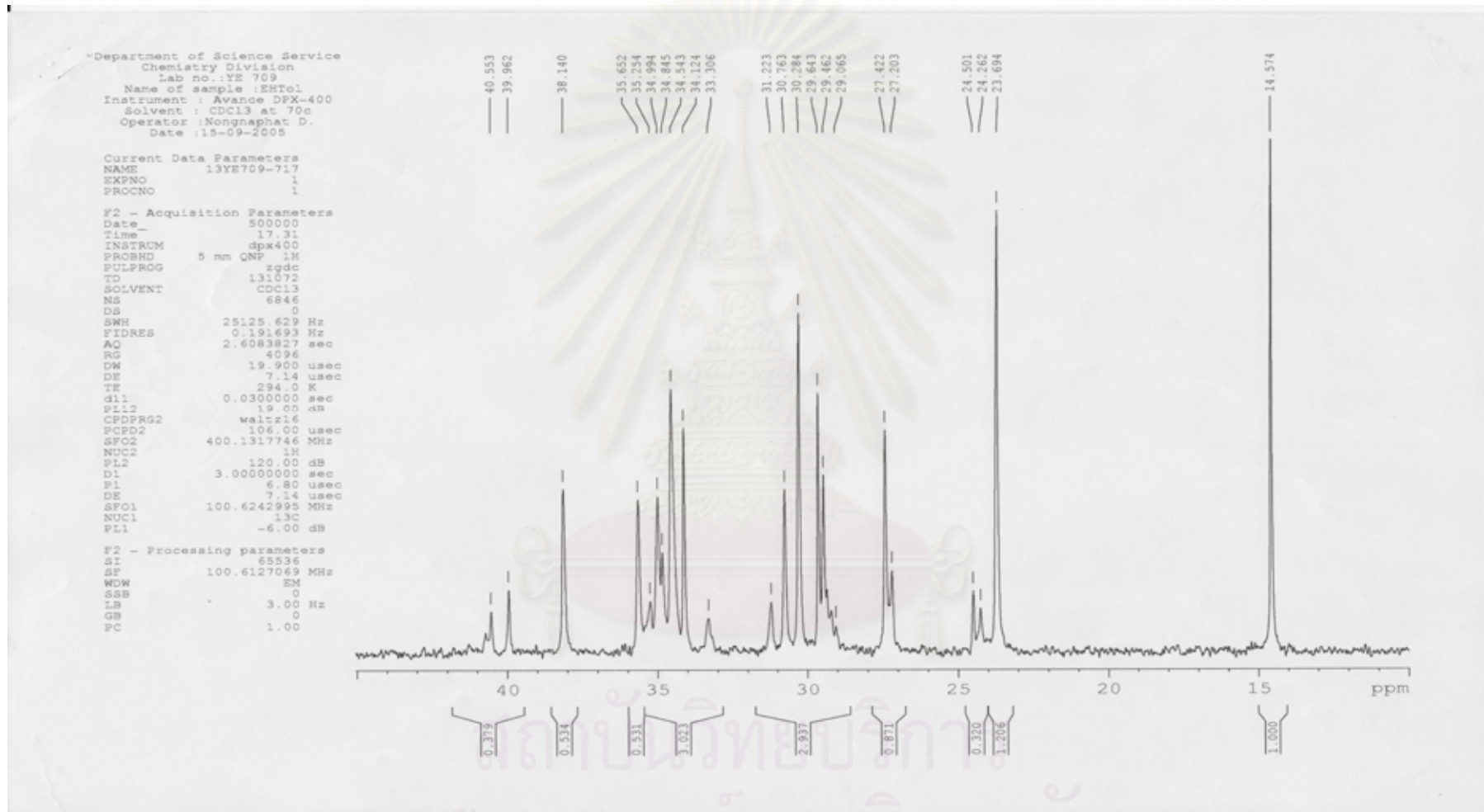


Figure B9 : ^{13}C -NMR spectrum of ethylene/1-hexene copolymer with catalyst 1/MMAO in toluene at 0 °C

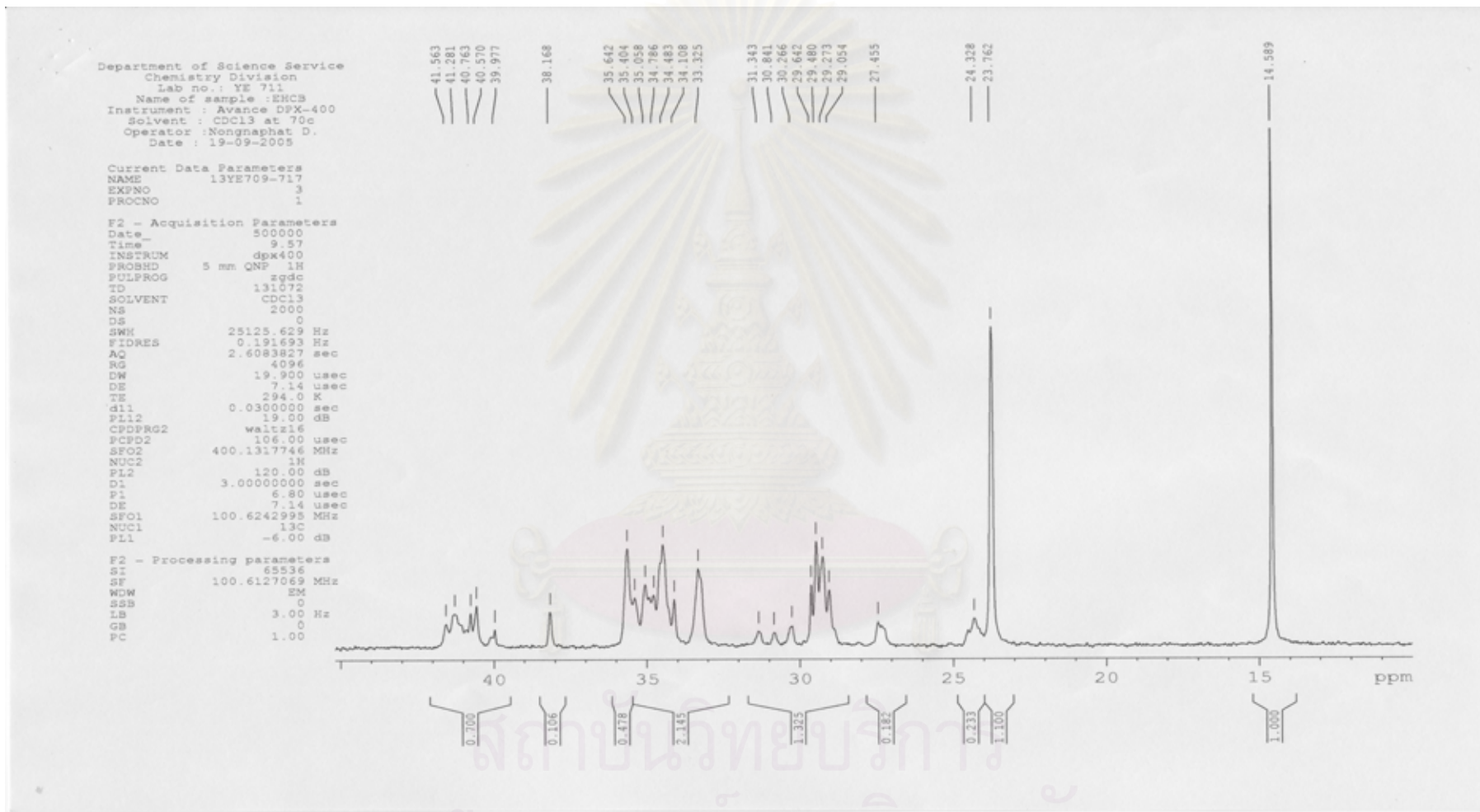


Figure B10 : ^{13}C -NMR spectrum of ethylene/1-hexene copolymer with catalyst 1/MMAO in chlorobenzene at 0 °C

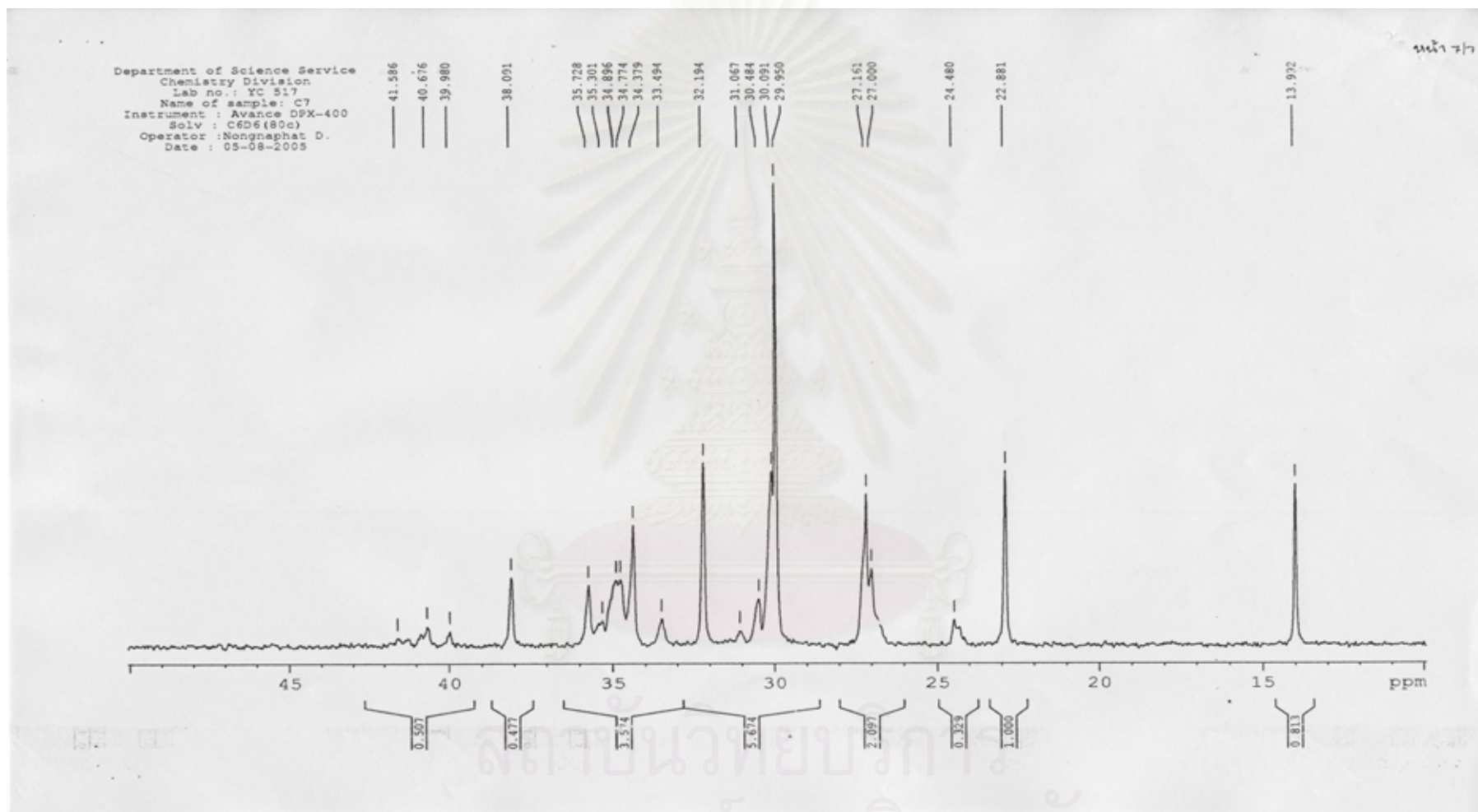


Figure B11 : ^{13}C -NMR spectrum of ethylene/1-octene copolymer with catalyst 1/MMAO in heptane at 70 °C

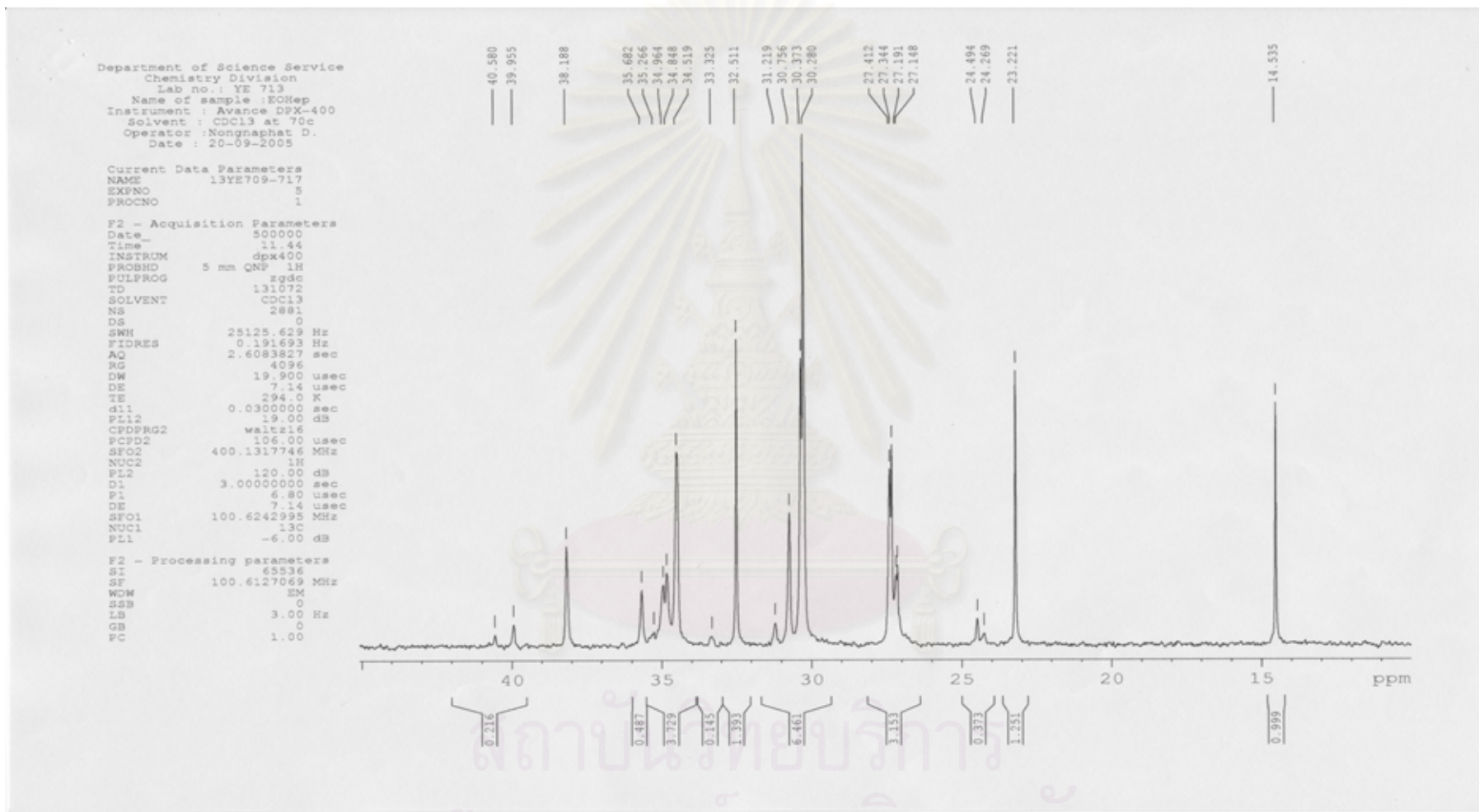


Figure B12 : ^{13}C -NMR spectrum of ethylene/1-octene copolymer with catalyst 1/MMAO in heptane at 0 °C

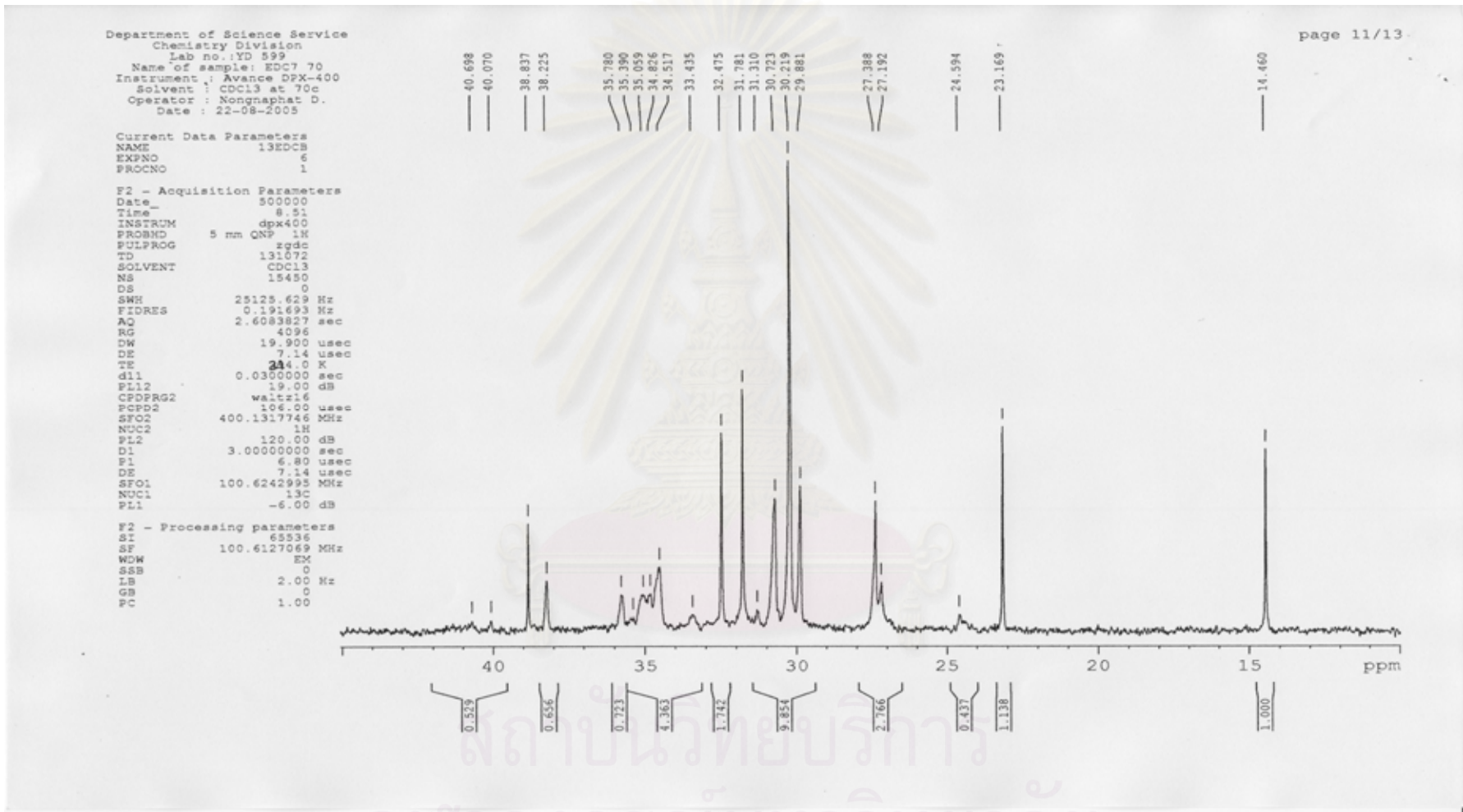


Figure B13 : ¹³C-NMR spectrum of ethylene/1-decene copolymer with catalyst 1/MMAO in heptane at 70 °C

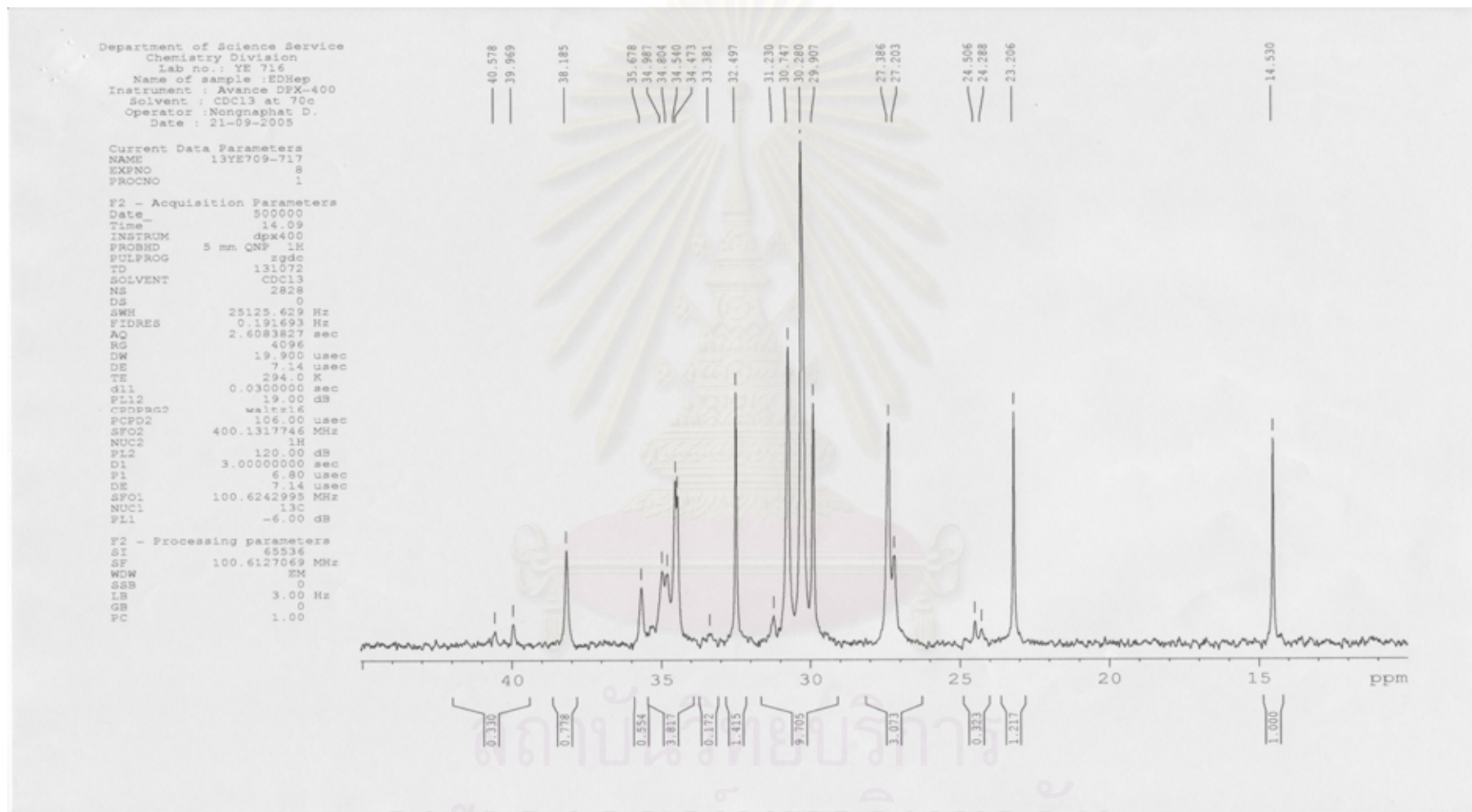


Figure B14 : ^{13}C -NMR spectrum of ethylene/1-decene copolymer with catalyst 1/MMAO in heptane at 0 °C

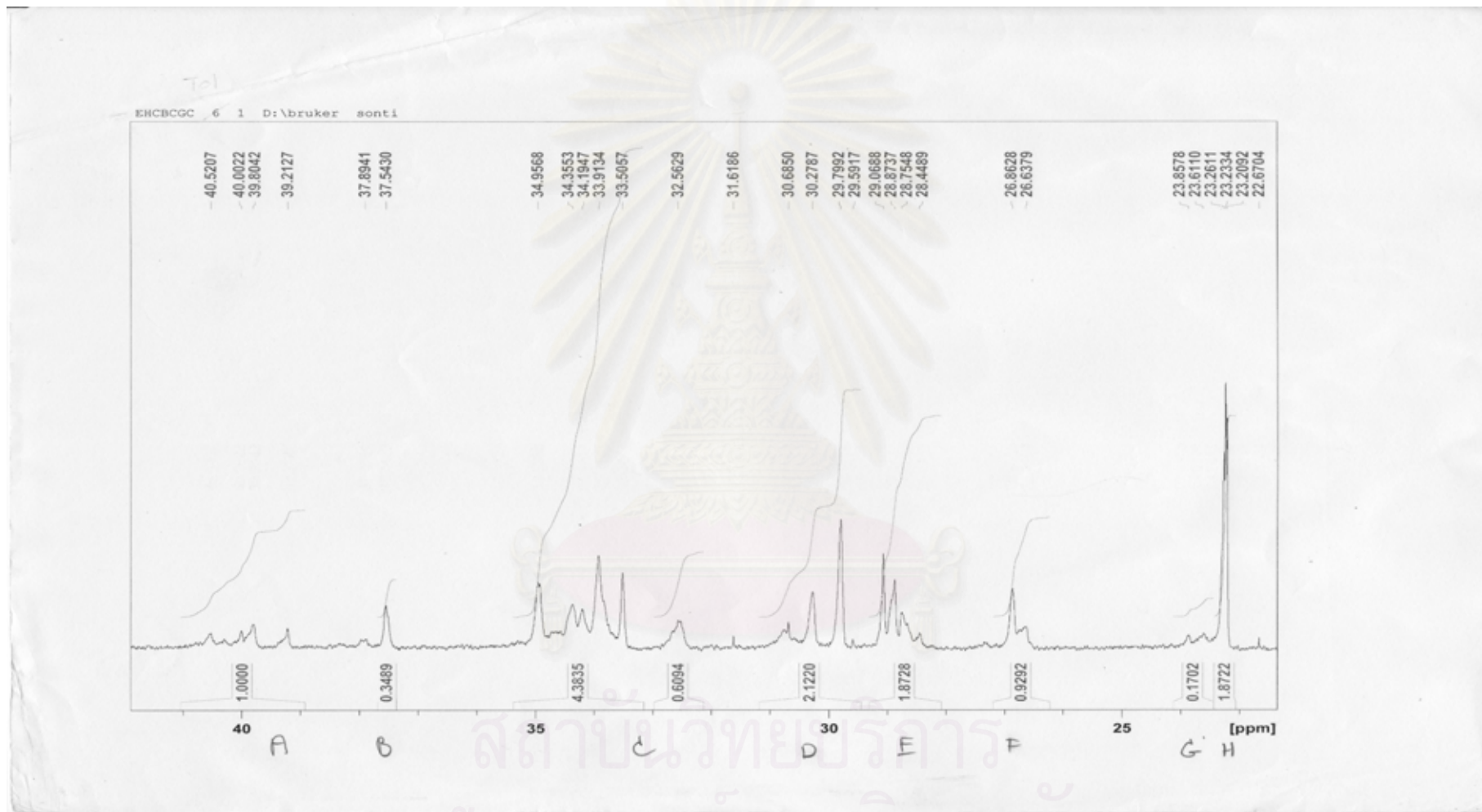


Figure B15 : ^{13}C -NMR spectrum of ethylene/1-hexene copolymer with catalyst 2/MMAO in heptane at 70 °C

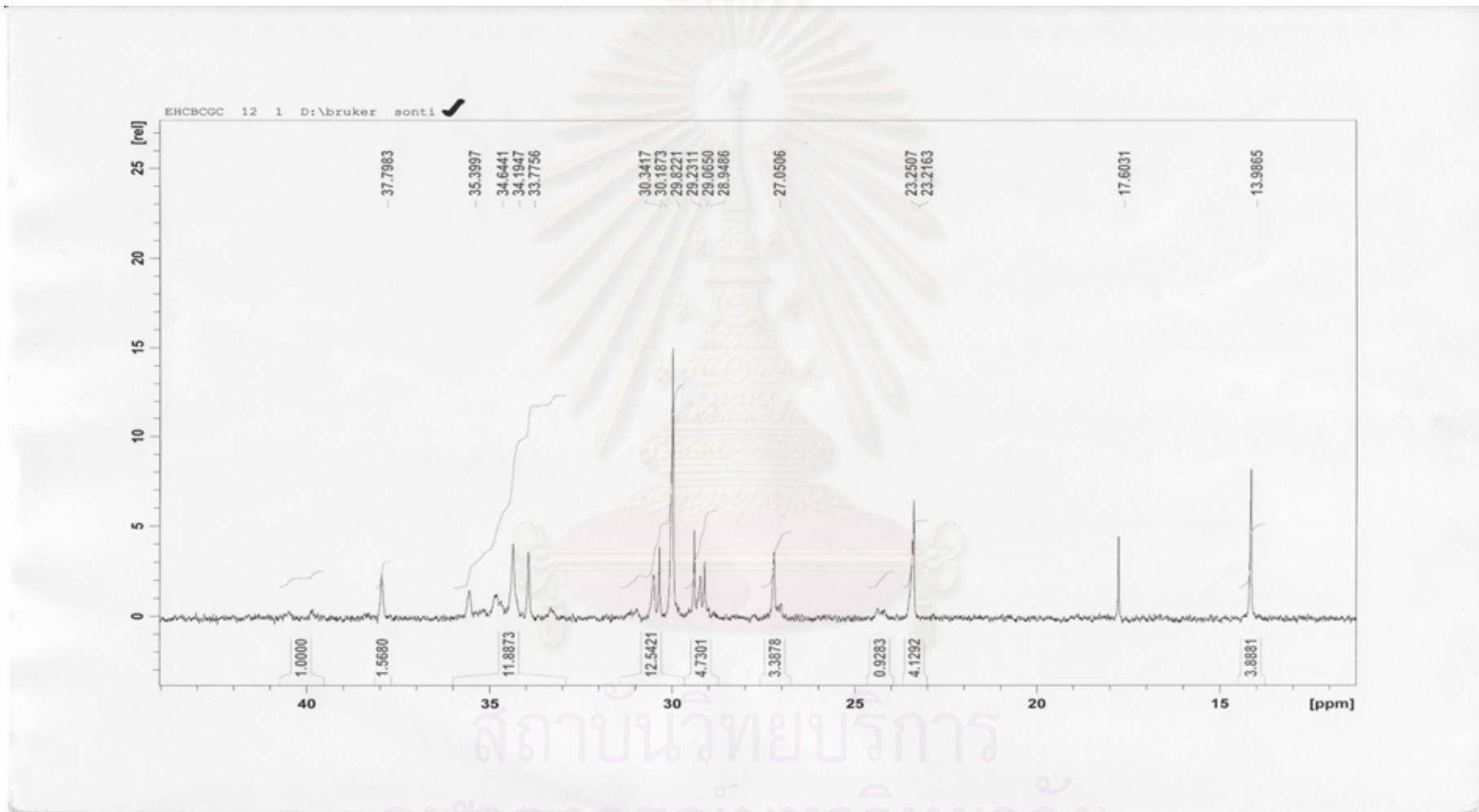


Figure B16 : ^{13}C -NMR spectrum of ethylene/1-hexene copolymer with catalyst 2/MMAO in heptane at 0 °C

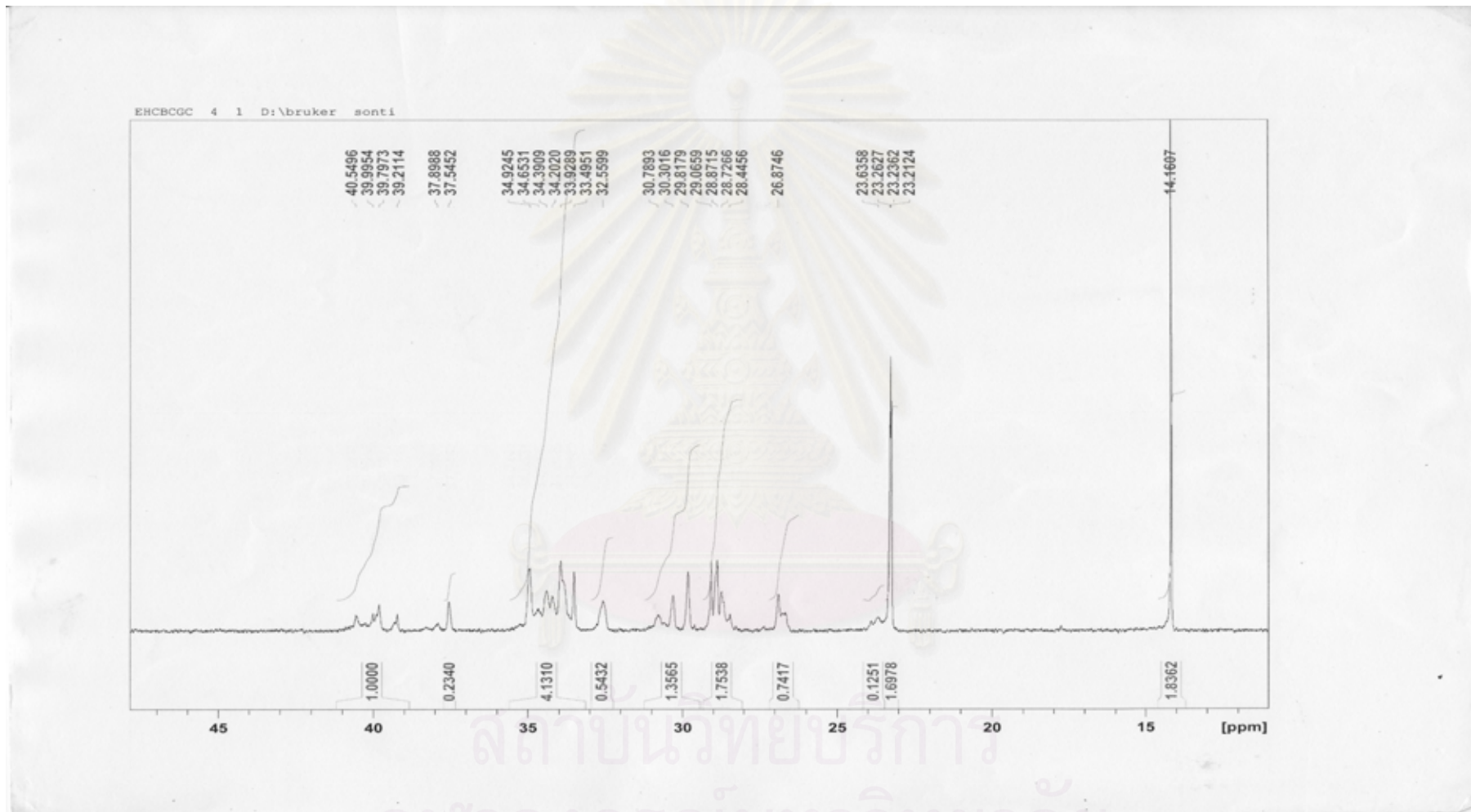


Figure B17 : ^{13}C -NMR spectrum of ethylene/1-hexene copolymer with catalyst 2/MMAO in toluene at $70\text{ }^\circ\text{C}$

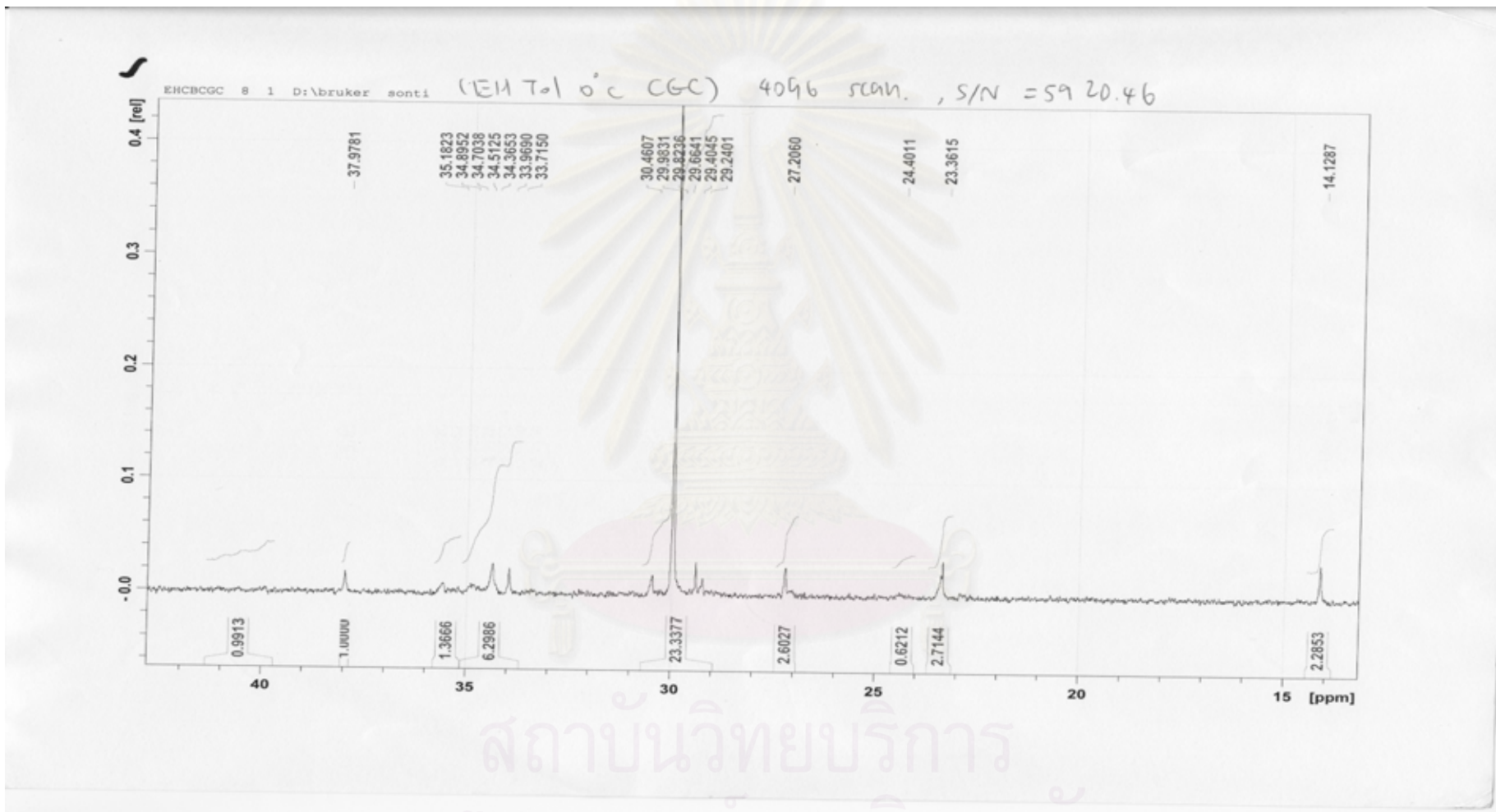
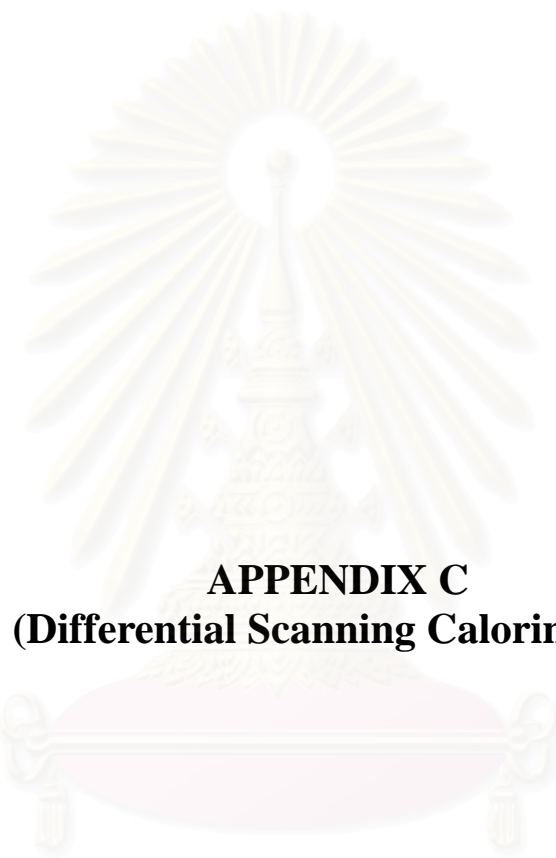


Figure B18 : ^{13}C -NMR spectrum of ethylene/1-hexene copolymer with catalyst 2/MMAO in toluene at 0 °C



Figure B19 : ^{13}C -NMR spectrum of ethylene/1-hexene copolymer with catalyst 2/MMAO in chlorobenzene at 70 °C



APPENDIX C
(Differential Scanning Calorimeter)

สถาบันวิทยบริการ
จุฬาลงกรณ์มหาวิทยาลัย

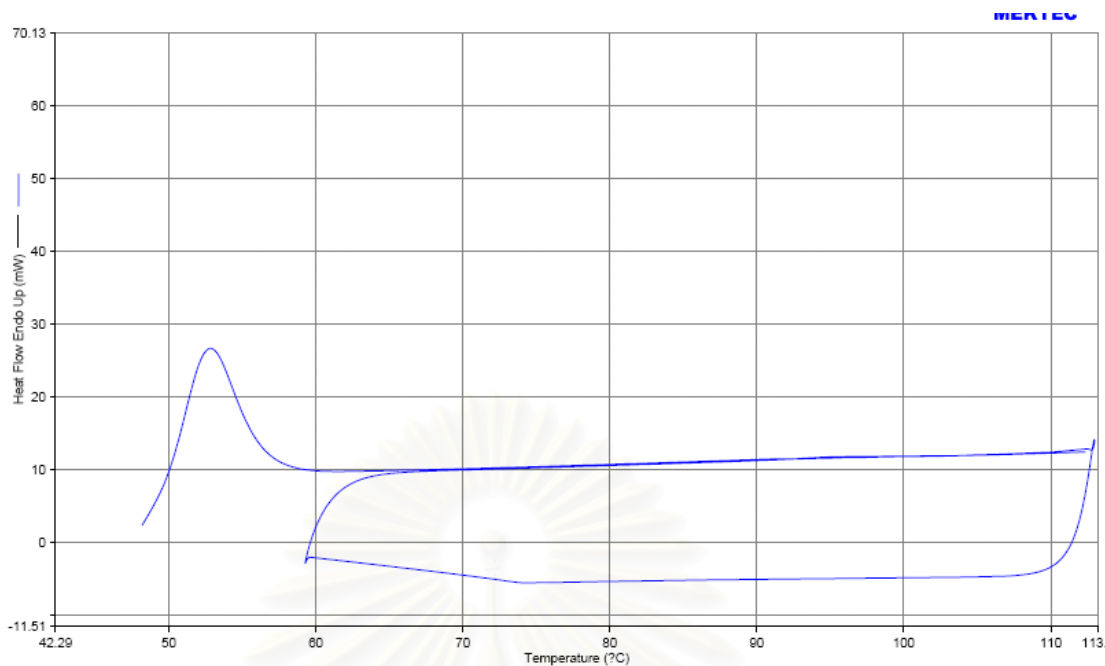


Figure C1: DSC scanning of Ethylene/1-hexene copolymer with catalyst 1/MMAO in heptane at 70° C

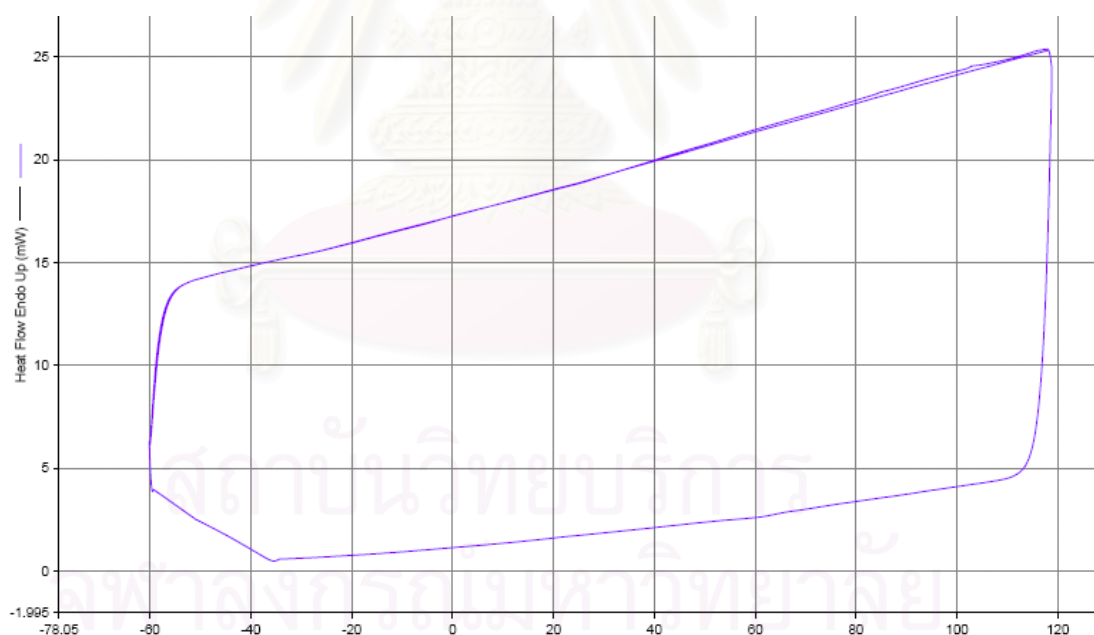


Figure C2: DSC scanning of Ethylene/1-hexene copolymer with catalyst 1/MMAO in toluene at 70° C

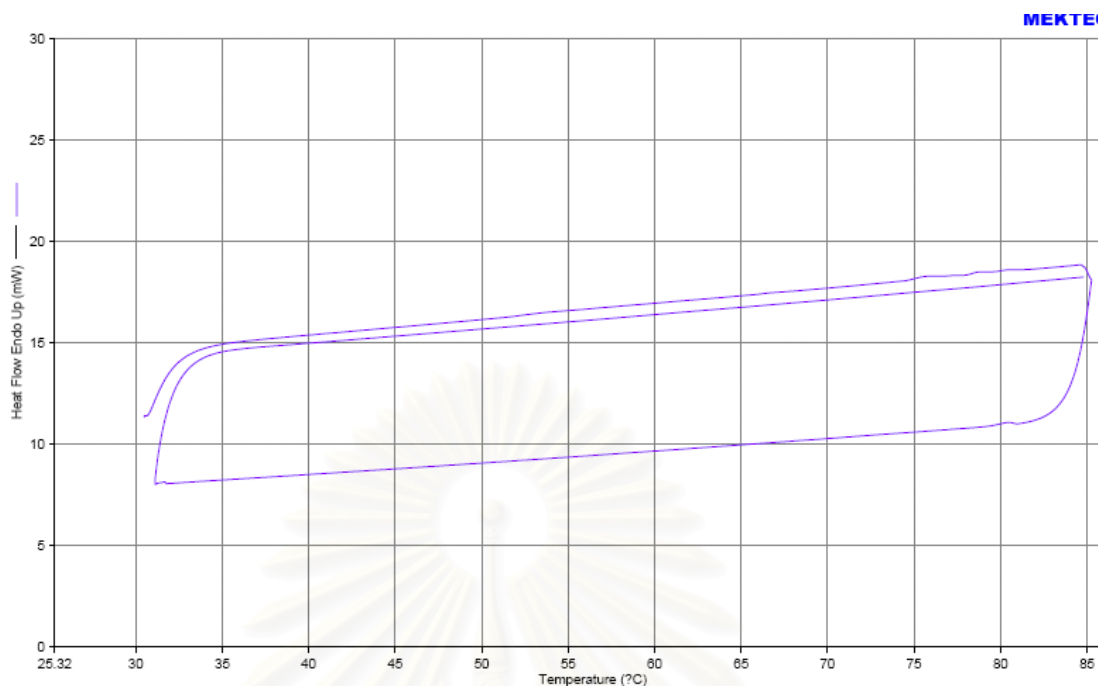


Figure C3: DSC scanning of Ethylene/1-hexene copolymer with catalyst 1/MMAO in chlorobenzene at 70° C

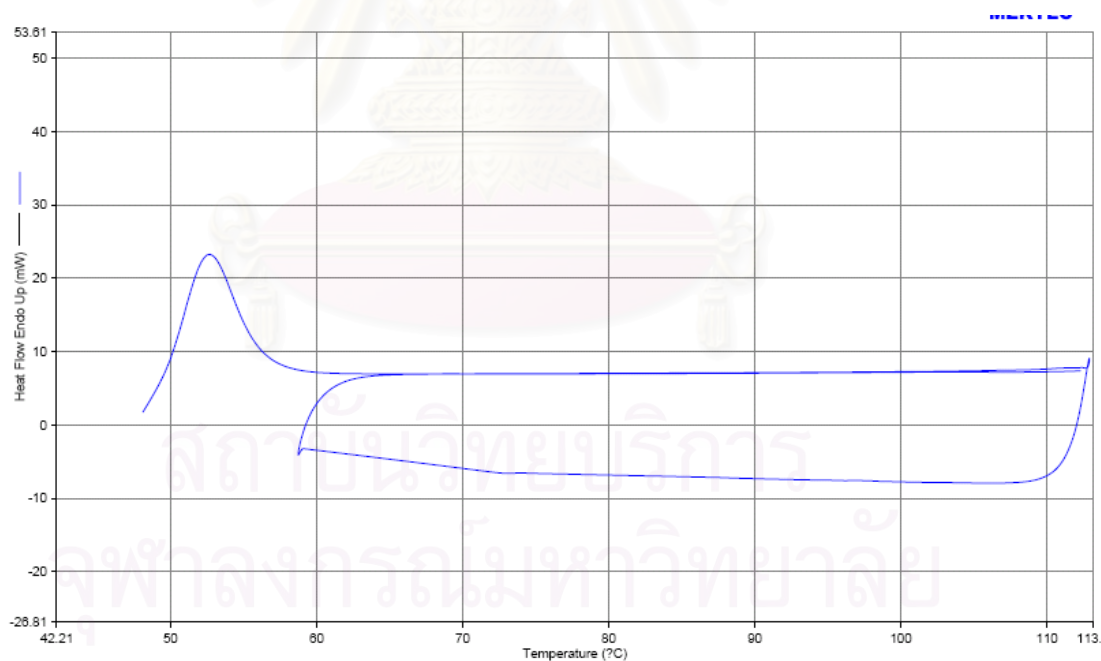


Figure C4: DSC scanning of Ethylene/1-octene copolymer with catalyst 1/MMAO in heptane at 70° C

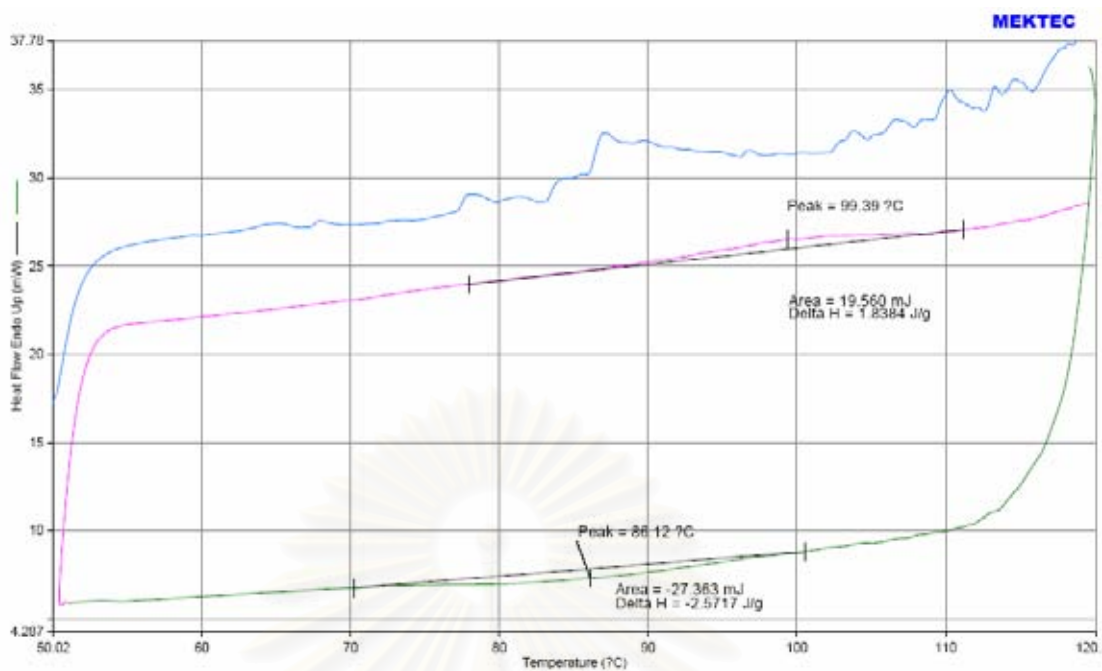


Figure C5: DSC scanning of Ethylene/1-decene copolymer with catalyst 1/MMAO in heptane at 70° C

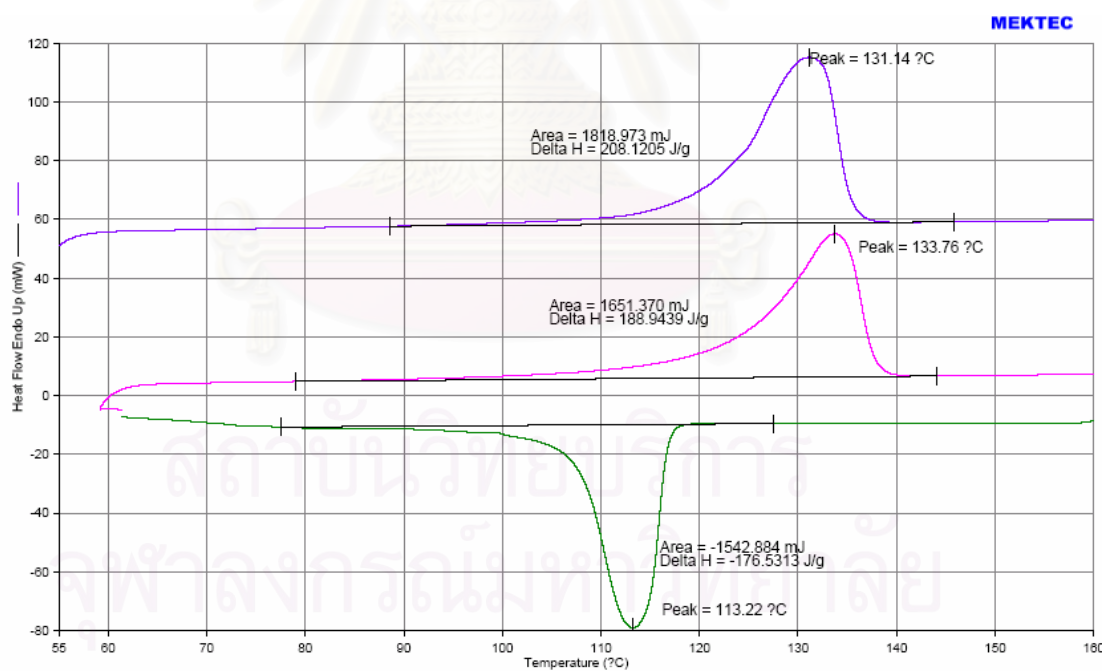


Figure C6: DSC scanning of polyethylene with catalyst 1/MMAO in heptane at 70° C

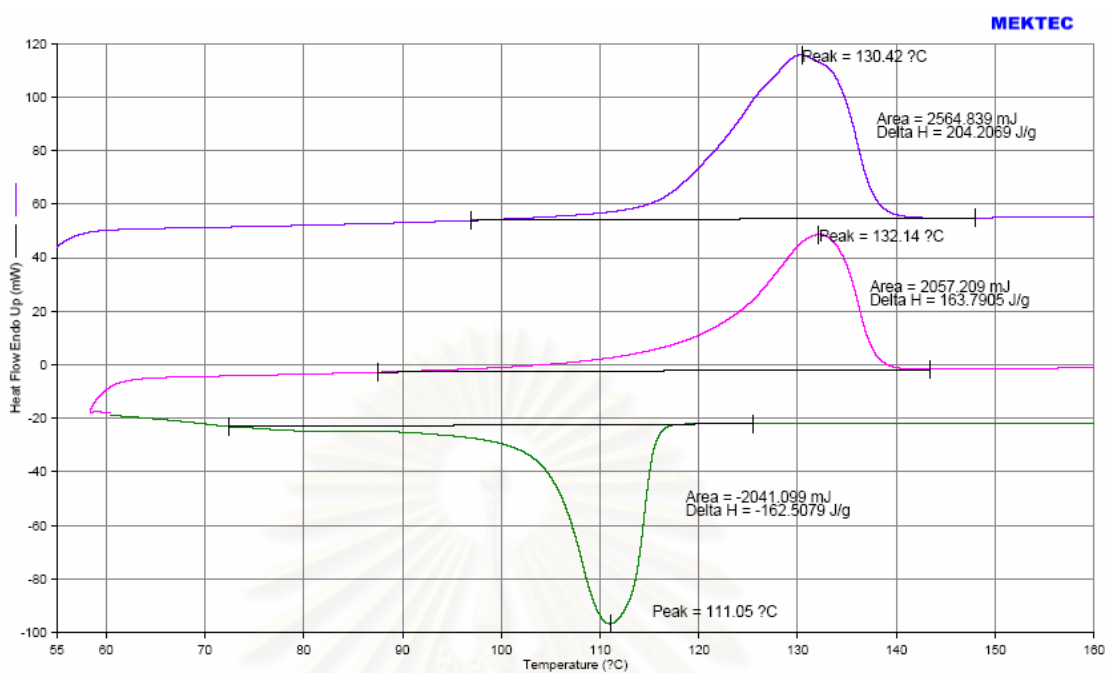


Figure C7: DSC scanning of polyethylene with catalyst 1/MMAO in toluene at 70°C

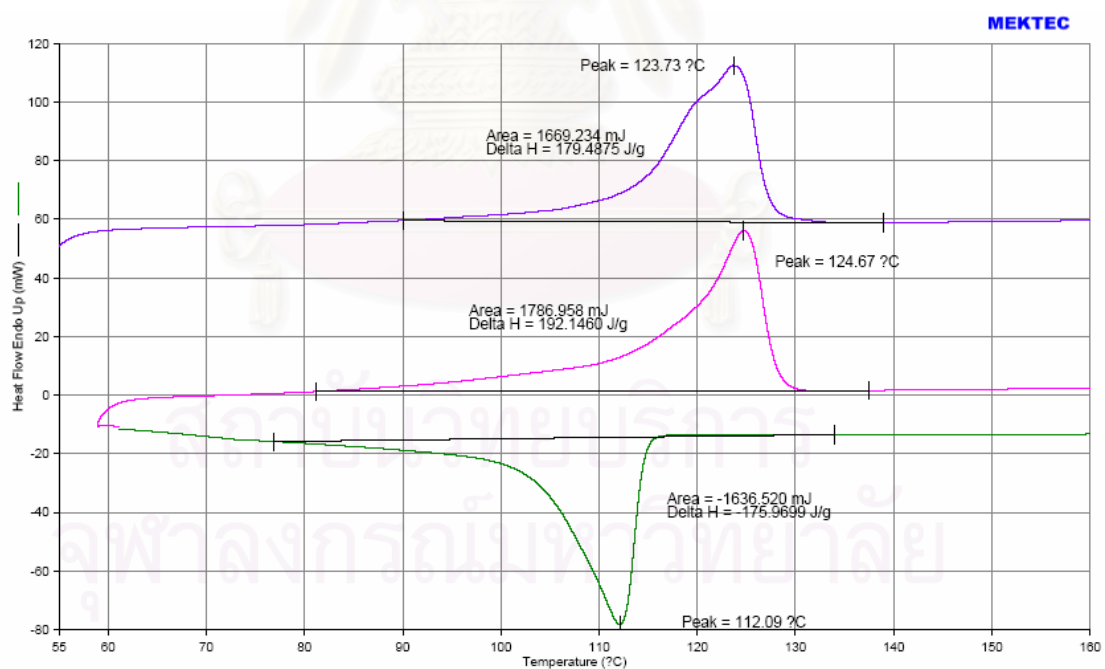


Figure C8: DSC scanning of polyethylene with catalyst 1/MMAO in chlorobenzene at 70°C

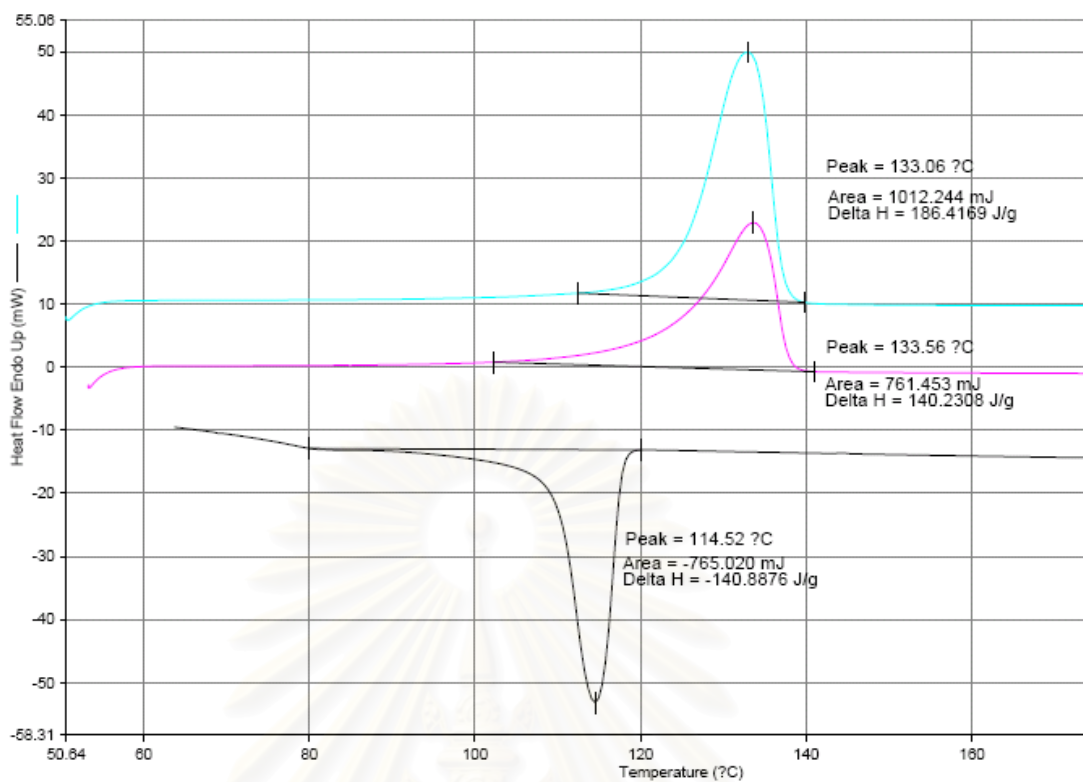


Figure C9: DSC scanning of polyethylene with catalyst 2/MMAO in heptane at 70°C

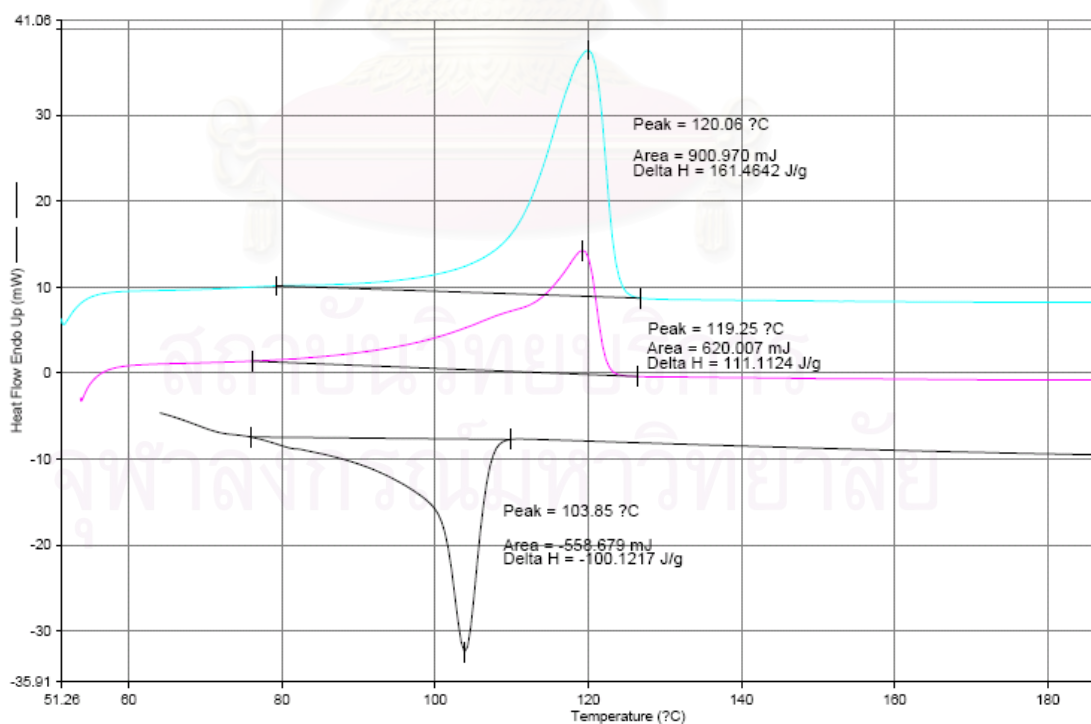


Figure C10: DSC scanning of polyethylene with catalyst 2/MMAO in toluene at 70°C

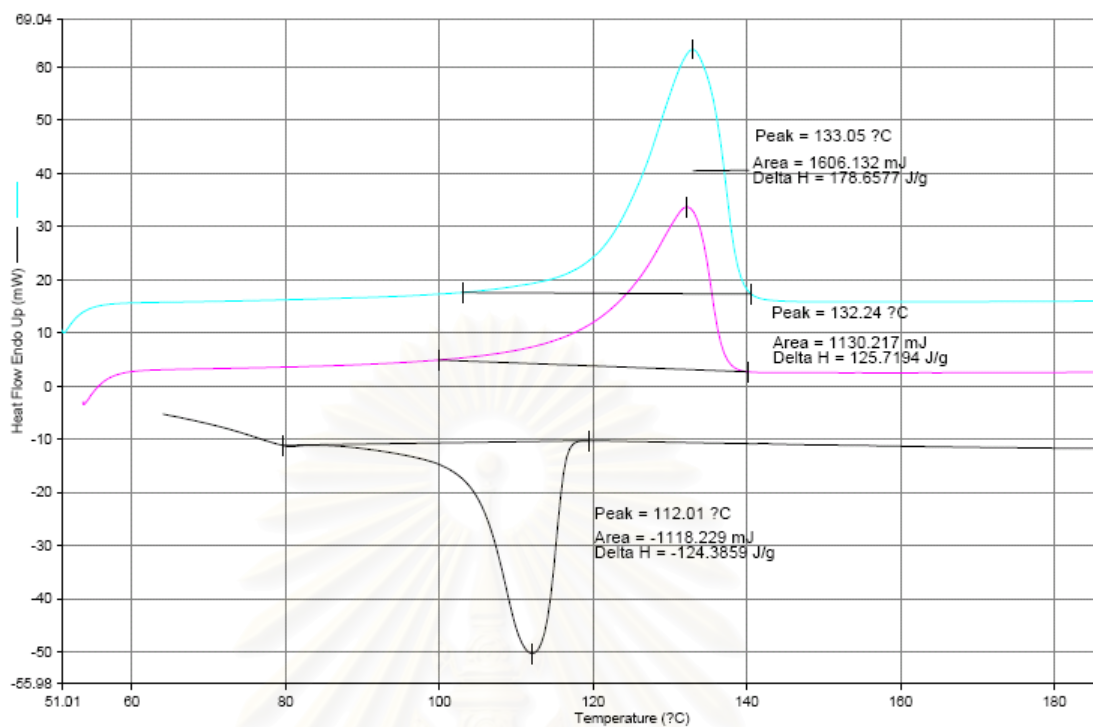
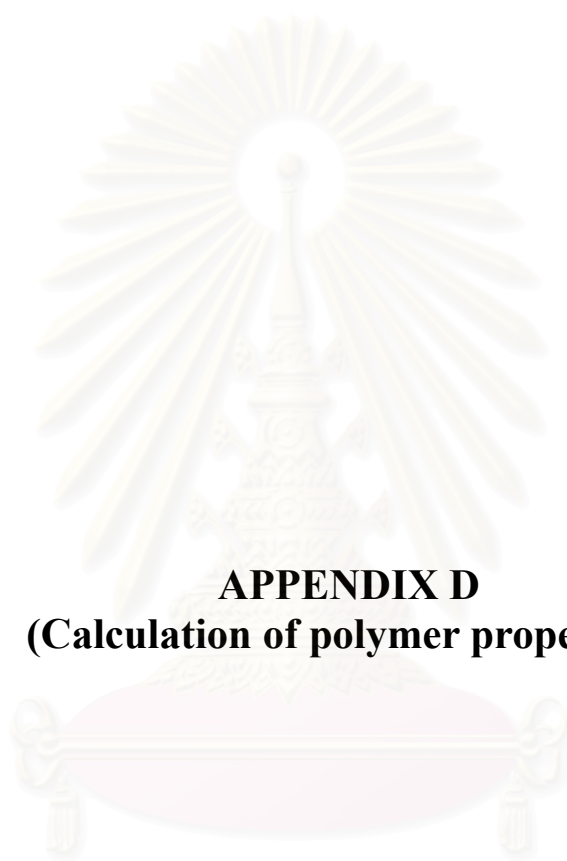


Figure C11: DSC scanning of polyethylene with catalyst 2/MMAO in chlorobenzene at 70° C

สถาบันวิทยบริการ
จุฬาลงกรณ์มหาวิทยาลัย



APPENDIX D
(Calculation of polymer properties)

สถาบันวิทยบริการ
จุฬาลงกรณ์มหาวิทยาลัย

D.1 Calculation of polymer microstructure

Polymer microstructure and also triad distribution of monomer can be calculated according to the Prof. James C. Randall [57] in the list of reference. The detail of calculation was be interpreted as follow

D.1.1 Ethylene/1-hexene copolymer

The integral area of ^{13}C -NMR spectrum in the specify range are listed.

T_A	=	39.5 - 42	ppm
T_B	=	38.1	ppm
T_C	=	33 - 36	ppm
T_D	=	28.5 - 31	ppm
T_E	=	26.5 - 27.5	ppm
T_F	=	24 - 25	ppm
T_G	=	23.4	ppm
T_H	=	14.1	ppm

Triad distribution was calculated as the followed formular

$k[\text{HHH}]$	=	$2T_A - T_C + T_G + 2T_F + T_E$
$k[\text{EHH}]$	=	$2T_C - 2T_G - 4T_F - 2T_E - 2T_A$
$k[\text{EHE}]$	=	T_B
$k[\text{EEE}]$	=	$0.5T_D - 0.5T_G - 0.25T_E$
$k[\text{HEE}]$	=	T_E
$k[\text{HEH}]$	=	T_F

D.1.2 Ethylene/1-octene copolymer

The integral area of ^{13}C -NMR spectrum in the specify range are listed.

T_A	=	39.5 - 42	ppm
T_B	=	38.1	ppm
T_C	=	36.4	ppm
T_D	=	33 - 36	ppm
T_E	=	32.2	ppm
T_F	=	28.5 - 31	ppm
T_G	=	25.5 - 27.5	ppm
T_H	=	24 - 25	ppm

$$\begin{aligned} T_I &= 22 - 23 \quad \text{ppm} \\ T_J &= 14 - 15 \quad \text{ppm} \end{aligned}$$

Triad distribution was calculated as the followed formula

$$\begin{aligned} k[\text{OOO}] &= T_A - 0.5T_C \\ k[\text{EOO}] &= T_C \\ k[\text{EOE}] &= T_B \\ k[\text{EEE}] &= 0.5T_F - 0.25T_E - 0.25T_G \\ k[\text{OEE}] &= T_G - T_E \\ k[\text{OEO}] &= T_H \end{aligned}$$

D.1.3 Ethylene/1-decene copolymer

The integral area of ^{13}C -NMR spectrum in the specify range are listed.

$$\begin{aligned} T_A &= 39.5 - 42 \quad \text{ppm} \\ T_B &= 38.1 \quad \text{ppm} \\ T_C &= 36.4 \quad \text{ppm} \\ T_D &= 33 - 36 \quad \text{ppm} \\ T_E &= 32.2 \quad \text{ppm} \\ T_F &= 28.5 - 31 \quad \text{ppm} \\ T_G &= 25.5 - 27.5 \quad \text{ppm} \\ T_H &= 24 - 25 \quad \text{ppm} \\ T_I &= 22 - 23 \quad \text{ppm} \\ T_J &= 14 - 15 \quad \text{ppm} \end{aligned}$$

Triad distribution was calculated as the followed formular

$$\begin{aligned} k[\text{DDD}] &= T_A - 0.5T_C \\ k[\text{EDD}] &= T_C \\ k[\text{EDE}] &= T_B \\ k[\text{EEE}] &= 0.5T_F - 0.5T_E - 0.5T_G - T_I \\ k[\text{DEE}] &= T_G - T_I \\ k[\text{DED}] &= T_H \end{aligned}$$

All copolymer was calculated for the relative comonomer reactivity (r_E for ethylene and r_C for the comonomer) and monomer insertion by using the general formula below

$$r_E = 2[EE]/([EC]X) \qquad r_C = 2[CC]X/[EC]$$

where

$$r_E = \text{ethylene reactivity ratio}$$

$$r_C = \text{comonomer } (\alpha\text{-olefin) reactivity ratio}$$

$$[EE] = [EEE] + 0.5[CEE]$$

$$[EC] = [CEC] + 0.5[CEE] + [ECE] + 0.5[ECC]$$

$$[CC] = [CCC] + 0.5[ECC]$$

$$X = [E]/[C] \text{ in the feed} = \text{concentration of ethylene (mol/L) / concentration of comonomer (mol/L) in the feed.}$$

$$\%E = [EEE] + [EEH] + [HEH]$$

$$\%H = [HHH] + [HHE] + [EHE]$$

D.2 Calculation of crystallinity for ethylene/ α -olefin copolymer

The crystallinities of copolymers were determined by differential scanning calorimeter. %crystallinity of copolymers is calculated from equationn [71].

$$\chi(\%) = \frac{\Delta H_m}{\Delta H_m^0} \times 100$$

Where $\chi(\%)$ = %crystallinity

$$\Delta H_m = \text{the heat of fusion of sample (J/g)}$$

$$\Delta H_m^0 = \text{the heat of fusion of perfectly crystalline polyethylene (286 J/g) [71]}$$

VITA

Mr. Nawaporn Intaragamjon was born on May 4, 1981 in Bangkok, Thailand. He received the Bachelors Degree of Chemical Engineering from the Department of Chemical Engineering, Faculty of Engineering, Chulalongkorn University in May 2002, He continued his Doctor degree study at Chulalongkorn University in June, 2002.

In his research has been accepted and/or submitted for the publication as describe below.

1. A comparative study ethylene/1-hexene copolymerization with $[t\text{-BuNSiMe}_2\text{Flu}]\text{TiMe}_2$ catalyst via various activators, **Study in surface science and catalysis**, in press
2. Elucidation of solvent effects on the catalytic behaviors for $[t\text{-BuNSiMe}_2\text{Flu}]\text{TiMe}_2$ complex during ethylene/1-hexene copolymerization. **Catalysis Communications** 7(2006): 721-727
3. Effect of α -olefin on copolymerization of ethylene and α -olefin with $[t\text{-BuNSiMe}_2\text{Flu}]\text{TiMe}_2$ catalyst: **Study in surface science and catalysis**, in press

สถาบันวิทยบริการ
จุฬาลงกรณ์มหาวิทยาลัย